2013

# The Effects of N-Butonol on the Model and Reconstituted Membrane of *Clostridium Pasteurianum*

Yogi Kurniawan
*University of Rhode Island*, yogik@my.uri.edu

# THE EFFECTS OF N-BUTANOL ON THE MODEL AND RECONSTITUTED MEMBRANE OF *CLOSTRIDIUM PASTEURIANUM*

BY

YOGI KURNIAWAN

A DISSERTATION SUBMITTED IN PARTIAL FULFILLMENT OF THE

REQUIREMENTS FOR THE DEGREE OF

DOCTOR OF PHILOSOPHY

IN

CHEMICAL ENGINEERING

UNIVERSITY OF RHODE ISLAND

**2013**

DOCTOR OF PHILOSHOPHY DISSERTATION

OF

YOGI KURNIAWAN

APPROVED:

Thesis Committee:

Major Professor Dr. Geoffrey Bothun

Dr. Lenore Martin

Dr. Mercedes Rivero

Nasser H. Zawia
DEAN OF THE GRADUATE SCHOOL

UNIVERSITY OF RHODE ISLAND
2013

## ABSTRACT

During n-butanol fermentation, n-butanol partitions into microbial membranes result indestabilizing cellular lipid membranes by altering their lipid composition(generally the ratio of saturated to unsaturated lipids) whereas adapted microorganisms respond by altering the ratio of unsaturated to saturated lipids. The mechanism of how microbes achieve a high adaptation in response to n-butanol is barely known. This dissertation describes the role of unsaturated lipids and charged lipid composition in modulating n-butanol partition into membrane using model bacteria (i.e. lipid bilayer vesicles or liposomes and Langmuir monolayers) and those studies were compared with reconstituted membranes (*Clostridium pasteurianum*) that represented an original sample which was collected during batch fermentation as a function of different fermentation conditions.

Calorimetric, spectroscopic, Langmuir balance and chromatographic techniques were used to examine the effects of unsaturated lipid, charged lipid and n-butanol on membrane phase behavior, membrane packing, and membrane structure. The effects of n-butanol on heterogeneous membrane phase behavior was dependent onn-butanol concentration and which phase was continuous (saturated or unsaturated lipids). An increase of unsaturated lipid ratios increased n-butanol partitioning into the membranes due to “binding pocket” on acyl chain of unsaturated lipid and increased area per molecule resulting in enhancing membrane elasticity.

Heterogenous monolayer membrane of DPPC/DOPC with n-butanol was also examined using Langmuir balance trough and fluorescence microscope. Lipid phase behavior, lipid packing, and monolayer elasticity were evaluated by surface pressure-

area (*Π-A*) analysis. This study shows that n-butanol partitioning in DPPC, DOPC domain and at DPPC/DOPC interface. n-Butanol partitioning into DPPC monolayers led to lipid expansion and decreased elasticity. Lipid expansion became greater when DOPC content increased. n-Butanol accumulation at equimolar DPPC/DOPC was amplified at the interface between coexisting liquid expanded (*LE*, DOPC-rich) phases and liquid condensed (*LC*, DPPC-rich)domains. The accumulation of n-butanol also reduced *LE-LC* line tension and changed the domain size and morphology of *LC* domains.

The integrity of charged lipid membrane was driven by electrostatic interactions between cations and negatively charged lipid headgroups and hydrophobic effects on lipid tails. However, above interdigitation concentration (0.13 M) of n-butanol, n-butanol partitioning into membrane transformed the gel phase to the interdigitated phase disregarding DPPG content and salt concentration. Increasing DPPG content in the DPPC/DPPG membrane and salts above 0.13 M of n-butanol concentration, aggregation/ fusion could be prevented and the transformation of LUV-SUVs could be observed. Increasing salt and DPPG concentration, screening electrostatic repulsion between PG headgroups was apparent to promote more rigid bilayer structures and reduced butanol partition.

Reconstituted membrane of *C.pasteurianum* have been examined to determine membrane composition, membrane phase behavior, and membrane fluidization using different techniques such as chromatographic, spectroscopic, and Langmuir balance. n-Butanol adapted membrane was the result of lipid modification by increasing longer

fatty acids and decreasing the amount of unsaturation and protein improvement that increased membrane rigidity that counter-acted the fluidizing effect of butanol.

Model and reconstituted membrane studies revealed that membrane rigidity and stability were promoted by decreasing unsaturated lipids, increasing the length of lipid tails and increasing charged lipid ratios in the electrolyte solution. The accumulation of n-butanol within membrane influenced membrane fluidity and membrane packing. These results demonstrate a fundamental link of the disordering effects of butanol and lipid compositions on cell membranes.

## ACKNOWLEDGMENTS

I would like to first thank Dr. Geoffrey Bothun for his vital guidance, mentorship, patience, and support over the last four years. Thanks to my Ph.D. committees (Dr. Martin, Dr. Rivero, Dr. Greenfield, Dr. Parang) for their time, support, thoughtful comments and guidance. I would like to acknowledge the Department of Chemical Engineering at the University of Rhode Island for giving me opportunity to study for my doctorate degree. I deeply appreciate each contribution made towards my evolving into a scholar and a well-equipped person: All members in Blab group, Dr. Keerti Ventakaramanan, Dr. Scholz, Hong Yin, Varun, Amitesh, Prateesh, Brenda Moyer, and Sheryl Girard.

I am so grateful to my family, friends, colleagues and brothers-sisters in the church life, who have involved in a major contribution in my doctoral study. Their prayer, love and support inspired me to pass through the tough times. Specifically, dreams from my parents strengthen my perseverance to have a higher education and a better life. Last but not least, I am so happy to finish my doctoral program and pass through tough times with the love, the prayer and the support of Jennie, my wife.

"I tell you the truth, no one can enter the kingdom of God unless he is born of water and the Spirit. Flesh gives birth to flesh, but the Spirit gives birth to spirit. You should not be surprised at my saying, 'You must be born again.' The wind blows wherever it pleases. You hear its sound, but you cannot tell where it comes from or where it is going. So it is with everyone born of the Spirit." John 3 5-8.

## PREFACE

This dissertation was prepared in the manuscript format. This dissertation is a compilation of one published manuscript, one submitted manuscript, and two manuscripts under preparation.

The first manuscript entitled "n-Butanol Partitioning and Phase Behavior in DPPC/DOPC Membranes" comprises chapter 2 of this dissertation and provides information on the role of unsaturated lipid in modulating butanol partition with model bacterial membrane. It was published in Journal of Physical Chemistry B (2012) 116(20):5919-5924.

The second manuscript "n-Butanol Partitioning at the Interface Between Liquid Expanded and Liquid Condensed Phases in Heterogeneous Lipid Monolayers" was submitted for publication to Langmuir journal. This manuscript comprises chapter 3 of this dissertation and evaluates the molecular packing, elasticity and phase behavior of heterogenous monolayer membranes affected by n-butanol.

The third manuscript "Role of Ionic Strength on n-Butanol Partitioning into Anionic Dipalmitoyl Phosphatidylcholine/Phosphatidylglycerol Vesicles" is being prepared for submission to Journal of Physical Chemistry B. This manuscript comprises chapter 4 of this dissertation and describes the synergetic effects of the interactions between negatively charged lipid (DPPG) in liposome and salt, and n-butanol on membrane phase behavior and fluidization.

The fourth manuscript "Differential Homeoviscous Response of *Clostridium Pasteurianum* by Membrane Composition and Structural Adaptations to Butanol Toxicity" is being prepared for submission to ACS Chemical Biology. This manuscript comprises chapter 5 of this dissertation and characterizes membrane

composition, membrane fluidity, and membrane compressibility of the homeoviscous cell membrane of *Clostridium pasteurianum* affected by addition of exogeneous n-butanol in media.

## TABLE OF CONTENTS

## LIST OF TABLES

## LIST OF FIGURES

# CHAPTER 1

# INTRODUCTION

Interest in n-butanol as a potential renewable biofuel has increased during the last four years due to its favorable physicochemical properties (hydrophobicity, high energy density, low vapor pressure) that enable it to be used directly or blended with gasoline in combustion engines.[1]Fermentation is the preferred route for n-butanol synthesis because it utilizes cellulosic (e.g. lignocellulose), sugar (e.g. glucose), and/or sugar-alcohol (e.g. glycerol) feedstocks that are available or can be derived naturally. For example, *Clostridium pasteurianum* is a potential microorganism that can convert crude glycerol, a waste product of biodiesel production, to n-butanol.[2] However, as with most fermentation processes, n-butanol product yields are low (typically lower than 2 % by weight[3,4]) due to low n-butanol-tolerance of the microorganism. The cause for this low tolerance lies within the cellular membrane. n-Butanol is a short-chain aliphatic alcohol consisting of a polar hydrophilic hydroxyl group and a nonpolar hydrophobic hydrocarbon chain (Figure 1.1).Thus, n-butanol can be described as an amphiphilic molecule that has high affinity for lipid membranes (lipophilic).[5] When n-butanol partitions into cellular membranes, it accumulates within the lipid headgroup region near the membrane/water interface destabilizing the membrane[6,7]and adversely affecting the structure and function of the cell.[3,8]

Compared to ethanol, which has been extensively examined because of its relevance to human physiology and fermentation,[9] relatively little is known on how n-butanol interacts with cellular membranes on a biophysical level. Biophysical studies are conducted primarily on lipid bilayers or monolayers employed as model cellular

membranes to eliminate complexities associated with cellular metabolism and growth – they provide a platform for quantifying membrane restructuring in response to n-butanol. However, most biophysical studies on membrane response to alcohols have relied on homogeneous single-lipid membranes that do not adequately account for the compositional and phase heterogeneity of actual cellular membranes. Quantifying restructuring of heterogeneous membranes in response to n-butanol would have direct implications to understanding/enhancing bacterial tolerance during n-butanol fermentation, which underpins the motivation of this dissertation. Connecting model membranes to reconstituted membranes comprised of cellular membrane extracts brings us one step closer to understanding the effects of n-butanol on membrane phenomena in *C. pasteurianum*.

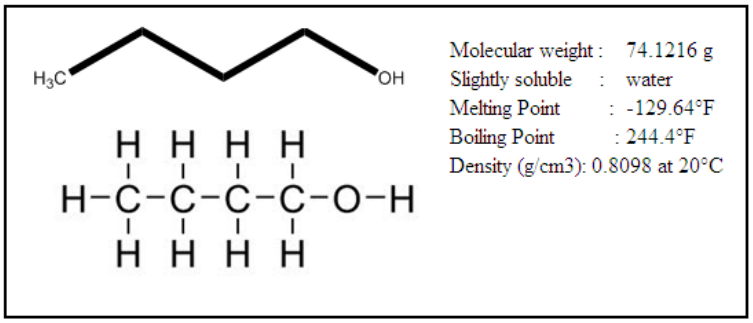


Figure 1.1.n-Butanol structure and its properties.

### 1.1. Bacterial cellular membranes

Lipid composition varies greatly in bacterial membranes depending on the species and changes during cell growth and metabolism, and in response to environmental stress. The major lipids include phosphatidylcholine (PC), phosphatidylethanolamine (PE), phosphatidylglycerol (PG), and

diphosphatidylglycerol (DPG) and their hydrocarbon tail groups, R, can vary in length and degree of unsaturation (Figure 1.2). PC and PE are zwitterionic lipids with net neutral charge and PG is an anionic lipid with a negative charge. PG lipids are the major anionic components found in gram positive and gram negative bacteria.[10] For example, *C. acetobutylicum* membranes contain 46% PE, 29% PG, and 15% DPG; and *C. butyricum* membranes contain 46% PE, 21% PG, and 21% DPG. The lipid tail groups, R, range from saturated dipalmitoyl ($C_{16}$, 16:0) to monounsaturated dioleoyl ($C_{18}$, 18:1). Prior to our work (Chapter 5) the lipid composition of *C. pasteurianum* membranes had not been determined.

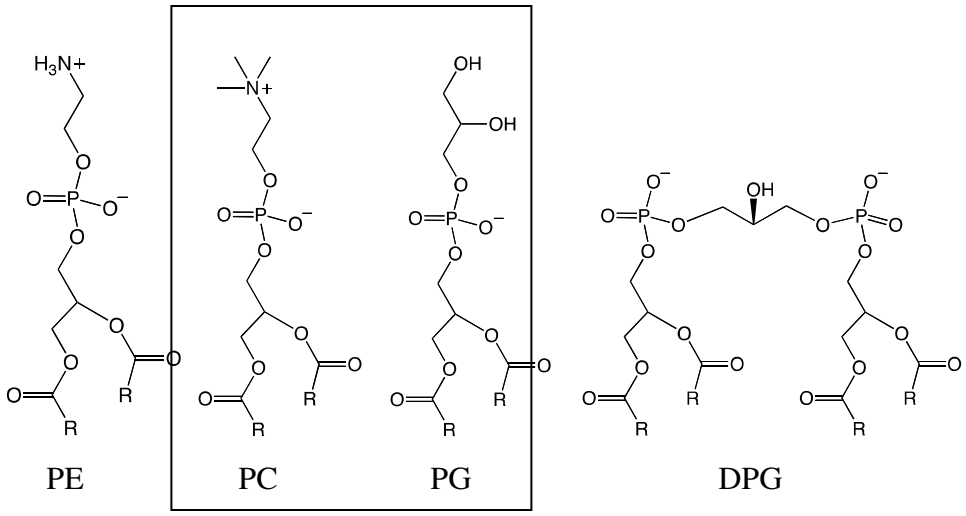


Figure 1.2.Chemical structures ofthe major phospholipids in bacterial membrane. A solid square marksthe types of lipids that were used as a model system for this dissertation.

### 1.2. n-Butanol tolerance in *Clostridium pasteurianum*

When cell membranes of *C. acetobutylicum*, *C. butyricum*, or *C. thermocellum* are exposed to n-butanol, they are fluidized (i.e. disordered or less viscous)and, in response to counteract this fluidization, the lipid composition is altered. A similar

response is observed when *C. pasteurianum* is exposed to n-butanol during fermentation. However, *C. pasteurianum,* an anaerobic bacterium, has a natural ability to tolerate n-butanol toxicity at higher concentrations than other species of solventogenic clostridia and it can utilize biodiesel-derived crude glycerol or mixing purified glycerol as substrates to produce n-butanol.[3,11,12]These advantages make *C. pasteurianum* a potential candidate for n-butanol fermentation and a model for studying the correlation between lipid membrane composition and n-butanol concentration.*C. pasteurianum* ferments glycerol as the sole substrate generating a mixture of n-butanol, ethanol, acetone and 1,3-propanediol (PDO) as shown (Figure 1.3).

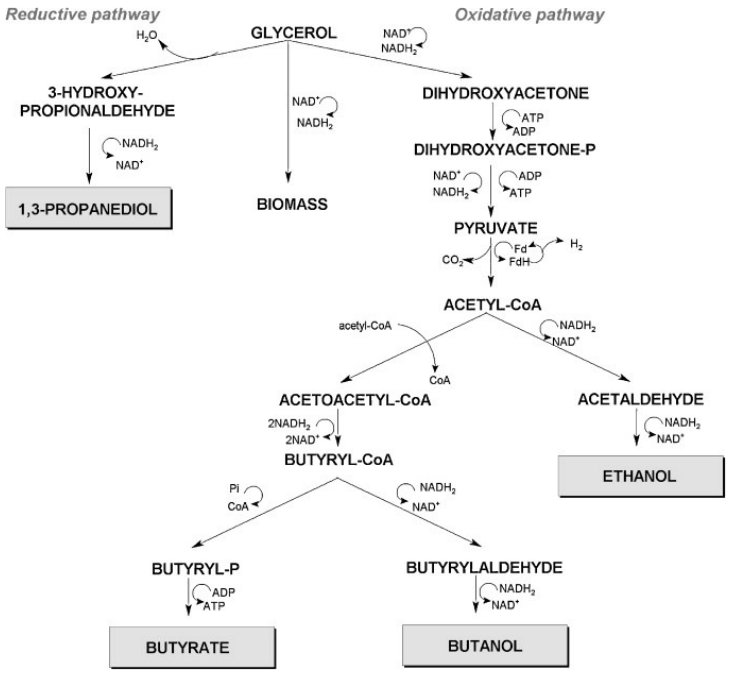


Figure 1.3. Metabolic pathways in the glycerol fermentation of *C. Pasteurianum.*[13]

By modifying the composition of the lipid membrane, *C. pasteurianum*adapts to tolerate the toxic solvents through homeoviscous adaptation. To counteract the fluidizing effects of n-butanol, *Clostridia* adjust the ratio of saturated to unsaturated fatty acids (SFA/UFA) and the chain length of SFA in the lipid membrane to yield a rigid membrane.[14-16] The fluidity of the lipid membrane is directly proportional to the amount of SFA in the tails of the lipid bilayer.[15] Hence, the n-butanol-tolerant bacteria may a much higher SFA/UFA ratio in the lipid bilayer. It is critical to understand how SFA/UFA ratio of homeoviscous microbes achieves their adaptation in response to n-butanol. Thus, a fundamental link between model and intact cell membranes has to be identified. The goal of this research is to identify and to understand how n-butanol restructures model membranes and to draw comparisons with reconstituted cell membranes of *C. Pasteurianum.*

It is very difficult to study the phenomena of membrane surface at molecular level due to the complexities of cell membranes. Reconstituted membranes of *C. pasteurianum* are the best way to simplify experiment processes, reduce complexity in data interpretation, and improve greater experimental control. By extracting cell membrane, reconstituted membrane can be obtained and formed as lipid bilayer model membranes and lipid monolayer membranes. Reconstituted membranes are an excellent model membrane that can be studied as a comparison with model membrane.

### 1.3. Lipid bilayers and monolayers as model cellular membranes

#### *Lipid bilayers as model membranes*

Lipid bilayers are the scaffold for cellular membranes, which separate intracellular components from the extracellular environment and determine the cell

shape[1].The effect of n-butanol toxicity on bilayer membranes forces cells to adjust their membrane composition and intrinsic curvature, which are related to the function of several membrane proteins[2,3]Lipid bilayer model membranes (liposomes) have been used to mimic the complex biological membranes to understand membrane-alcohol interactions. By modifying lipid bilayer composition, fundamental insight into n-butanol-membrane interactions can be gained.

Phosphatidylglycerol (PG) lipid, negatively charged phospholipid, is the major component found in gram positive and gram negative bacteria.[10] A model consisting of PC and PG system is a suitable model to mimic cytoplasmic bacterial membrane to investigate the effect of n-butanol partitioning into negative charged lipid membranes.

Table 1.1.List of lipids used in the study.

| Components | Chemical Structure | Melting Temperature ($T_m$, oC) |
|---|---|---|
| Dipalmitoylhosphatidylcholine (DPPC, zwitterionic lipid, 734.05MW) | 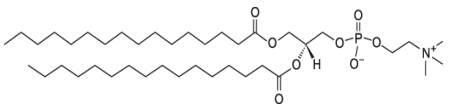 | 42 $^{o}$C |
| Dioleoylphosphatidylcholine (DOPC, zwitterionic lipid, 786.13MW) | 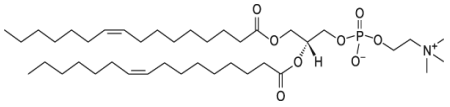 | -20 $^{o}$C |
| Dipalmitoylphosphatidylglycerol (DPPG, anionic lipid, 744.95MW) | 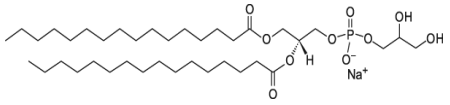 | 41 $^{o}$C |

When amphiphilic phospholipids are dispersed in water, hydrophilic lipid headgroups point toward aqueous environment and hydrophobic lipid tails interacts between opposing phospholipid monomers resulting in the formation of lipid bilayer

vesicles or liposomes (Figure 1.4). A liposome resembles biological membranes and it can be prepared simply.[17]

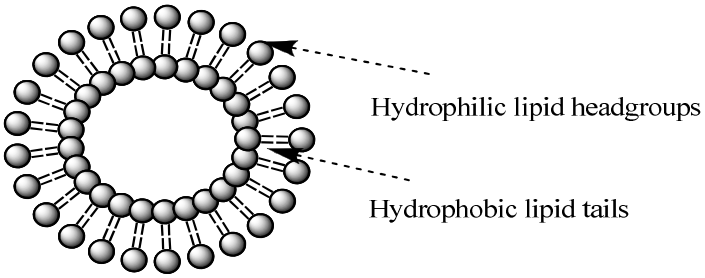


Figure 1.4.Schematic of a lipid bilayer vesicle (liposome). The hydrophobic thickness is approximately 3 nm and the total bilayer thickness is approximately 4-5 nm depending on the lipid composition and phase state.

The most characteristic property of a lipid bilayer is its phase transition temperature. The main phase transition of lipids, denoted as the melting temperature ($T_m$), is associated with conformational changes of the lipid acyl chains. Below the phase transition temperature (T $<T_m$), membrane is in ordered gel like phase ($L_{\beta'}$) and above melting temperature, membrane is in disordered fluid phase ($L_\alpha$). A phase between $L_{\beta'}$ and $L_\alpha$phase is called ripple phase ($P_{\beta'}$) where flat membrane in the gel phase transforms into an undulated bilayer (Figure 1.5).[18]

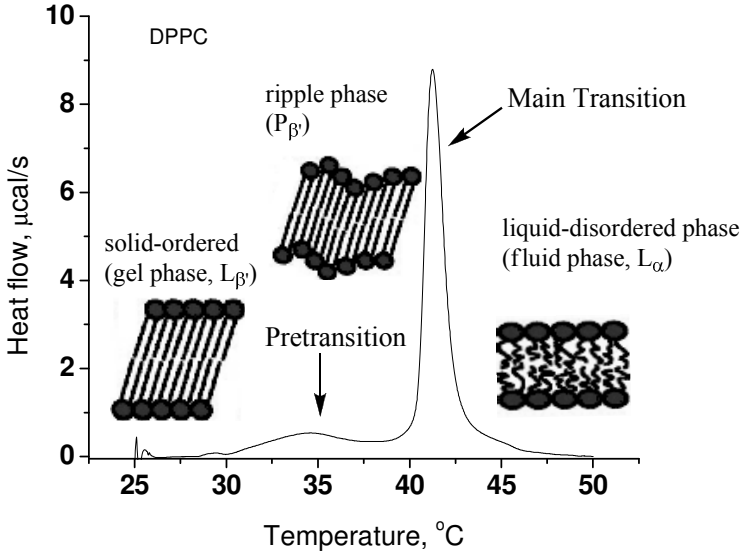


Figure 1.5.Calorimetric melting profile of dipalmitoylphosphatidylcholine(DPPC). The melting curve displays two peaks called pretransition ($T_P$) and main transition ($T_m$). Above the main transition the liquid-disordered state (fluid phase) occurs. The ripple phase is an intermediate between the gel and fluid phase.

***Monolayers as model membranes***

Lipid monolayer membranes are excellent as model membranes, represent a single membrane lipid leaflet, to investigate interactions between membrane components or the mechanism of solute partitioning into the membrane interface. Comparatively, monolayers are more controllable than bilayers. The physicochemical properties of monolayer membrane can be carefully adjusted to define molecular density with altering molecular area and surface pressure; and the size and shape of the monolayer domain formation due to phase separation can be visualized analytically with Brewster angle microscopy (BAM) [19] or fluorescence microscopy.[20] The interactions between monolayer molecules can be represented with the surface pressure($\Pi$) – area ($A$) isotherms under compressive or expansive force. Dipalmitoylphosphatidylcholine (DPPC) has been used for many monolayer studies.

In general, DPPC monolayer isotherms consists of different phases under different surface pressures and area per molecule; gas (*G*)- liquid-expanded (*LE*), liquid condensed (*LC*), solid (*S*), and collapsed phases (Figure 1.6).

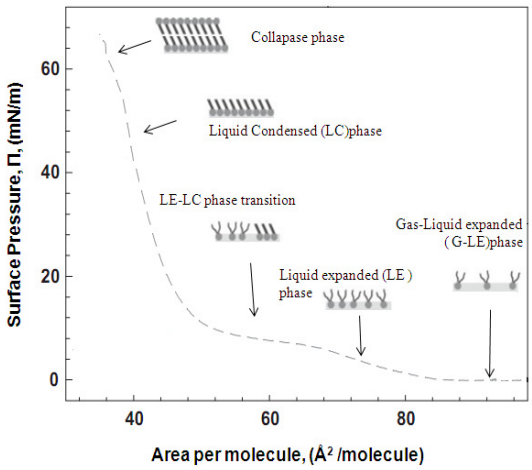


Figure 1.6.The *Π-A*isotherms of dipalmitoylphosphatidylcholine (DPPC) exhibiting different phases under different surface pressures and area per molecule; gas- liquid-expanded (*G-LE*), liquid-expanded (*LE*), liquid condensed (*LC*), and collapse phase.[21]

The surface pressure in *G* phase is very low. The lipid tails are not curled and lie extended on the surface. The lipid molecules also move freely at air/water interface. When a compressive force on water surface is increased, the surface pressure is also increased. Monolayers enter the *G-LE* phase transitions and then *LE* phase which lipid tails are still disordered. Further compressing the monolayer enters the *LE-LC* phase and the *LC* phase where lipid tails are tilted orderly. Further a high compression, monolayer experiences in collapse phase at which the monolayer films are collapsed and packed to their maximum density.[22]

The interactions between DPPC monolayers and short chain alcohols such as methanol and ethanol have been previously studied. Increasing surface excess of alcohol molecules adsorbed at the interface promotes alcohol partitioning into

monolayers and results in increases in area per molecule and surface pressure (see Figure 1.7), and decreases inelasticity and molecular packing density.[23] Molecular packing density, elasticity, and the excess free energy of mixing between lipid/alcohol are dependent on the particular alcohol and its concentration. Longer hydrocarbon chain length alcohols have a stronger impact on molecular arrangement and membrane structure, creating different sizes and shapes of monolayer domains at different surface pressures.[24] Even though the interactions of short chain alcohols (methanol, ethanol and propanol)[25] and homogeneous monolayers have been studied, understanding the interactions between mixed saturated/unsaturated monolayers with n-butanol are not well known. Thus, this dissertation will reveal the mechanism and the interactions between heterogeneous monolayers and n-butanol.

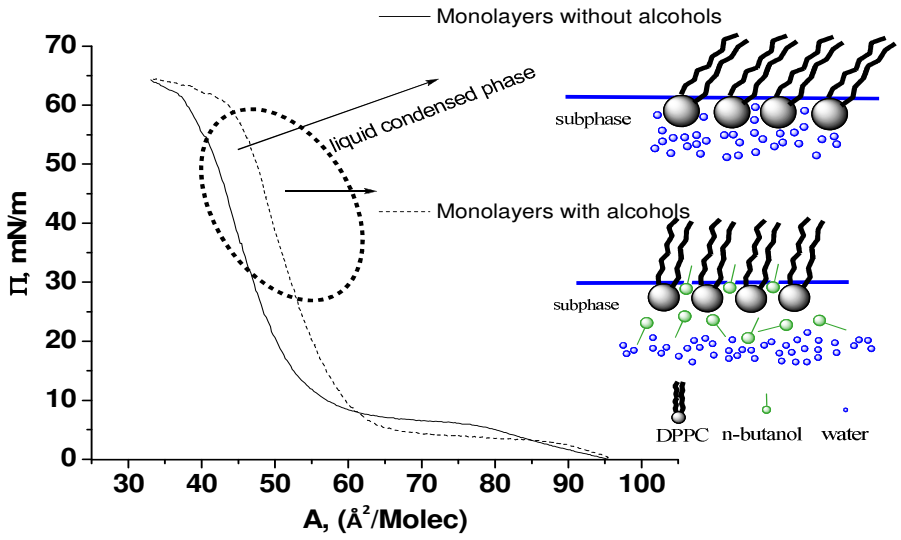


Figure 1.7.*Π-A*isotherms of dipalmitoylphosphatidylcholine (DPPC) monolayers with and without alcohols adsorption at air/water interface. The schematic illustration exhibits the interaction between lipid monolayers and alcohols in liquid condensed phase.

### 1.4. n-Butanol interactions with lipid membranes

Alcohol partitioning into membrane is correlated to hydrophobicity in the *alkyl chain* length of the alcohol molecule.[26] Longer chain alcohols are more hydrophobic and, hence, n-butanol that is more hydrophobic than methanol, ethanol or propanol interacts more strongly with lipid membranes. n-Butanol resides near the lipid polar headgroup and its alkyl chain extends parallel into the hydrophobic tails of the lipids. The effects of n-butanol partitioning into membrane produce a large disorder in the glycerol backbone of the lipid membrane.[27]

Previous studies show that incorporation of n-butanol in lipid bilayer membrane perturbs lipid–lipid and lipid-water interaction resulting in a disturbance of membrane functions. Zhang et al. found that n-butanol concentration affects on homogeneous membrane phase behavior of phosphatidylcholine and lipid ordering.[28] An increased fluidity of the lipid membrane reflects with decreasing the melting temperature of the membrane and loosing membrane packing. They also determined that restructuring membrane is dependent on n-butanol concentration exhibiting a changing membrane phase, gel phase to interdigitated phase ($L_{\beta'} \rightarrow L_{\beta I)}$ (Figure 1.8). It is clear that determination of n-butanol concentration accumulated in the membrane (n-butanol partition coefficients) becomes more pronounce to maintain the membrane fluidity and stability.

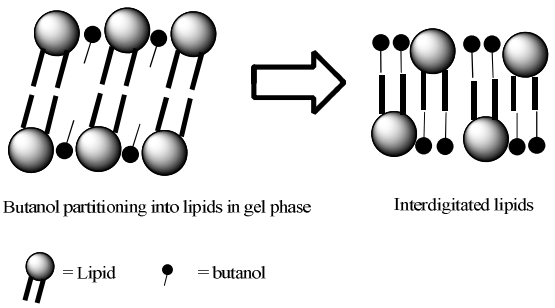


Figure 1.8. Schematic of n-butanol partitioning into lipids in gel phase resulting in interdigitated lipids

At low concentrations n-butanol disorders the lipid tails and promotes a lower transition temperature ($T_m$), a broader main phase transition $P_{\beta'} \rightarrow L\alpha$, and a larger phase pretransition $L_{\beta'} \rightarrow P_{\beta'}$. At high concentrations of n-butanol molecular packing is tightened orderly due to interdigitation, resulting in an increase of $T_m$and a disappearance of pretransition. When high n-butanol concentration is present, n-butanol replaces the interfacial lipid water molecules. The hydrophobic tail of n-butanol is aligned to the hydrophobic core of the bilayer and the hydroxyl group of n-butanol binds to the lipid headgroup, creating an expansion of lateral space or voids between the lipid headgroups. The voids are energetically unfavorable contributing the formation of an interdigitated phase ($L_{\beta I}$) to minimize the energy and the tail ends of the alcohol molecules shield the tail ends of the lipids. The interdigitated lipids gain energy due to stronger van der Waals interaction in the hydrophobic tails of lipids.[27-29]

**1.5 Effect of short-chain alcohols on lipid membrane**

Short chain alcohols (i.e ethanol and n-butanol) have important applications as a biofuel.[11] The fundamental understanding of the molecular mechanism of ethanol interacts on the lipid membrane is well studied through experimental and simulation results.[5,26,27]To date, homogenous model systems such as unilamellar vesicles,

supported bilayers or monolayers have been used to elucidate the effects of ethanol or n-butanol on the physical and thermodynamic properties of lipid membranes.[23-26,28,30] Ethanol partitioning into the headgroup region disturbs the lipid membrane. In addition, ethanol partition can modulate properties of membranes. With higher ethanol concentration partitioning into membrane, the fluidity of the membrane increases; the main phase transition temperature decreases; the membrane thickness decreases; and it can induce the formation of interdigitated bilayer structures.[31]Pastworks have also shown that n-butanol decreases the main phase transition temperature, induces the formation of interdigitated bilayer and decreases membrane thickness.[28] However, there are a few studies of the interactions between n-butanol and lipid membrane and understanding of n-butanol interacts with heterogeneous membranes is limited. Thus, quantitative studies of the n-butanol effects on coexisting phase in membrane will be more realistic resembling the real cell membrane. Motivated by realistic model systems, this dissertation will expand the understanding of the interactions between n-butanol and heterogeneous membrane, and apply this understanding as the best approach for gaining insight into how *C.pasteurianum* membranes respond to n-butanol partitioning.

**1.6. Dissertation objectives**

Determining the effects of n-butanol on model and reconstituted cell membranes will advance the understanding of how lipid composition modulates the effects of n-butanol cell membranes. The goal of this research is to identify and to understand how n-butanol restructures model membranes and to draw comparisons with reconstituted cell membranes of *C.Pasteurianum*. Model membranes are used to

mimic a bacterial membrane and simplify the complexities of whole cell membrane. Thus, the objectives of this research are to characterize structural perturbations in model membrane and reconstituted cell membranes by:

1. Examining the role of unsaturated lipid in modulating n-butanol partitioning into heterogeneous bilayer membrane (Chapter 2).
2. Examining surface pressure-area (*Π-A*) of heterogeneous monolayer to analyze lipid phase behavior, molecular packing, and elasticity (Chapter 3).
3. Evaluating the modulation of n-butanol partition into negatively charged/neutral membrane influenced by the role of ionic strength (Chapter 4).
4. Quantifying anisotropy and surface pressure-area (*Π-A*) of reconstituted cell membranes (Chapter 5).
5. Analyzing the lipid compositions of homeoviscous cell membrane in respond to exogenous n-butanol at different concentration (Chapter 5).

In Chapter 2 the effects of n-butanol on heterogeneous membranes are examined. Lipid bilayers as a model membrane are varied with different compositions. Calorimetry and fluorescence technique will be introduced. This study demonstrates liposome fluidization and interdigitation correlated to n-butanol and dioleoylphosphatidylcholine (DOPC) concentration. To our knowledge, this is the first study to examine the effects of n-butanol partitioning on membranes composed of saturated and unsaturated lipids that exhibit coexisting phase states.

Chapter 3 evaluates the effects of n-butanol on lipid phase behavior, lipid packing, and monolayer elasticity. n-Butanol partition at dipalmitoylphosphatidylcholine/ dioleoylphosphatidylcholine (DPPC/DOPC)

interfaces are evaluated by detailed analysis of surface pressure-area isotherms at 25 $^{o}$C coupled with visual analysis of lipid monolayer images using fluorescence microscopy. This study demonstrates the effects of n-butanol on reduction of line tension between the coexisting liquid expanded (*LE*, DOPC-rich) phases and liquid condensed (*LC*, DPPC-rich).The changes of size and morphology due to n-butanol accumulation at LE/LC interface will be presented. To our knowledge this is the first study depicting the effects of n-butanol partitioning on heterogeneous monolayers with coexisting *LE* and *LC* phases.

Chapter 4 examines the effects of ionic strength on n-butanol partitioning into charged and neutral lipid membranes. Dipalmitoylphosphatidylglycerol /dipalmitoylphosphatidylcholine DPPC/DPPG membrane phase behavior, size and n-butanol partitioning affected by DPPG and salts concentration will be presented. This study demonstrates that the presence of DPPG in DPPC/DPPG liposome and salts do not prevent the lipid interdigitation but they prevent aggregation/fusion and small unilamellar vesicle (SUV).This is the first study to our knowledge to examine the effects of n-butanol partitioning on model cell membranes composed of negatively charged lipid in the presence of salts.

Chapter 5 presents the effects of n-butanol on reconstituted membranes of *C. pasteurianum* grown under different conditions. The study discusses stability and change in the cell membrane composition that constitute a homeoviscous response under different conditions. The mechanical properties of cell membrane monolayer producing solvents will be elaborated. This is the first study to our knowledge to

analyze the homeoviscous adaptation to butanol by *C. pasteurianum* and this study is also the first study that quantifies lipid composition in *C. pasteurianum*.

## 1.7. References


(1) Harvey, B. G.; Meylemans, H. A., *Journal of Chemical Technology and Biotechnology* **2011,** 86, 2.

(2) Taconi, K. A., et al., *Environmental Progress & Sustainable Energy* **2009,** 28, 100.

(3) Biebl, H., et al., *Applied Microbiology and Biotechnology* **1992,** 36, 592.

(4) Jones, D. T.; Woods, D. R., *Microbiological Reviews* **1986,** 50, 484.

(5) Mccreery, M. J.; Hunt, W. A., *Neuropharmacology* **1978,** 17, 451.

(6) Bowles, L. K.; Ellefson, W. L., *Appl Environ Microbiol* **1985,** 50, 1165.

(7) Vollherbst-Schneck, K., et al., *Appl Environ Microbiol* **1984,** 47, 193.

(8) Dabrock, B., et al., *Appl Environ Microbiol* **1992,** 58, 1233.

(9) Benedict, F., *Industrial and Engineering Chemistry* **1925,** 17, 423.

(10) Goni, F. M.; Alonso, A., *Progress in Lipid Research* **1999,** 38, 1.

(11) Biebl, H., *Journal of Industrial Microbiology & Biotechnology* **2001,** 27, 18.

(12) Jensen, T. O., et al., *Journal of Industrial Microbiology & Biotechnology* **2012,** 39, 709.

(13) Kubiak, P., et al., *Process Biochemistry* **2012,** 47, 1308.

(14) Lepage, C., et al., *Journal of General Microbiology* **1987,** 133, 103.

(15) Liu, S. Q.; Qureshi, N., *New Biotechnology* **2009,** 26, 117.

(16) Matta-el-Ammouri, G., et al., *Biochimie* **1987,** 69, 109.

(17) Carmona-Ribeiro, A. M., *Chemical Society Reviews* **2001,** 30, 241.

(18) Riske, K. A., et al., *Biochimica Et Biophysica Acta-Biomembranes* **2009,** 1788, 954.

(19) Toimil, P., et al., *Phys Chem Chem Phys* 12, 13323.

(20) Nakahara, H., et al., *Colloids Surf B Biointerfaces* **2005,** 41, 285.

(21) Guzman, E., et al., *Colloids and Surfaces a-Physicochemical and Engineering Aspects* **2012,** 413, 174.

(22) Hossain, M. M., et al., *Langmuir* **2006,** 22, 1074.

(23) Weis, M., et al., *Applied Surface Science* **2006,** 253, 2425.

(24) Myrick, S. H.; Franses, E. I., *Colloids and Surfaces a-Physicochemical and Engineering Aspects* **1998,** 143, 503.

(25) Wittenberg, N. J., et al., *Langmuir* **2008,** 24, 2637.

(26) Ly, H. V.; Longo, M. L., *Biophysical Journal* **2004,** 87, 1013.

(27) Kranenburg, M., et al., *Biophysical Journal* **2004,** 87, 1596.

(28) Zhang, F. L.; Rowe, E. S., *Biochemistry* **1992,** 31, 2005.

(29) Simon, S. A.; Mcintosh, T. J., *Biochimica Et Biophysica Acta* **1984,** 773, 169.

(30) Vemuri, S.; Rhodes, C. T., *Pharm Acta Helv* **1995,** 70, 95.

(31) Lobbecke, L.; Cevc, G., *Biochim Biophys Acta* **1995,** 1237, 59.

# CHAPTER 2

## n-Butanol Partitioning and Phase Behavior in DPPC/DOPC Membranes

Yogi Kurniawan[1], Keerthi P.Venkataramanan[2], Carmen Scholz[3], and Geoffrey D. Bothun[1,*]

[1]Department of Chemical Engineering, University of Rhode Island, 16 Greenhouse Rd, Kingston, RI

[2]Biotechnology Science and Engineering program, University of Alabama in Huntsville, 301 Sparkman Dr, Huntsville, AL

[3]Department of Chemistry, University of Alabama in Huntsville, 301 Sparkman Dr, Huntsville, AL

*Corresponding author: bothun@egr.uri.edu (email); +1-401-874-9518 (tel); +1-401-874-4689 (fax)

Published in Journal of Physical ChemistryB. (2012)116(20):5919-5924.

## 1. Abstract

Membrane phase behavior and fluidization has been examined in heterogeneous membranes composed of dipalmitoylphosphatidylcholine (DPPC, a saturated lipid) and dioleoylphosphatidylcholine (DOPC, an unsaturated lipid) at n-butanol concentrations below and above the interdigitation threshold of DPPC. Our results show that the presence of DOPC did not influence the interdigitation concentration of n-butanol on DPPC (0.1 to 0.13 M) despite the fact that DOPC increased n-butanol partitioning into the membranes. When DPPC was the continuous phase, up to equimolar DPPC:DOPC, n-butanol partitioning into the gel or interdigitated DPPC was only slightly affected by the presence of DOPC. In this case a 'cooperative effect' of DOPC + n-butanol eliminated the DPPC pretransition phase and yielded an untilted gel-like phase. When DOPC was the continuous phase, more n-butanol was needed to cause DPPC interdigitation (0.2 M), which was attributed to n-butanol residing at the interface between DOPC and DPPC domains. To our knowledge this is the first study to examine the effects of n-butanol partitioning on membranes composed of saturated and unsaturated lipids that exhibit coexisting phase states.

## 2. Introduction

The partitioning of primary alcohols into homogenous lipids bilayer membranes has been well studied. Generally speaking, the partitioning of short alcohols (up to $C_6$) dehydrates lipid headgroups at the membrane/water interface, reduces membrane surface tension, leads to a reduction in lipid ordering (i.e. membrane fluidization), and, at high concentrations, causes lipid interdigitation.[1-12] As the carbon-chain length of the alcohol increases, the partitioning coefficient increases and fluidization or interdigitation occurs at lower alcohol concentrations. While well characterized in homogenous membranes, there has been relatively little work on alcohol partitioning and its effects on heterogeneous membranes that contain multiple lipid species and coexisting phase states.

This work examines n-butanol partitioning and membrane restructuring which, compared to ethanol, have not been examined extensively. n-Butanol is a viable biofuel and platform chemical for biorefining. It is also lipophilic and, when produced by fermentation, partitions into microbial membranes and compromises membrane integrity.[13,14] This can ultimately inhibit or eliminate microbial activity. Microorganisms respond by altering their lipid composition, specifically the ratio of saturated to unsaturated lipids and/or lipid tail length, to maintain a homeoviscous membrane state.[14] Studying the effects of n-butanol on heterogeneous membranes composed of saturated and unsaturated lipids is an important step towards understanding this response mechanism.

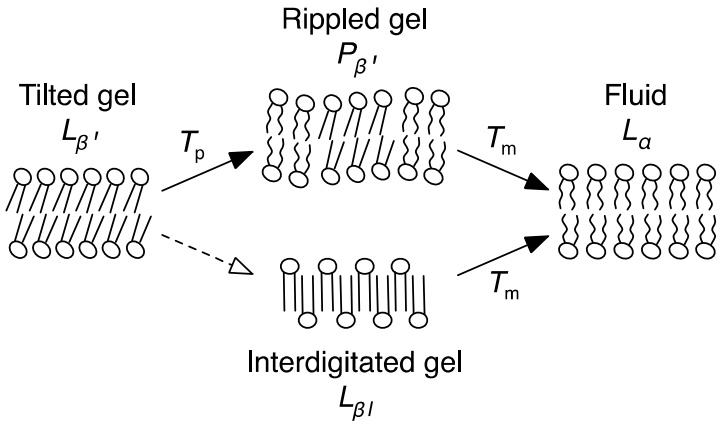


Figure 2.1. Schematic of membrane phase behavior and nomenclature. With heating, a tilted gel to rippled gel transition, $L_{\beta'} \rightarrow P_{\beta'}$, occurs at the pretransition temperature ($T_p$) and a rippled gel to fluid transition, $P_{\beta'} \rightarrow L_\alpha$, occurs at the main transition or melting temperature ($T_m$). At a critical alcohol concentration the titled gel phase becomes interdigitated, $L_{\beta'} \rightarrow L_{\beta I}$, and the pretransition is eliminated.

One common way to probe the effects of an alcohol on the membrane structure is through lipid phase behavior (Figure 2.1). In homogeneous membranes composed of saturated lipids, such as dipalmitoylphosphatidylcholine (DPPC), n-butanol partitioning can disorder the lipids and reduce the pretransition and melting temperatures.[8,12] Above a threshold concentration (0.14 M to 0.18 M)[4,12] n-butanol leads to complete lipid interdigitation. Previous work has shown that short-chain alcohols exhibit greater partitioning into unsaturated lipid membranes than into saturated lipids of membranes. Alcohols partition into the lipid/water interface, and greater partitioning into unsaturated lipid membranes can be attributed to a greater interfacial area stemming from the packing properties of unsaturated acyl tails.[10,15] It is unclear what effect this might have on the phase behavior of a heterogeneous membrane with saturated and unsaturated lipids. Using atomic force microscopy, Marques et al.[16] have shown that phase separation in DPPC/ dioleoylphosphatidylcholine (DOPC) membranes caused by ethanol is dependent on

which lipid phase is continuous. When DOPC was continuous at low ethanol concentrations, ethanol preferentially partitioned into and thinned the fluid DOPC phase. Increasing ethanol concentration then thinned both the DOPC and gel DPPC domains. When gel DPPC was the continuous phase and fluid DOPC domains were present, ethanol first partitioned at the gel/fluid interface and did not lead to the expansion of the fluid domains. These experiments were performed below the ethanol interdigitation concentration.

To our knowledge the effects of n-butanol on heterogeneous membranes have not yet been examined. In this study, DPPC/DOPC liposomes were used as a model system to investigate n-butanol partitioning, membrane phase behavior, and membrane fluidization at n-butanol concentration up to 0.27 M (20 g/l). The DPPC:DOPC molar ratio was varied to study membranes where DPPC (1:0, 3:1, and 1:1) or DOPC (1:3 and 0:1) was the continuous phase.

## 3. Experimental

1,2-Dipalmitoyl-*sn*-glycero-3-phosphocholine (DPPC, >99% purity) and 1,2-dioleoyl-*sn*-glycero-3-phosphocholine (DOPC, >99% purity) were purchased from Avanti Polar Lipids (Alabaster, AL) and used without further purification. The fluorescent membrane probe, 1,6-diphenyl-1,3,5-hexatriene (DPH, >98%), was purchased from Sigma Aldrich (St. Louis, MO). HPLC grade n-butanol and chloroform were purchased from Fisher Scientific. Deionized (DI) ultrafiltered water was obtained from a Millipore Direct Q-3 purifier.

### 3.1. Liposome preparation

Liposomes were prepared by the Bangham method.[17] Briefly, DPPC and DOPC dissolved in chloroform were mixed to achieve the desired ratio of DPPC to DOPC. The chloroform was then evaporated under a stream of nitrogen and the samples were dried under vacuum for at least 30 minutes. The dry films were then hydrated with 1.5 ml of deionized water to yield a total lipid concentration of 0.5 mM. Liposome suspensions were formed by sonication at 50 $^{o}$C for 30 min using a bath ultrasonicator (Branson, Danbury, CT). The average liposome diameters are summarized in Table 1. Butanol was then added to the samples at the desired concentration. The samples were briefly vortexed and stored for 2 h after the butanol addition before further processing or analysis.

**Table 2.1**. Liposome hydrodynamic diameter ($d_h$) and polydispersity index (PDI) based on dynamic light scattering (DLS).

| DPPC:DOPC (molar ratio) | $d_h$ (nm) | PDI |
|---|---|---|
| 1:0 | 343 | 0.282 |
| 3:1 | 271 | 0.310 |
| 1:1 | 118 | 0.329 |
| 1:3 | 108 | 0.366 |

### 3.2. High performance liquid chromatography (HPLC)

HPLC was one of the three methods to determine the lipid/water n-butanol partitioning coefficient. Sample preparation began by taking liposomes (no n-butanol) and liposomes + n-butanol, and centrifuging the suspensions at 10,000 rpm for 30 min at 4 $^{o}$C (Megafuge 16 R, Germany). The aqueous supernatant was separated from the liposomes and analyzed by HPLC for n-butanol concentration. HPLC was conducted with a resin-based column (Aminex HPX-87H, Bio-Rad, CA) and a refractive index

detector (Varian, CA) using with 0.5 mM $H_2SO_4$ as the mobile phase. Standard calibration curves were prepared with aqueous butanol solutions containing 0.007 M to 0.135 M n-butanol ($R^2 = 0.994$).

The partition coefficient, $K_P$, was calculated as

$$K_P = \frac{x_b^m}{x_b^w} \qquad (1)$$

where $x_b^m$ and $x_b^w$ are the mole fractions of n-butanol (*b*) in the membrane (*m*) and aqueous (*w*) phases. n-Butanol mole fractions were determined based on mole balance, $x_b^m = n_b^m/(n_b^w + n_b^m)$ and $x_b^w = n_b^w/(n_b^w + n_b^m)$, where $n_b^m$ and $n_b^w$ are the number of moles of n-butanol in the membrane and aqueous phases, respectively. The number of moles of n-butanol in the membrane was calculated as $n_b^m = n_b - n_b^w$ where $n_b$ was the total number of moles of n-butanol in the system.

**3.3. Differential scanning calorimetry (DSC)**

DSC was performed using a TA Instruments Nano DSC with capillary cells. The reference cell was filled with degassed water and the sample cell was filled with 760 µl of degassed sample. The cell chamber was sealed and pressurized to 3 atm under nitrogen. Samples were analyzed by consecutive heating/cooling cycles between 25 $^oC$ and 50 $^oC$ at a rate of 1 $^oC$/min. Pretransition temperature, $T_p$, melting temperature, $T_m$, and melting enthalpy, $\Delta H_m$, were determined using the Universal Analysis software. The melting temperature was taken as the temperature at maximum peak height.

$K_P$ was calculated from DSC results as:

$$\Delta T_m = -\frac{RT_{m,o}^2}{\Delta H_m}\left(\frac{C_b K_P}{C_w + C_l}\right) \qquad (2)$$

where$\Delta T_m$ is the measured change in melting temperature ($T_m - T_{m,0}$), $R$ is the gas constant, $T_{m,0}$ is the melting temperature of DPPC without n-butanol, and $\Delta H_m$ is the lipid melting enthalpy. $C_b$, $C_w$, and $C_l$ are the n-butanol, water, and lipid molar concentrations, respectively.

### 3.4. Fluorescence anisotropy

Liposome preparation for fluorescence anisotropy was similar to that for DSC. In this case, DPH was added to the lipids in chloroform as a probe at a DPH:lipid molar ratio of 1:400. The samples were hydrated with 3 ml of DI water to yield a total lipid concentration of 0.04 mM. DPH anisotropy, <*r*>, in DPPC/DOPC bilayers was measured as a function of n-butanol concentration using a LS55 Luminescence Spectrometer with a Peltier system (Perkin-Elmer, Shelton,CT). Heating and cooling scans were conducted between 25 $^{o}$C and 50 $^{o}$C at a rate of 1 $^{o}$C/min, and the sample was continuously mixed with a magnetic stirrer. Steady-state DPH anisotropy was determined at an excitation wavelength of 350 nm and an emission wavelength of 452 nm with a 10 nm slit width. The anisotropy was calculated as

$$< r >= \frac{I_{VV} - I_{VH}}{I_{VV} + G I_{VH}} \qquad (3)$$

where $I$ represents the fluorescence intensity, the subscripts $V$ and $H$ represent the vertical and horizontal orientation of the excitation and emission polarizers, respectively, and $G$ is the grating factor ($G = I_{HV}/I_{VH}$), which accounts for the correction factor of the sensitivity of the instrument towards vertically and horizontally polarized light. Anisotropy is dependent upon the fluorescence lifetime of DPH ($\tau$), which changes with temperature and lipid composition.[18,19] However, in this work steady-state anisotropy was measured and changes in $\tau$ are not considered.

## 4. Results

### 4.1. Membrane phase behavior

Results are first presented for DPPC with n-butanol, which has been previously studied.[4,8,12] DSC was conducted by adding n-butanol at room temperature followed by sequential heating and cooling scans (Figure 2.2). Without n-butanol, DPPC underwent a pretransition at 35.8 $^{o}$C with heating ($L_{\beta'} \rightarrow P_{\beta'}$) and melted at 41.2 $^{o}$C with heating ($P_{\beta'} \rightarrow L_{\alpha}$) and 41.1 $^{o}$C with cooling ($L_{\alpha} \rightarrow L_{\beta'}$), no pretransition was observed with cooling). Adding n-butanol up to 0.1 M decreased $T_p$ to 31.1 $^{o}$C, and beyond 0.1 M the pretransition disappeared. With respect to $T_m$, increasing the n-butanol concentration up to 0.13 M led to a significant decrease in $T_m$ with no appreciable melting hysteresis between heating and cooling. Above 0.13 M n-butanol, $T_m$plateaued with heating and there was a significant melting hysteresis.

Melting enthalpies, $\Delta H_m$, are shown in Figure 2.3 $\Delta H_m$ describes tail disordering and bilayer expansion, which is resisted by interlipid van der Waals attraction.[1,20] Increases in $\Delta H_m$ were observed within increasing n-butanol concentration and, upon cooling, $\Delta H_m$ hysteresis was evident. $\Delta H_m$hysteresis became most pronounced above 0.13 M n-butanol. Evidence of lipid interdigitation with increasing n-butanol concentration includes the disappearance $T_p$, a plateauing or increase in $T_m$, $T_m$ hysteresis, and increases in $\Delta H_m$.[4,12] Interdigitated phases ($L_{\beta I}$) exhibit greater ordering than rippled gel phases ($P_{\beta'}$) and yield higher $\Delta H_m$ upon melting. Our results show that DPPC was interdigitated above 0.13 M n-butanol ($L_{\beta'} \rightarrow L_{\beta I}$), which is in agreement with previous work.[4,12]

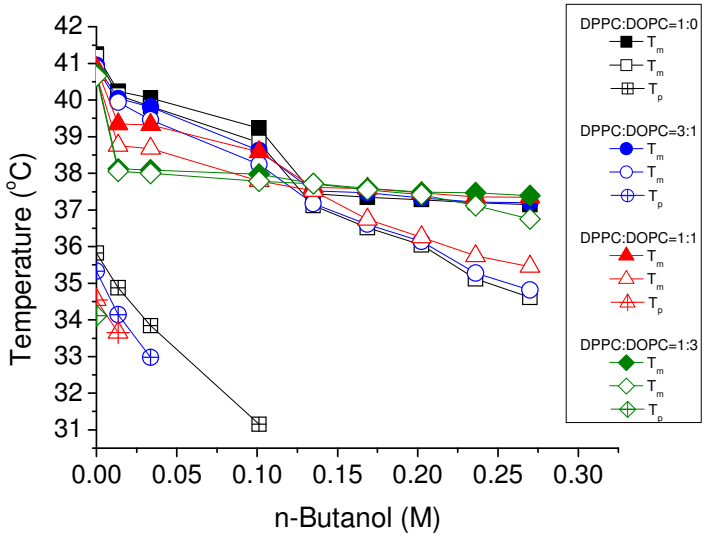


Figure 2.2. DSC thermographs of membrane phase behavior at DPPC:DOPC ratios of (■,□) 1:0, (●,○) 3:1, (▲,△) 1:1, and (◆,◇) 1:3 as a function of n-butanol concentration. Melting temperatures ($T_m$) are shown as filled symbols for heating and unfilled symbols for cooling scans. Pretransition temperatures ($T_p$) are shown for heating scans at DPPC:DOPC ratios of (⊞) 1:0, (⊕) 3:1, (⧋) 1:1, and (✧) 1:3.

DOPC had little effect on the $T_p$ or$T_m$ of DPPC in the absence of n-butanol, as shown in Figures 2.2, and confirms the two-phase coexistence of DOPC-rich $L_\alpha$ and DPPC-rich $L_{\beta'}$ phases below the pretransition. At DPPC:DOPC ratios of 3:1 and 1:1, the pretransition disappeared above 0.03 M and 0.01 M n-butanol, respectively. This indicates that less n-butanol was needed to suppress the pretransition with increasing DOPC concentration. With respect to melting, the trends in $T_m$with increasing n-butanol concentration were similar to that for DPPC and suggest that the DPPC/DOPC membranes were interdigitated above 0.13 M n-butanol. However, when DOPC was the continuous phase $T_m$ hysteresis was observed above 0.2 M n-butanol.

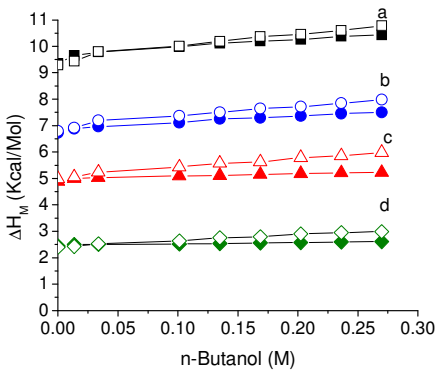


Figure 2.3.Melting enthalpy as a function of n-butanol concentration at different DPPC:DOPC ratios of (a; ■,□) 1:0, (b; ●,○) 3:1, (c; ▲,△) 1:1, and (d; ◆,◇)1:3. Filled symbols represent heating scans and unfilled symbols represent cooling scans.

Evidence for interdigitation from $T_p$ and $T_m$is contradictory and was addressed by considering the melting enthalpies (Figure 2.3). $\Delta H_m$was directly proportional to the DPPC concentration, which shows that the DPPC present within the membranes existed within gel phases and melted. Increases in $\Delta H_m$ were observed with increasing n-butanol concentration in all DPPC/DOPC membranes and, upon cooling, $\Delta H_m$ was higher than that for heating. $\Delta H_m$hysteresis became most pronounced at or above 0.13 M n-butanol at all DPPC:DOPC ratios. While trends in $T_p$ and $T_m$ were contradictory, trends in $T_m$ and $\Delta H_m$ indicate that DPPC was interdigitated at 0.13 M n-butanol up to equimolar DPPC:DOPC ratios, and at 0.2 M when DOPC was the continuous phase.

### 4.2.n-Butanol partitioning ($K_p$)

Calculated n-butanol partitioning coefficients ($K_p$) were 62, 54, and 45 at DPPC:DOPC ratios of 1:0, 3:1, and 1:1. These are based on $\Delta T_m$ (equation 2) and reflect the amount of n-butanol in the DPPC phases during melting. The results suggest that increasing DOPC concentration led to a decrease in n-butanol partitioning into DPPC. $K_p$was also measured at 25 $^{o}$C as a function of n-butanol and DOPC

concentration (Figure 2.4A). Corresponding values for the number of n-butanol molecules per lipid are shown (Figure 2.4B). For DPPC, $K_p$ was dependent on the phase state; 101 in the $L_{\beta'}$ phase (0.03 M n-butanol) and 200 in the $L_{\beta I}$ phase (0.27 M n-butanol). Greater partitioning into $L_{\beta I}$ phases was consistent with previous results.[12]It should be noted that the $K_p$ values were larger than previously reported for gel or interdigitated DPPC.[12]

For DPPC/DOPC, the membranes were in coexisting $L_{\beta'}$ (DPPC) + $L_\alpha$ (DOPC) phases at 0.03 M, and coexisting $L_{\beta I}$ (DPPC) + $L_\alpha$ (DOPC) phases at 0.10 M and 0.27 M. n-Butanol partitioning increased proportional to the DOPC content when the membrane was in a $L_{\beta'} + L_\alpha$ state. In contrast, the increase in $K_p$ was modest when the membrane was in a $L_{\beta I} + L_\alpha$ state. Only at a DPPC:DOPC ratio of 1:3, when DOPC was the continuous phase, did $K_p$ increase. Comparing measured and calculated $K_p$ values suggests that, below the interdigitation concentration, additional n-butanol partitioning was dependent on DOPC concentration and that the presence of DOPC did not increase partitioning into DPPC. However, above the interdigitation concentration $K_p$ was dependent upon which lipid was the continuous phase.

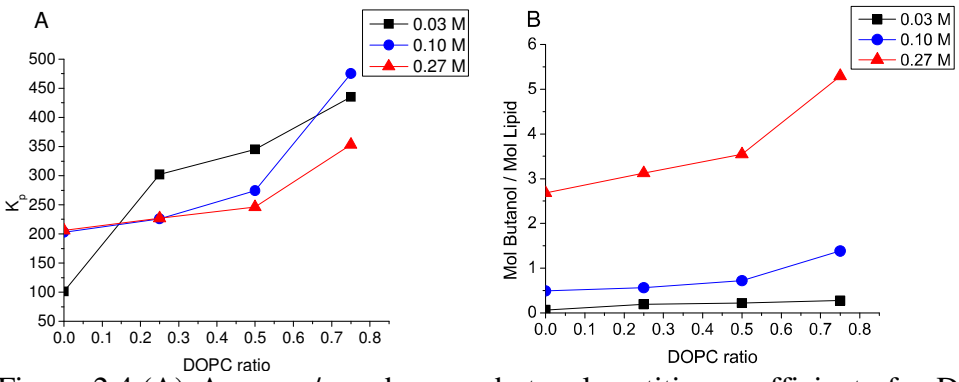

Figure 2.4.(A) Aqueous/membrane n-butanol partition coefficients for DPPC/DOPC liposomes as a function of DOPC fraction and n-butanol concentration. Measurements were performed at 25 $^{o}$C. (B) Number of n-butanol molecules per lipid determined from $K_p$.

### 4.3.Membrane fluidization

Fluorescence anisotropy was conducted using the probe DPH to assess membrane fluidization due to lipid disordering. Anisotropy, <*r*>, is shown in Figure 2.5 at 25 $^{o}$C and 50 $^{o}$C as a function of the n-butanol concentration. Increases in <*r*> denote lipid ordering or a decrease in membrane fluidity while decreases in <*r*> denote lipid disordering or an increase in membrane fluidity. At 25 $^{o}$C, increasing the n-butanol concentration had little effect on <*r*> in DPPC, which was between 0.29 and 0.32 with heating or cooling (Figure 2.5). This indicates that the lipid ordering experienced by DPH was similar in gel and interdigitated gel phases. At 50 $^{o}$C there was modest fluidization that shows increasing n-butanol concentration led to lipid disordering in the fluid phase.

At DPPC:DOPC ratios of 3:1 and 1:1, DPH anisotropy at 25 $^{o}$C and 50 $^{o}$C was similar to that for DPPC at low n-butanol concentrations. This shows that DPH preferentially partitioned into the $L_{\beta'}$ or$L_{\alpha}$ DPPC phase. However, above a critical n-butanol concentration (0.23 M and 0.14 M, respectively) a sharp decrease in <*r*> was observed at both temperatures. When DOPC was the continuous phase, greater

membrane fluidity was observed over the entire range of n-butanol concentrations when compared to the other membranes. There was also a pronounced <*r*> hysteresis with heating and cooling that indicates reorganization within the membrane.

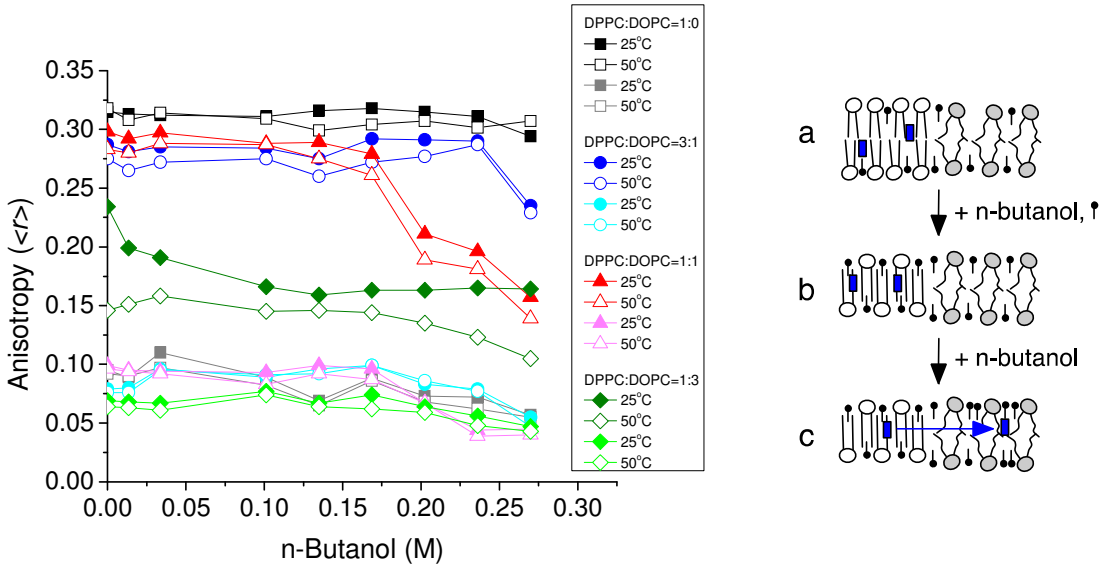


Figure 2.5.DPH fluorescence anisotropy at DPPC:DOPC ratios of (square) 1:0, (triangle) 3:1, (circle) 1:1, and (diamond) 1:3 as a function of n-butanol concentration at 25 °C (■,●,▲,◆) and 50 °C (■,●,▲,◆). Filled symbols represent heating scans and unfilled symbols represent cooling scans. (right) Schematic depicting the location of DPH within the membranes. DPH preferentially resides in the DPPC phase (a, b) until a critical n-butanol concentration is reached. DPH then partitions into the DOPC phase (c).

## 5. Discussion

For DPPC, it has been reported that n-butanol partitioning is greater in $L_\alpha$ phases than in $L_{\beta'}$ phases.[12]Although the same information is not available for membranes with saturated verses unsaturated lipids, previous work for ethanol has shown that partitioning into unsaturated $L_\alpha$ membranes is approximately 4-fold greater than into saturated $L_\alpha$ membranes.[10] While homogenous membranes have been well studied, there is no direct information available on the partitioning behavior in mixed

saturated/unsaturated membranes (for ethanol or n-butanol) or on how the partitioning affects membrane structure.

Heterogeneous membranes, specifically those containing DPPC and DOPC, attract interest due to their unique phase behavior and relevance as model membranes. However, conflicting results have been published for gel-fluid phase coexistence in DPPC/DOPC membranes. Microscopy studies on giant unilamellar vesicles (GUVs) have shown that when DPPC is in abundance, $L_{\beta'}$ and $P_{\beta'}$ phases coexist with DOPC ($L_{\alpha}$).[23] Up to 50% DOPC, gel DPPC was the continuous phase and contained fluid DOPC domains, while above 50% DOPC, DOPC was continuous and contained DPPC domains. For DOPC concentrations of 50% and greater, only the $P_{\beta'}$ was observed. Wide angle x-ray spectroscopy studies on multilamellar vesicles (MLVs) contradict these results and indicate that, at equimolar DPPC:DOPC, the gel DPPC phase does not form a $L_{\beta'}$ phase, but rather an untilted $L_{\beta}$-like phase.[24]Our DSC results show that a pretransition did occur at all DPPC:DOPC ratios in the absence of n-butanol, but quickly disappeared with increasing DOPC and n-butanol concentration. We do not attribute the disappearance of the pretransition to interdigitation, but rather a cooperative effect of DOPC + n-butanol that restricts lipid tilt and eliminates the $L_{\beta'} \rightarrow P_{\beta'}$ transition. This is based in part on evidence of $T_m$ and $\Delta H_m$ hysteresis that infers a common interdigitation concentration between 0.1 M and 0.13 M n-butanol when gel DPPC is the continuous phase.

Surface tension ($\gamma$) in lipid membranes is related to the area compressibility modulus ($\gamma \propto K_A$) and, with solute concentration ($c$), the partition coefficient ($d\Delta\gamma/dc \equiv K_p$). $K_A$is lower for fluid phases and unsaturated lipids than for gel phases and

saturated lipids. Hence, increasing DOPC and/or n-butanol concentrations would lower membrane surface tension and reduce $T_m$. This was not observed in the absence of n-butanol, consistent with the observation that DPPC (continuous or as domains) was not influenced by DOPC at the conditions examined. However, a reduction in $T_m$ was observed in the presence of n-butanol below the interdigitation concentration. In this case, increasing the DOPC concentration up to an equimolar DPPC:DOPC ratio did not affect this $T_m$ reduction. This suggests that increasing DOPC concentration did not increase n-butanol partitioning into gel DPPC and that increases in $K_p$, when gel DPPC was the continuous phase, can be attributed to additional partitioning into fluid DOPC. This is in agreement with $K_p$ calculated from DSC.

$K_p$increased linearly with DOPC concentration below the n-butanol interdigitation concentration and appeared to be independent of which phase was continuous. The linear relationship suggests that greater partitioning correlated with greater fluid phase fraction. Above the interdigitation concentration, $K_p$ was dependent upon which phase was continuous. Up to a DPPC:DOPC ratio of 1:1, interdigitated DPPC was the continuous phase and there was a modest increase in $K_p$. This indicates that n-butanol had a similar affinity for the interdigitated and fluid phases, which has been shown for ethanol.[20]At a DPPC:DOPC ratio of 1:3, fluid DOPC was the continuous phase and there was a notable increase in $K_p$. At this stage we attribute the increase in $K_p$ to n-butanol partitioning at the $L_{\beta I}/L_{\alpha}$ interface. This concept is supported by theoretical[25] and experimental[25-27] evidence that the dynamic wetting layer at gel/fluid interfaces become more influential when the fluid phase fraction is increased and becomes the continuous phase.

Fluorescence anisotropy provides additional insight into membrane structure. Assuming that DPH has equal affinity for gel and fluid phases,[28]<*r*> would represent the weighted average of DPPC gel and DOPC fluid domains. The anisotropy of DPPC at 25 $^{o}$C was greater than 0.3 across the range of n-butanol concentrations, which shows that the lipid ordering experienced by DPH in the $L_{\beta I}$ and$L_{\beta'}$ phases was similar. For DOPC at 25 $^{o}$C without n-butanol, <*r*> was 0.1 (not shown). The weighted average of <*r*> calculated at DPPC:DOPC ratios of 3:1, 1:1, and 1:3 are approximately 0.25, 0.2, and 0.15, respectively. This was not observed at ratios of 3:1 or 1:1 until n-butanol concentrations of 0.27 M and 0.2 M were reached, respectively. Below these concentrations, <*r*> was consistent with gel DPPC phases ($L_{\beta'}$or $L_{\beta I}$). DPH aligns parallel to lipid tails near the bilayer center, and its apparent preference for DPPC rather than DOPC may reflect unfavorable tail packing within DOPC that leads to large areas per headgroup (more interfacial void space) and exposes the hydrophobic core to water. When n-butanol is added, it partitions to the lipid/water interface and occupies these void spaces. This shields the hydrophobic core from water and makes it more favorable for DPH to partition into DOPC. This concept is supported by the high number of n-butanol molecules per lipid at high DOPC concentrations (Figure 2.4B). Considering that this occurs above the interdigitation concentration, we can conclude that DPPC, when it was the continuous phase, was interdigitated before DPH partitioned into DOPC. When DOPC was the continuous phase, <*r*> appeared to reflect the weighted average.

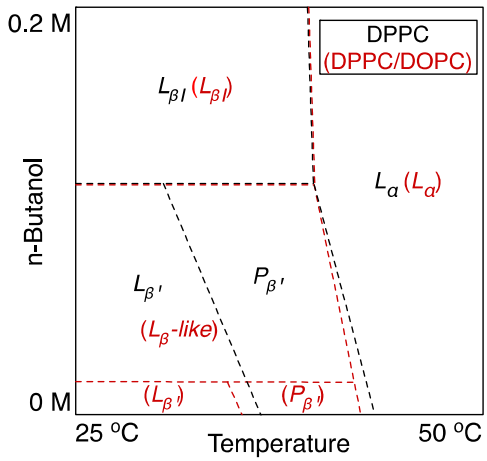

Figure 2.6.Schematic depicting the phase behavior of DPPC (black) and DPPC/DOPC (1:1; red, phases further indicated in parentheses) as a function of n-butanol concentration and temperature.

The cooperative effects of DOPC + n-butanol proceeded as follows based on our interpretation of the data (Figure 2.6). Below the interdigitation concentration, n-butanol partitioning increased with DOPC concentration proportionally to the fluid phase fraction. This resulted in DPPC converting from a $L_{\beta'}$ phase to an untilted $L_\beta$-like phase, upon which point the $P_{\beta'}$ phase was not observed. Above the interdigitation concentration, n-butanol had similar affinity for $L_{\beta I}$ and $L_\alpha$ phases and there was little change in the partition coefficient when DPPC was the continuous phase. However, when DOPC was the continuous phase, n-butanol partitioning increased due to the dynamic wetting effect at the gel/fluid interface.

## 6. Conclusions

Results from this work depict a cooperative effect of DOPC + n-butanol on membrane phase behavior that was dependent on n-butanol concentration and which phase (DPPC or DOPC) was continuous. Below the interdigitation concentration with a continuous gel DPPC phase, the total n-butanol partitioning increased proportional to the fluid phase fraction (DOPC), but partitioning into DPPC was unchanged. In this

case DOPC alone did not eliminate ripple gel formation by DPPC, but DOPC + n-butanol did by promoting a $L_\beta$-like DPPC phase. Fluidization results showed that the fluorophore preferentially partitioned into gel or interdigitated gel phases at low n-butanol concentrations, but distributed more evenly between DPPC and DOPC at high n-butanol concentrations (twice that for interdigitation). We propose that this was achieved by n-butanol filling the membrane/water interface and reducing unfavorable tail packing conditions normally experienced DOPC that expose the hydrophobic region to water. This study infers a cooperative effect of unsaturated lipids and alcohols in heterogeneous membranes, which aids our understanding of how membranes with mixtures of saturated to unsaturated lipids restructure in response to alcohols.

## 7. References


(1) Herold, L. L.; Rowe, E. S.; Khalifah, R. G. *Chem. Phys. Lipids***1987**, *43*, 215.

(2) Ho, C. J.; Stubbs, C. D. *Biochemistry-Us***1997**, *36*, 10630.

(3) Krill, S. L.; Knutson, K.; Higuchi, W. I. *J. Controll. Release***1993**, *25*, 31.

(4) Löbbecke, L.; Cevc, G. *BBA. Biomembranes***1995**, *1237*, 59.

(5) Ly, H. *Biophys. J.***2004**, *87*, 1013.

(6) Patra, M.; Salonen, E.; Emma, T.; llpo, V. *Biophys. J.***2006**, *90*, 1121.

(7) Pillman, H. A.; Blanchard, G. J. *J. Phys. Chem. B***2010**, *114*, 3840.

(8) Reeves, M. D.; Schawel, A. K.; Wang, W.; Dea, P. *Biophys. Chem.***2007**, *128*, 13.

(9) Rowe, E. S.; Zhang, F.; Leung, T. W.; Parr, J. S.; Guy, P. T. *Biochemistry***1998**, *37*, 2430.

(10) Terama, E.; Ollila, O. H. S.; Salonen, E.; Rowat, A. C.; Trandum, C.; Westh, P.; Patra, M.; Karttunen, M.; Vattulainen, I. *J. Phys. Chem. B***2008**, *112*, 4131.

(11) Vierl, U.; Löbbecke, L.; Nagel, N.; Cevc, G. *Biophys. J.***1994**, *67*, 1067.

(12) Zhang, F.; Rowe, E. S. *Biochemistry***1992**, *31*, 2005.

(13) Bowles, L. K.; Ellefson, W. L. *Appl. Environ. Microb.***1985**, *50*, 1165.

(14) Vollherbst-Schneck, K.; Sands, J. A.; Montenecourt, B. S. *Appl. Environ. Microbiol.***1984**, *47*, 193.

(15) Cantor, R. S. *J. Phys. Chem. B***2001**, *105*, 7550.

(16) Marques, J. T.; Viana, A. S.; De Almeida, R. F. M. *Biochimica Et Biophysica Acta- Biomembranes***2011**, *1808*, 405.

(17) Bangham, A. D.; Standish, M. M.; Watkins, J. C. *J. Mol. Biol.***1965**, *13*, 238.

(18) Lakowicz, J. R.; Prendergast, F. G.; Hogen, D. *Biochemistry***1979**, *18*, 520.

(19) Parasassi, T.; Conti, F.; Glaser, M.; Gratton, E. *J Biol Chem***1984**, *259*, 14011.

(20) Kranenburg, M.; Vlaar, M.; Smit, B. *Biophys. J.***2004**, *87*, 1596.

(21) Parasassi, T.; Stasio, G. D.; Rusch, R. M.; Gratton, E. *Biophys. J.***1991**, *59*, 466.

(22) Miccoli, L.; Szczepaniak, C.; Dumas, D.; Savonniere, S.; Muller, S.; Carr, M. C.; Donner, M. *J.Fluoresc***1993**, *3*, 251.

(23) Li, L.; Cheng, J.-X. *Biochemistry***2006**, *45*, 11819.

(24) Mills, T. T.; Huang, J.; Feigenson, G. W.; Nagle, J. F. *Gen. Physiol. Biophys.***2009**, *28,*126.

(25) Jorgensen, K.; Mouritsen, O. G. *Biophys. J***1995**, *69*, 942.

(26) Leidy, G.; Wolkers, W. F.; Jorgensen, K.; Mouritsen, O. G.; Crowe, J. H. *Biophys. J***2001**, *80*, 1819.

(27) Almeida, R. F. M. D.; Loura, L. M. S.; Fedorov, A.; Prieto, M. *Biophys. J***2002**, *82*, 823.

(28) Florinecasteel, K.; Feigenson, G. W. *Biochim Biophys Acta***1988**, *941*, 102.

# CHAPTER 3

## n-Butanol Partitioning at the Interface Between Liquid Expanded and Liquid Condensed Phases in Heterogeneous Lipid Monolayers

Yogi Kurniawan[1], Carmen Scholz[2], and Geoffrey D. Bothun[1,*]

[1]Department of Chemical Engineering, University of Rhode Island, 16 Greenhouse Rd, Kingston, RI

[2]Department of Chemistry, University of Alabama in Huntsville, 301 Sparkman Dr, Huntsville, AL

*Corresponding author: bothun@egr.uri.edu (email); +1-401-874-9518 (tel); +1-401-874-4689 (fax)

Submitted to Langmuir Journal.

## 1. Abstract

Cellular adaptation to elevated alcohol concentrations involves altering membrane lipid composition to counteract fluidization. However, few studies have examined the biophysical response of biologically relevant heterogeneous membranes. Lipid phase behavior, molecular packing, and elasticity have been examined by surface pressure-area (*Π-A*) analysis inmixed monolayers composed of saturated dipalmitoylphosphatidylcholine (DPPC) and unsaturated dioleoylphosphatidylcholine (DOPC) as a function of DOPC and n-butanol concentration.n-Butanol partitioning into DPPC monolayers led to lipid expansion and decreased elasticity. Greater lipid expansion occurred with increasing DOPC concentration and a maximum was observed at equimolar DPPC:DOPCconsistent with n-butanol accumulation at the interface between coexisting liquid expanded (*LE*, DOPC-rich) phases and liquid condensed (*LC*, DPPC-rich)domains. This effectively reduced the *LE-LC* line tension and altered the size and morphology of *LC* domains. In DOPC-rich monolayers the effect of n-butanol adsorption on *Π-A* behavior was less pronounced due to DOPC tail kinking. These results point to the importance of n-butanol partitioning at membrane domain interfaces.

## 2. Introduction

Primary alcohols are lipophilic and can partition into cellular membranes and cause lipid disordering, which increases membrane fluidity (reduces membrane viscosity). Cells counteract membrane fluidization through homeoviscous adaptation by altering their membrane lipid composition. Homeoviscous adaptation varies based on cell type andcan involve either an *increase* in the ratio of saturated to unsaturated lipids, where saturated lipids restore lipid ordering, or a *decrease* in the ratio of saturated to unsaturated lipids, where unsaturated lipids reduce the extent of membrane expansion.[1]Biophysical studies using lipid bilayers or monolayers as model cell membranes have provided a great deal of insight into how lipid structure and composition modulate membrane fluidization, and how this varies with the hydrocarbon chain length of the alcohol.[2-5] With implications in physiology and biofuel production, much of what is known for alcohol-induced membrane fluidization has been gained using ethanol and homogenous single-component lipid bilayers. Ethanol, like other short chain alcohols (up to $C_6$), partitions to the membrane/water interface, hydrogen bonds to carbonyl groups in the lipid headgroups, leads to lipid expansion and reduced interlipid van der Waals attraction, and increases membrane elasticity.[6-9] Above a critical concentration, short chain alcohols also induce lipid interdigitation in gel-phase membranes composed of saturated phosphatidylcholine (PC) such as dipalmitoyl PC (DPPC).[2,9-11]

Recent studies on alcohol-induced membrane fluidization have focused on heterogeneous membranes comprised of different lipid species and phase states (i.e. lipid domains in membranes containing saturated and unsaturated lipids), which better reflect the complex structure of cellular membranes.[7,12,13] Marques et al.[13]have shown

that restructuring in planar supported DPPC/dioleoylphosphatidylcholine (DOPC, unsaturated, fluid phase) membranes caused by ethanol is dependent on which lipid phase is continuous. When DOPC was the continuous phase at low ethanol concentrations, ethanol preferentially partitioned into and thinned the fluid DOPC phase. Increasing ethanol concentration then thinned both the DOPC and gel DPPC domains. When gel DPPC was the continuous phase and fluid DOPC domains were present, ethanol first partitioned at the gel/fluid interface and did not lead to the expansion of the fluid domains. These results are consistent with greater partitioning of short-chain alcohols into unsaturated than saturated lipid phases, and can be attributed to a greater interfacial area stemming from the poor packing properties of unsaturated lipid tails.[3,8]

Similar to ethanol, much of what is known of the fluidizing effects of n-butanol has been gained through biophysical studies of homogenous lipid bilayers.[5,8,9,11,14-21] Ly and Longo[4] studied the influence of short-chain alcohols on the interfacial tension and mechanical properties of unsaturated stearoyl-oleoylphosphatidylcholine (SOPC) lipid bilayers. Their results show that n-butanol led to greater mechanical destabilization and increased bilayer expansion than methanol, ethanol, and propanol. In addition, n-butanol had the highest membrane partitioning and permeability coefficients. Kurniawan et al.[13]have since shown that n-butanol partitioning in DPPC/DOPC bilayers increased with DOPC concentration and, when DOPC was the major component, n-butanol appeared to partition at the interface between gel and fluid phases. These observations were similar to those reported for ethanol.[7] Results from this work also suggested that DOPC reduced n-butanol

interdigitation in the DPPC phase, which is in agreement with recent work by Vanegas et al.[12]where DOPC prevented ethanol interdigitation in a yeast membrane model (DPPC/DOPC/ergosterol). The emergent role that unsaturated lipids play in modulating the response of heterogeneous membranes to alcohols should provide new insight into cellular homeoviscous adaptation, where increasing the ratio of saturated to unsaturated lipid does not always correlate with improved alcohol tolerance.[22]

In this study, heterogeneous DPPC/DOPC monolayers have been used to determine effects of n-butanol on lipid phase behavior, lipid packing, and monolayer elasticity. Monolayers were employed to better examine n-butanol partition at DPPC/DOPC interfaces. This was achieved by detailed analysis of surface pressure-area isotherms at 25 $^{o}$C coupled with fluorescence microscopy of lipid monolayers transferred onto glass slides. Monolayers were prepared over a range of DPPC:DOPC ratios and subjected to n-butanol subphase concentrations up to 0.27 mM (20 mg/L). DPPC is a saturated lipid with dual $C_{16}$ tails and a melting temperature of 41 $^{o}$C, while DOPC is an unsaturated lipid with dual $C_{18}$ tails (*cis* double bond in each tail at the 9-10 position) and a melting temperature of -20 $^{o}$C. DPPC/DOPC monolayers were used to yield heterogeneous monolayers with coexisting liquid expanded phase (*LE*, DOPC) and liquid condensed (*LC*, DPPC) and high surface pressures or low areas per lipid molecule representative of cellular membranes.

## 3. Materials and Methods

### 3.1. Chemicals.

1,2-Dipalmitoyl-*sn*-glycero-3-phosphocholine (DPPC, >99% purity),1,2-dioleoyl-*sn*-glycero-3-phosphocholine (DOPC, >99% purity) and 1,2-dipalmitoyl-*sn*-

glycero-3-phosphoethanolamine-N-(lissamine rhodamine B sulfonyl) (ammonium salt) (RhPE, >99% purity) were purchased from Avanti Polar Lipids (Alabaster, AL) and used without further purification. n-Butanol was purchased from Fisher Scientific and deionized (DI) ultrafiltered water was obtained from a Millipore Direct Q-3 purification system (18.2 MΩ.cm).

**3.2. Surface pressure-area (Π-A) isotherms**.

*Π-A*isotherms were measured in a Langmuir trough (model 102M, KSV NIMA) with a deposition area of 70 $cm^2$ at 25$^oC$. Surface pressure was measured with an accuracy of ±1μN/m using a Wilhelmy plateconnected to an electronic microbalance (Mini PS4, KSV NIMA). The subphase temperature was controlled by the external recirculating water bath (Haake B3). Monolayers were obtained by spreading diluted solutions of DPPC and/or DOPC in chloroform at the air/water interface using a 5 μl microsyringe (Hamilton, USA). After deposition, the spreading solvent was allowed to evaporate and the films to spread for 15 min. Prior to compression by PTFE barriers, n-butanol at a desired concentration was injected from the bottom of the trough into the subphase. The system was equilibrated for 10 min before being compressed at a speed of 10 $cm^2$/min. All experimental isotherms were recorded in duplicate.

Surface pressuremeasurements were conducted to confirm that n-butanol did not evaporate over the course of the experiments. n-Butanolwas injected in the subphase at 0.1 mM and 0.27 mM, and *Π*was recorded over 1.5 h. After stabilizing (~10 min) the change in *Π*did not exceed 0.2 mN/m.

### 3.3. Fluorescence microscopy.

A hydrophilic glass slide pretreated with piranha solution (2.54 cm x 1.27 cm) was immersed vertically into the subphase using a dipper assembly (KSV Nima). Monolayers were then formed as described in the preceding section with RhPE at 3 mol%.The labeled monolayer films were compressed at 10 $cm^2$/minto a surface pressure of 30 mN/m. Monolayers were transferred to the slides during withdrawal from the subphase at a rate of 3 mm/min.Imaging was performed at 100× magnification using a Nikon Diaphot-TMD inverted Epi-fluorescence microscope (Nikon, Japan). The microscope was equipped with phase contrast-2 ELWD 0.52 phase-contrast condenser, a12 V 100W mercury lamp (Nikon, Japan), and a digital sight DS-L2 camera (Nikon, Japan)equipped with G-2B filter cube.NIS-element software was used to capture the images and ImageJ was used for processing and analysis.[23]

## 4. Results and Discussion

### 4.1. Surface pressure-area isotherms and monolayer phase behavior

Surface pressure-area (*Π–A*)isotherms are shown in Figure 3.1.A-C for DPPC:DOPC ratios of 3:1, 1:1, and 1:3 (isotherms for pure DPPC and DOPC are shown in appendix D). Upon compression, the monolayers transitioned from single *LE* phases to coexisting phases with *LC* DPPC and *LE* DOPC. This transition, *LE-LC* for DPPC within the monolayers, occurred near 10 mN/m irrespective of DOPC concentration, but shifted to lower areas per molecule with increasing DOPC concentration. [24,25] DOPC, with dual monounsaturated tails, remained in *LE* phases and did not form *LC* domains upon compression as tail 'kinking' of the double bonds

hindered lipid packing. In DPPC/DOPC monolayers, the effects of poor DOPC packing are reflected in the increasing values for area per lipid molecule ($A_o$; Figure 3.1.D at $\Pi$ = 30 mN/m) with increasing DOPC concentration.

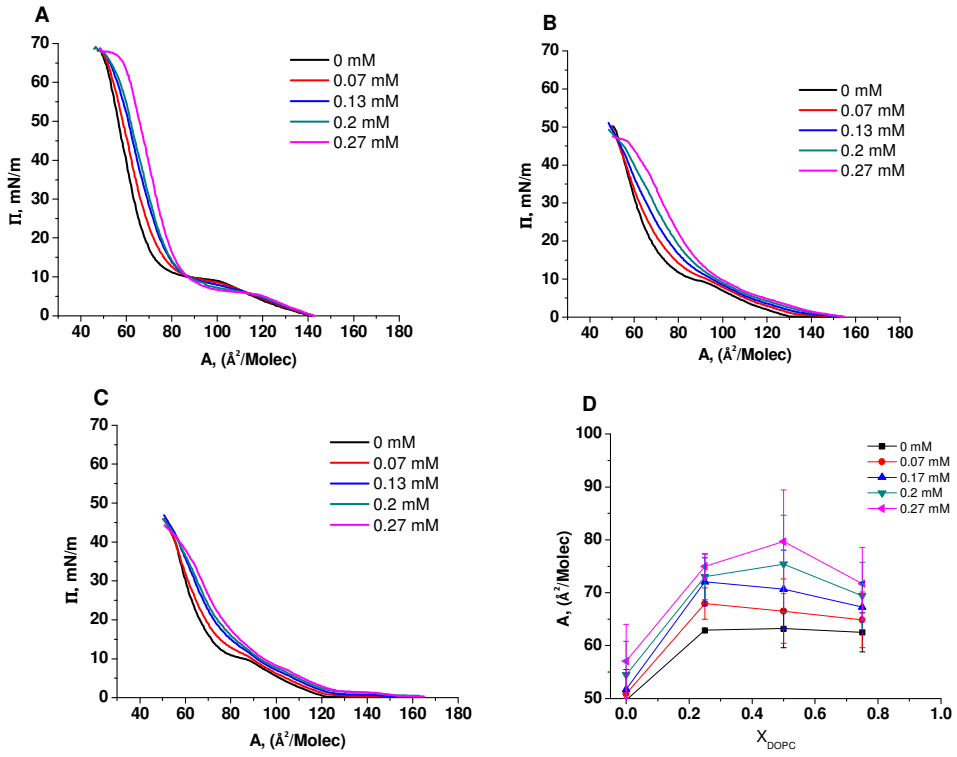


Figure 3.1.*Π–A* isotherms of DPPC/DOPC monolayers spread at air/water interfaces at 25°C as a function of the DPPC:DOPC molar ratio, (A) 3:1, (B) 1:1, and (C) 1:3, and the concentration of n-butanol in the subphase (legend). (D) Area per molecule, $A_o$, taken from the isotherms at 30 mN/m as a function of DOPC mole fraction and n-butanol concentration.

When n-butanol was added to the subphase (0.07 to 0.27 mM) it partitioned from water to the monolayer, leading to lipid expansion reflected as higher $A_o$ values. Monolayer expansion occurred because of the surface excess of alcohol molecules adsorbed at the interface.[26,27] *LE-LC* transitions with n-butanol present were observed when DPPC was the major component (3:1 DPPC:DOPC, Figure 3.1.A). In this case

increasing n-butanol concentration lowered the surface pressure associated ($\Pi_{LE\text{-}LC}$) with the LE-LC transition. A reduction in $\Pi_{LE\text{-}LC}$ suggests that n-butanol accumulated at the *LE-LC* domain boundary and allowed *LC* domains to form at lower surface pressures. The evidence for n-butanol accumulation at *LE-LC* domain boundaries is further supported by the results for $A_o$ (Figure 3.1D). The increase in $A_o$ with n-butanol concentration was greatest at 1:1 DPPC:DOPC; a condition that yields the largest net interfacial perimeter between *LE* and *LC* phases. Results for $A_o$ differ from simulation results performed by Dickey et al.[28]where they found that n-butanol did not affect the area per lipid molecule in DPPC bilayers. While changes in $A_o$ for DPPC and DOPC were modest, ~15% increase from 0 mM to 0.27 mM n-butanol (Figure 3.1D), phase separated DPPC/DOPC monolayers exhibited significant increase in $A_o$ (up to ~30%) owing to n-butanol at *LE-LC* interfaces.

When the DOPC mole fraction was ≥ 50% (1:1 and 1:3 DPPC:DOPC, Figures 3.1B and C, respectively) the *LE-LC* transitions became less pronounced with increasing n-butanol concentration. To verify *LE-LC* coexistence, fluorescence microscopy was conducted on supported monolayers transferred at $\Pi$ = 30 mN/m (Figure 3.2A). This surface pressure was selected because it is similar to that found in cellular membranes. The images confirm, despite not being evident from the $\Pi$–*A* isotherms, that the monolayers contained *LC* DPPC domains (dark regions) within continuous *LE* DOPC phases (light regions). Qualitatively, the surface area associated with *LE* and *LC* phases is consistent with the DPPC:DOPC ratio.

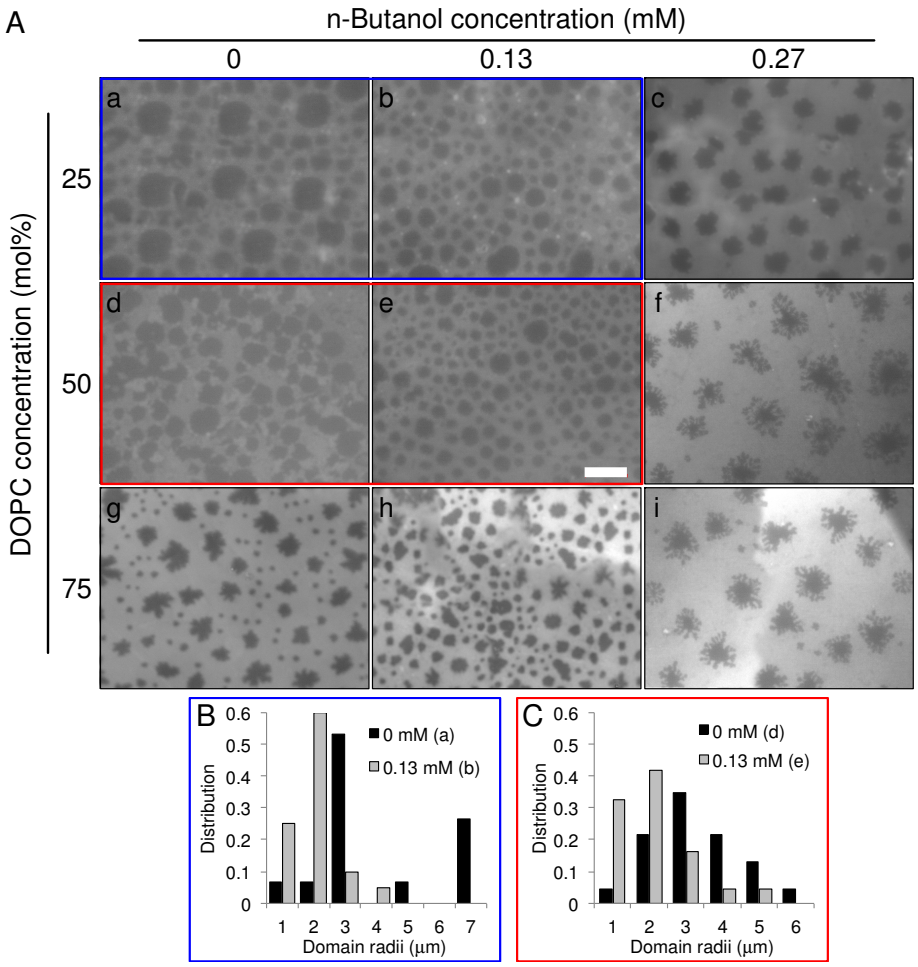


Figure 3.2.(A) Fluorescence microscopy images of DPPC/DOPC monolayers transferred at 30 mN/m. The scale bar in (e) is 20 μm and common to all images. Images (a-c) correspond to isotherms in Figure 3.1A, (d-f) isotherms in Figure 3.1B, and (g-h) isotherms in Figure 3.1C. Light regions reflect Rh-DPPE in liquid-disordered DOPC phases and dark regions reflect DPPC domains. (A) and (B) show distribution of domain radii determined by imaging analysis (ImageJ) at 3:1 and 1:1 DPPC/DOPC, respectively.

In the absence of n-butanol the *LC* domains were largely circular with some irregularities, particularly at 1:3 DPPC:DOPC or 75% DOPC (Figure 3.2A a, d, and g). At 0.13 mM n-butanol there were more, smaller LC domains present at all DPPC:DOPC ratios which suggests that n-butanol accumulated at the *LE-LC* interface and reduced line tension between the two phases (Figure 3.2A b, e, and h). At 0.27

mM n-butanol there were fewer domains relative to 0.13 mM n-butanol and the domains were irregular (Figure 3.2A c) or snowflake-like structures (Figure 3.2A f, i). It has been reported that snowflake-like structures are formed by diffusion-limited aggregation (DLA) of small *LC* nucleates into larger *LC* domains. At this point it is unclear whether DLA played a role in *LC* domain structure. However, what is clear is that n-butanol accumulates at the *LE-LC* interface and that the snowflake-like structures provided a significant amount of interfacial perimeter available for n-butanol partitioning.

Short chain alcohols are known to reduce the line tension between domains in lipid monolayers. Additional analysis of the *LC* domains was conducted to relate domain size to line tension reduction. This analysis was limited to the circular domains observed at 3:1 DPPC:DOPC (Figure 3.2A, a and b) and 1:1 DPPC:DOPC (Figure 3.2A, d and e). As described by Lee et al.,[29] the minimum energy domain radius ($R_o$) is proportional to $\exp[4\pi\varepsilon\varepsilon_o\lambda/\Delta m^2]$ where $\varepsilon$ is the dielectric constant of interfacial water, $\varepsilon_o$ is the permittivity of free space, $\lambda$ is the line tension at the domain interface (typically in femtonewtons, fN), and $\Delta m$ is the dipole density difference between the two phases. Distributions of domain radii are shown in Figure 3.2 for 3:1 and 1:1 DPPC:DOPC at 0 mM and 0.13 mM n-butanol. With n-butanol added there was a shift towards smaller domain sizes; the average domain radii decreased from 2.2±1.0 μm to 1.3±0.5 μm for 3:1 DPPC:DOPC and from 1.9±0.6 μm to 1.3±0.5 μm for 1:1 DPPC:DOPC. Assuming that $\Delta m$ was unchanged, this reduction in average domain radii represents a decrease in line tension of $0.5\times(4\pi\varepsilon\varepsilon_o\lambda/\Delta m^2)^{-1}$. As shown

theoretically by Lee et al.,[29] a 0.5 fN difference in line tension can significantly impact domain radii.

With regards to the *Π–A* isotherms, differences between single component and mixed DPPC/DOPC monolayers provide additional insight into n-butanol partitioning behavior. Unsaturated lipids within a monolayer or bilayer occupy larger areas than their saturated counterparts, yielding additional 'void area' at the lipid/water interface where the hydrocarbon tails are exposed to water. Hence, short chain alcohols, which are known to partition at the lipid/water interface, exhibit greater partitioning to unsaturated lipids than saturated lipids. For example, Cantor[3] has shown that ethanol partitioning in DOPC bilayers is 35% greater than in DPPC bilayers. *Π–A* results showed that n-butanol had the least effect on $A_o$ within a DOPC monolayer despite greater partitioning expected for DOPC. Unlike DPPC, DOPC was able to accommodate n-butanol at the lipid/water interface without greatly altering the area it occupied. This observation is consistent with simulation results for ethanol that showed that the increase in $A_o$ for DPPC was greater than that for palmitoyl-oleoylphosphatidylcholine (POPC).[5]

**4.2. Monolayer compressibility**

The bulk elastic moduli, ${C_s}^{-1}$, were determinedbased on the *Π-A* isotherms from

$$ {C_s}^{-1} = -A_o \left(\frac{\partial \Pi}{\partial A_o}\right)_T \qquad (1) $$

where *A* is the area per molecule at a given surface pressure.[30,31]. Figure 3.3 shows examples for ${C_s}^{-1}$ at 0 mM and 0.27 mM n-butanol, with corresponding *Π-A* isotherms, and maximum bulk modulus, $C_{Max}^{-1}$. DPPC forms rigid monolayers due to high packing and van der Waals attraction between its saturated tails, while DOPC

monolayers are less rigid due to unfavorable tail packing.[32] Not surprisingly $C_{Max}^{-1}$ occurred when the monolayers were *LC* or *LE-LC*. When DPPC was the major component, n-butanol increased the elastic moduli above 0.13 mM and $C_{Max}^{-1}$ increased with n-butanol concentration (Figure 3.3D). This observation is counterintuitive based on the known fluidizing effects of alcohols on lipid monolayers or bilayers. Compression isotherms of dipalmitoylphosphatidylcholine (DPPC) have revealed that methanol and ethanol expand the monolayer and decrease the elasticity modulus.[33] In contrast, at equimolar DPPC/DOPC, or when DOPC was the major component, there was little change in $C_{Max}^{-1}$. This suggests that, at sufficiently high concentrations, DOPC prevented the monolayer from rigidifying.

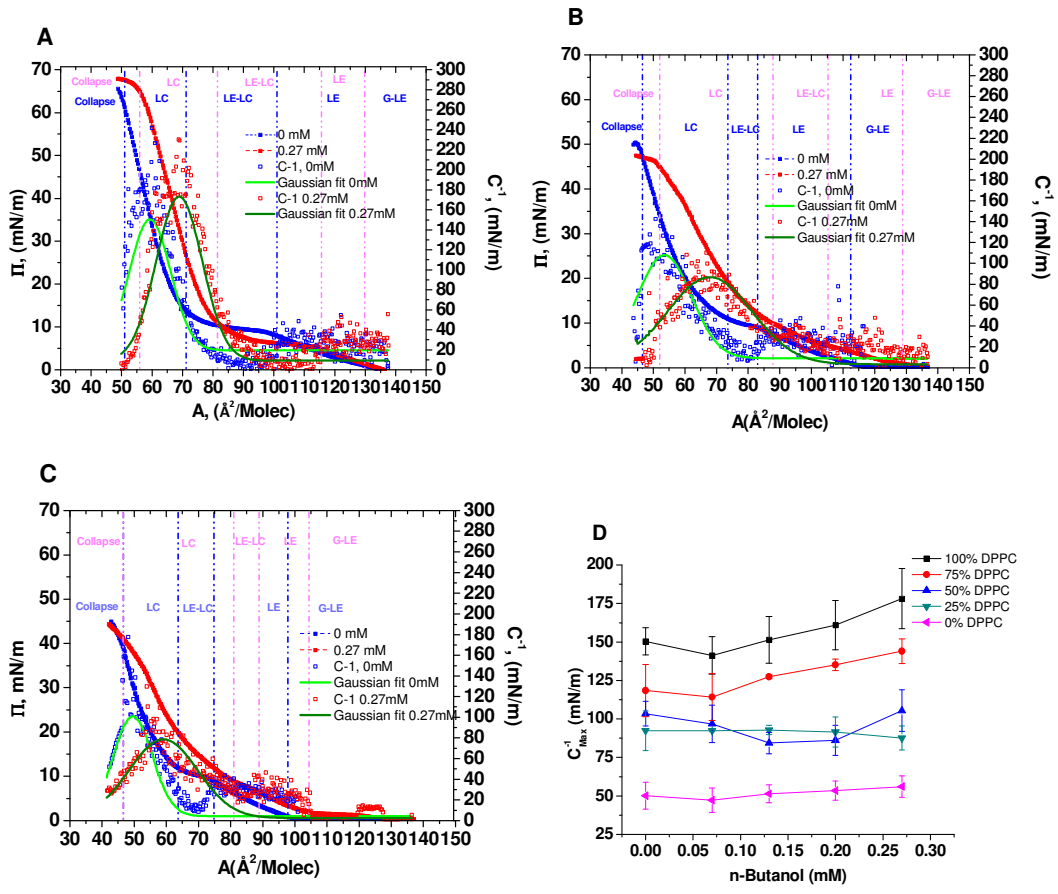

Figure 3.3.*Π–A* isotherms at 25 $^{o}$C with corresponding elastic moduli ($C^{-1}$) and phase diagrams of DPPC/DOPC monolayers at (A) 3:1, (B) 1:1, and (C) 1:3 DPPC:DOPC ratios for 0 mM and 0.27 mM n-butanol in the subphase. (D) Maximum elastic modulus as a function of n-butanol concentration and DPPC:DOPC ratio.

Ethanol partitioning into PC monolayers has been shown to reduce hydrogen-bonding between water and PC headgroups.[34]n-Butanol presumably has the same effect on PC monolayers but, due to its longer tail, exhibits greater van der Waals attraction between neighboring lipid tails. The combined effects of lipid dehydration, n-butanol hydrogen bonding with PC headgroups, and van der Waals attraction between PC tails may explain the increases in $C_{Max}^{-1}$ when DPPC was the main component.

**4. 3. Monolayer structure and n-butanol partitioning**

Additional analysis was conducted on the *Π–A* isotherms in the region between 25 mN/m and 35 mN/m where *Π* was a linear function of $A_o$ for DPPC:DOPC ratios from 1:0 to 1:3 ($R^2$> 0.99). At these pressures DPPC was in the *LC* phase. The DPPC hydrocarbon tilt angle normal to the air/water interface, $\theta$, was determined from $\cos\theta = A_{min}/A_o$ where $A_{min}$ is the minimum area occupied by the two carbon tails (40 Å$^2$).[35,36] The tilt angle decreased from 34.5$^{o}$ to 29.3$^{o}$ over this surface pressure range due to compression or increased packing. These values are in good agreement with previous work.[37,38] In contrast, DOPC was untilted in the *LE* phase. With *LE-LC* coexistence, DPPC tilt increased the gap between *LC* domains and the *LE* phase. This effectively increased the area for n-butanol partitioning and accumulation at *LE/LC* interfaces, which was further quantified by calculating the n-butanol mole fraction ($X_b$) in the monolayers based on a simple space-filling model. $X_b$ was determined as

$0.785(A_{o,b}–A_o)/A_b$ where $A_{o,b}$ is the area per lipid with n-butanol, $A_b$ is the area per n-butanol molecule (18 $Å^2$),[4] and 0.785 is the circular two dimensional packing factor. $X_b$ is shown in Figure 3.4 as function of $X_{DOPC}$ and $\Pi$ at n-butanol concentrations of 0.13 mM and 0.27 mM. For DPPC and 3:1 DPPC:DOPC$X_b$ was not greatly affected by surface pressure. In contrast, $X_b$ decreased with surface pressure at 1:1 and 1:3 DPPC:DOPC, see Figure 3.4. This analysis indicates that n-butanol was expelled or 'squeezed out' of the monolayers upon compression at higher DOPC concentrations. It also depicts the ability for DOPC to accommodate n-butanol with less lipid expansion ($A_o$) relative to DPPC.

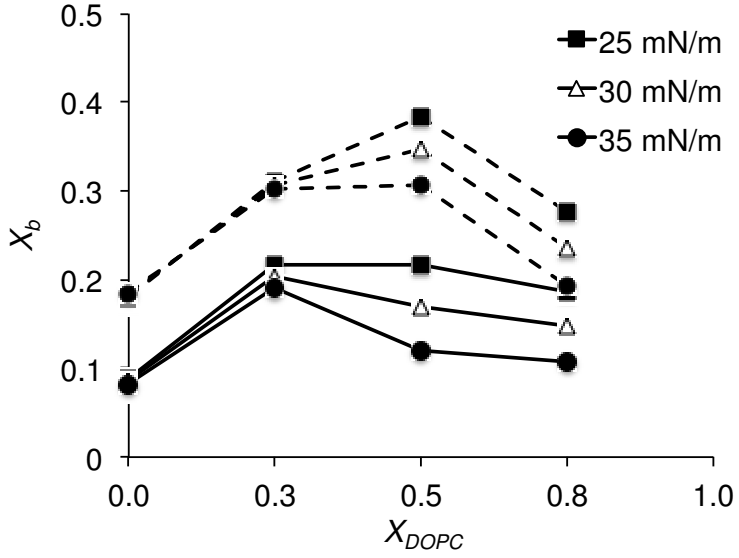


Figure 3.4.Mole fraction of n-butanol ($X_b$) in DPPC/DOPC monolayers as a function of DOPC mole fraction and surface pressure.$X_b$ was calculated at n-butanol concentrations of 0.13 mM (solid lines) and 0.27 mM (dashed lines).

The effects of n-butanol on DPPC and DPPC/DOPC are shown schematically in Figure 3.5 for *LC* or *LC/LE* monolayers ($\Pi$ ~30 mN/m), respectively. In case of DPPC without n-butanol at 25°C, the hydrocarbon chains of DPPC were packed in an all-trans conformation and tilted at the interface. When n-butanol was added it

adsorbed near the PC headgroups at the air/water interface. Inferred by simulation results for ethanol by Patra et al.,[5] n-butanol hydrogen bonded with the ester groups in the glycerol backbone of the lipids and reduced the amount of water bound to the lipid headgroups. n-Butanol adsorption increased the lipid area per molecule and, at high concentrations, increased the elastic moduli. In the case of DOPC, n-butanol adsorption presumably occurred in a similar fashion, but the effect on the *Π-A* behavior was less pronounced than for DPPC due to the larger interfacial voids caused by DOPC tail kinking. In the case of mixed DPPC/DOPC monolayers, n-butanol accumulated at the interface between *LE* and *LC* phases to reduce tail mismatch between DPPC and DOPC. *LC* domain size analysis by fluorescence microscopy suggests that this accumulation reduced line tension. However, additional work is needed to confirm this argument and determine whether n-butanol also affects the dipole density difference between the two phases.

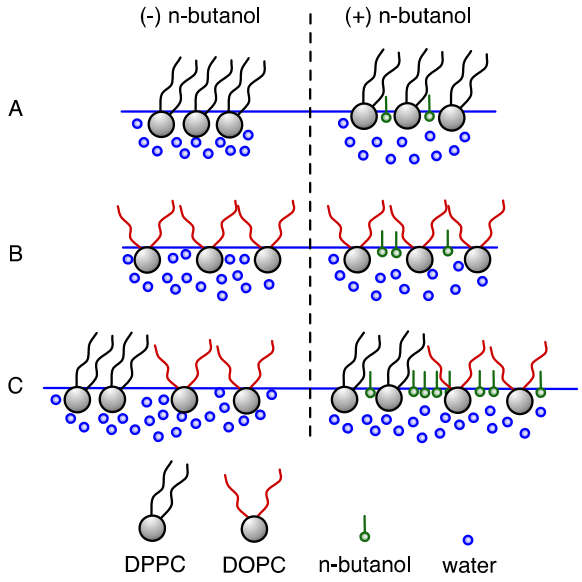


Figure 3.5. Schematicdepicting the partitioning behavior of n-butanol at 25 $^{o}$C into (A) DPPC, (B) DOPC, and (C) DPPC/DOPC monolayers at high surface pressure.

## 5. Conclusions

To the author's knowledge this is the first study depicting the effects of n-butanol partitioning on heterogeneous monolayers with coexisting *LE* and *LC* phases arising from a mixture of unsaturated and saturated lipids, respectively. Approaches such as this provide new insight into how complex, multicomponent cellular membranes are adapted to elevated alcohol concentrations. The effects of n-butanol on monolayer structure are not simply the cumulative effects on saturated + unsaturated lipids. Rather, the presence of both lipids exacerbates the effects of n-butanol due to dissimilarities between lipid tail structure and phase coexistence. This work suggests that n-butanol partitioning into monolayers increases with unsaturated lipid concentration and, more significantly, with increases in the total perimeter between *LE* and *LC* phases. Consistent with theories for homeoviscous adaptation, the unsaturated lipid (DOPC) accommodated high n-butanol concentrations without significant expansion. However, lipid packing based on saturated to unsaturated lipid ratios represents a new variable for understanding alcohol fluidization, particularly in heterogeneous membrane with coexisting phases.

## Supporting Information

Additional supporting informationincludes *Π–A* isotherms of DPPC/DOPC monolayers at different 1:0 and 0:1 DPPC:DOPC(Figure D.2) and corresponding phase diagrams (Figure D.3).

## 6. References


(1) Weber, F. J.; de Bont, J. A. *Biochimica Et Biophysica Acta***1996**, *1286*, 225.

(2)Adachi, T.; Takahashi, H.; Ohki, K.; Hatta, I. *Biophysical Journal***1995**, *68*, 1850.

(3) Cantor, R. S. *J. Phys. Chem. B***2001**, *105*, 7550.

(4)Ly, H. V.; Longo, M. L. *Biophysical Journal***2004**, *87*, 1013.

(5)Patra, M.; Salonen, E.; Emma, T.; llpo, V. *Biophys. J.***2006**, *90*, 1121.

(6)Holte, L. L.; Gawrisch, K. *Biochemistry***1997**, *36*, 4669.

(7)Marquês, J. T.; Viana, A. S.; De Almeida, R. F. M. *Biochim. Biophys. Acta***2011**, *1808*, 405.

(8) Terama, E.; Ollila, O. H. S.; Salonen, E.; Rowat, A. C.; Trandum, C.; Westh, P.; Patra, M.; Karttunen, M.; Vattulainen, I. *J. Phys. Chem. B***2008**, *112*, 4131.

(9)Vierl, U.; Löbbecke, L.; Nagel, N.; Cevc, G. *Biophys. J.***1994**, *67*, 1067.

(10)Kranenburg, M.; Vlaar, M.; Smit, B. *Biophys. J.***2004**, *87*, 1596.

(11)Zhang, F.; Rowe, E. S. *Biochemistry***1992**, *31*, 2005.

(12)Vanegas, J. M.; Contreras, M. F.; Faller, R.; Longo, M. L. *Biophysical Journal***2012**, *102*, 507.

(13)Kurniawan, Y.; Venkataramanan, K. P.; Scholz, C.; Bothun, G. D. *J. Phys. Chem. B***2012**, *116*, 5919.

(14)Herold, L. L.; Rowe, E. S.; Khalifah, R. G. *Chem. Phys. Lipids***1987**, *43*, 215.

(15)Ho, C. J.; Stubbs, C. D. *Biochemistry***1997**, *36*, 10630.

(16)Krill, S. L.; Knutson, K.; Higuchi, W. I. *J. Controll. Release***1993**, *25*, 31.

(17)Löbbecke, L.; Cevc, G. *BBA. Biomembranes***1995**, *1237*, 59.

(18)Ly, H. *Biophys. J.***2004**, *87*, 1013.

(19)Pillman, H. A.; Blanchard, G. J. *J. Phys. Chem. B***2010**, *114*, 3840.

(20)Reeves, M. D.; Schawel, A. K.; Wang, W.; Dea, P. *Biophys. Chem.***2007**, *128*, 13.

(21) Rowe, E. S.; Zhang, F.; Leung, T. W.; Parr, J. S.; Guy, P. T. *Biochemistry***1998**, *37*, 2430.

(22)Huffer, S.; Clark, M. E.; Ning, J. C.; Blanch, H. W.; Clark, D. S. *Appl. Environ. Microb.***2011**, *77*, 6400.

(23)Abramoff, M. D.; Magelhaes, P. J.; Ram, S. J. *Biophotonics Intl.***2004**, *11*, 36.

(24)Ma, G.; Allen, H. C. *Langmuir***2006**, *22*, 5341.

(25)Sabatini, K.; Mattila, J. P.; Kinnunen, P. K. J. *Biophysical Journal***2008**, *95*, 2340.

(26)Wittenberg, N. J.; Zheng, L.; Winograd, N.; Ewing, A. G. *Langmuir***2008**, *24*, 2637.

(27)Yano, Y. F. *Journal of Colloid and Interface Science***2005**, *284*, 255.

(28)Dickey, A. N.; Faller, R. *Biophysical Journal***2007**, *92*, 2366.

(29)Lee, D. W.; Min, Y. J.; Dhar, P.; Ramachandran, A.; Israelachvili, J. N.; Zasadzinski, J. A. *Proceedings of the National Academy of Sciences of the United States of America***2011**, *108*, 9425.

(30)Duncan, S. L.; Larson, R. G. *Biophysical Journal***2008**, *94*, 2965.

(31)Panda, A. K.; Vasilev, K.; Orgeig, S.; Prestidge, C. A. *Materials Science & Engineering C-Materials for Biological Applications***2010**, *30*, 542.

(32)Lucero, A.; Nino, M. R. R.; Gunning, A. P.; Morris, V. J.; Wilde, P. J.; Patino, J. M. R. *Journal of Physical Chemistry B***2008**, *112*, 7651.

(33)Weis, M.; Kopani, M.; Jakubovsky, J.; Danihel, L. *Applied Surface Science***2006**, *253*, 2425.

(34)Brezesinski, G.; Muller, H. J.; Toca-Herrera, J. L.; Krustev, R. *Chem. Phys. Lipids***2001**, *110*, 183.

(35)Kaganer, V. M.; Mohwald, H.; Dutta, P. *Reviews of Modern Physics***1999**, *71*, 779.

(36)Bringezu, F.; Ding, J.; Brezesinski, G.; Zasadzinski, J. A. *Langmuir***2001**, *17*, 4641.

(37)Yun, H.; Choi, Y. W.; Kim, N. J.; Sohn, D. *Bulletin of the Korean Chemical Society***2003**, *24*, 377.

(38)Tu, K.; Tobias, D. J.; Blasie, J. K.; Klein, M. L. *Biophysical Journal***1996**, *70*, 595.

# CHAPTER 4

## Role of Ionic Strength on n-Butanol Partitioning intoAnionic Dipalmitoyl Phosphatidylcholine/PhosphatidylglycerolVesicles

Yogi Kurniawan[1], Keerthi P.Venkataramanan[2], Mar Piernavienja[4], Carmen Scholz[3], and Geoffrey D. Bothun[1,*]

[1]Department of Chemical Engineering, University of Rhode Island, 16 Greenhouse Rd, Kingston, RI

[2]Biotechnology Science and Engineering program, University of Alabama in Huntsville, 301 Sparkman Dr, Huntsville, AL

[3]Department of Chemistry, University of Alabama in Huntsville, 301 Sparkman Dr, Huntsville, AL

[4]Department of Chemical and Materials Engineering, University of Alabama in Huntsville, 301 Sparkman Dr, Huntsville, AL

*Corresponding author: bothun@egr.uri.edu (email); 401-874-9518 (tel)

Prepared for submission to Journal of Physical Chemistry B

## 1. Abstract

Bacteria adjust their membrane lipid composition to counteract the fluidizing effects of alcohol and to adapt to elevated alcohol concentrations during fermentation. Bacterial membranes are rich in anionic phosphatidylglycerols (PG), but little is known regarding alcohol partitioning into anionic membranes, particularly for n-butanol. This work examines the effects of lipid charge on n-butanol partitioning into anionic membrane vesicles composed of dipalmitoylphosphatidylcholine (DPPC) anddipalmitoylphosphatidylglycerol (DPPG) in the absence and presence of salt. Above 0.13 M n-butanol the membraneswere interdigitated irrespective of DPPG or salt concentration, consistent with previous results for neutral membranes such as DPPC. Increasing salt concentration let to greater n-butanol partitioning in DPPC membranes and caused aggregation/fusion. However, aggregation/fusion was prevented with increasing DPPG concentration (i.e. increasing membrane charge) and small vesicles were observed. The results suggest that n-butanol partitioning, and subsequent changes in membrane and vesicle structure, was driven by a balance between the 'salting-out' of n-butanol, interlipid electrostatic interactions, and interfacial cation binding and hydration. This is the first study to our knowledge to examine the effects of n-butanol partitioning on model cell membranes composed of negatively charged lipid in the presence of salts.

## 2. Introduction

The partitioning of n-butanol into zwitterionic lipid bilayer membranes (e.g. dipalmitoylphosphatidylcholine or DPPC) in non-electrolyte solutions has been well studied.[1-3]At low n-butanol concentration(< 0.13M), n-butanol partitioning near the lipid headgroups and expands the lateral area of the membrane, reducing membrane surface tension and decreasing lipid ordering. At high n-butanol concentrations (> 0.13 M),n-butanol partitioning increases and promotes lipid interdigitation.[1-4]Interdigitationby short chain alcohols can induce aggregation and fusion of zwitterionic lipid bilayers when they are dispersed in an electrolyte solution at neutral pH.[5,6] While the partitioning of short chain alcohols into saturated phosphatidylcholine (PC) lipids is well known, n-butanol partitioning into saturated anionic phosphatidylglycerol (PG) lipids and the effects of electrolyte on partitioning and membrane structure are unknown.

n-Butanol is a biorefinery key platform chemical that can be used to produce polymers and resins.[7] n-Butanol also can be used for a viable biofuel.[8] However, the lipophilic solvent n-butanol is toxic during fermentation, destabilizing cell membranes and disrupting membranecomponents.[9]Bacteria, which generally have negatively charged membranesand exist in electrolyte media, respond to butanol toxicity by altering their lipid composition to compensate the fluidizing effects of butanol.[10] Studying the effects of n-butanol and electrolytes on charged lipids membranes is important to understand bacterial response mechanism.

n-Butanol partitioning can restructure lipid molecules resulting in changes inPC lipid phase behavior such as a decrease in the pretransition ($T_p$)and melting

temperatures ($T_m$), which reflect tilted gel to rippled gel ($L_{\beta'} \rightarrow P_{\beta'}$) and rippled gel to fluid ($P_{\beta'} \rightarrow L_{\alpha}$) phase transitions, respectively.[1-3]Previous resultshave shown that above 0.13 M (10 g/l),n-butanol can promote the transition from a gel to an interdigitated gel ($L_{\beta'} \rightarrow L_{\beta I}$)phase.[1,3]This behavior can persist even when DPPC is present as domains within a continuous unsaturated lipid phase; however, the presence of unsaturated lipids can reduce or even eliminate interdigitation at high concentrations.[11,12]

In addition to lipid composition, electrolytes play a central role in determining lipid membrane phase behavior and agglomeration in vesicle dispersions.[13-17] With increasing electrolyte concentration from 0 to 3M, $T_p$and$T_m$of DPPC phase transition increases due to ion binding to PC headgroups.[6] Komatsu et al show that short-chain alcohols; such as ethanol, in electrolyte solutions are able to induceinterdigitation andvesicle aggregation,causing bilayer mixing between adjacent membranes and leadingto fusion.[18] Comparatively, the effect of electrolytes on n-butanol partitioning into PG lipids is unknown. Manyes et al reported that cations in electrolyte solution adsorb ontoanionicPG headgroups,enhancing the mechanical stability of the lipid membrane. Their results showed that dipalmitoylphosphatidylglycerol (DPPG) membranes have stronger mechanical stability in the presence of electrolytesthan DPPC.[19]

To our knowledge the effects of ionic strength on n-butanol partitioning into charged or neutral lipid membranes has not been examined. In this study, large unilamellar vesicles (LUVs) composed of DPPC/DPPG in the absence and the presence of electrolyte solution (1x and 10x Phosphate-Buffered Saline,PBS) were

used as a model bacterial membrane system to investigate n-butanol partitioning and membrane phase behavior at n-butanol concentration up to 0.27 M (20 g/l). The DPPC:DPPG molar ratio was varied from 1:0 to 1:3 to study membranes with different anionic surface charge densities and, hence, different intermolecular interactions that will impact n-butanol partitioning and membrane structure. DPPC/DPPG represents a model bacterial membrane, which are known to have high PG content (e.g. 20-30% in *Clostridium* species).[20]

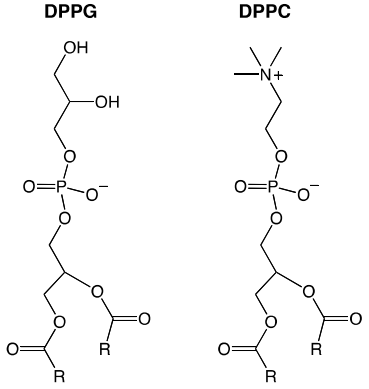


Figure 4.1.Molecular structures of DPPG and DPPC. The alkyl tail, R, is $(CH_2)_{14}CH_3$.

**3. Experimental**

1,2-Dipalmitoyl-*sn*-glycero-3-phosphatidylcholine (DPPC, >99% purity) and 1,2-dipalmitoyl-*sn*-glycero-3-phosphatidylglycerol (DPPG, >99% purity) were purchased from Avanti Polar Lipids (Alabaster, AL) and used without further purification (Figure 4.1).HPLC grade n-butanol and chloroform were purchased from Fisher Scientific. Deionized (DI) ultrafiltered water was obtained from a Millipore Direct Q-3 purifier.PBS at 10x concentration and pH 7.4 was prepared with 1.37 M NaCl, 27 mM KCl, 100 mM $Na_2HPO_4$, and 18 mM $KH_2PO_4$.PBS at 1x concentration was prepared by diluting with distilled water and readjusting to pH 7.4.

### 3.1.Vesicle preparation

LUVs were prepared by thin-film hydration method.[21] DPPC and DPPG were dissolved and mixed in chloroform to achieve 1:0, 3:1, 1:1, and 3:1 DPPC:DPPG ratios. A stream of nitrogen was used to evaporate the chloroform and then the samples were dried under vacuum for at least 30 min. The dry films were then hydrated with 3 ml of DI water or PBS solution to yield a total lipid concentration of 10 mM as a vesicle solution sample stock. Vesicle suspensions were formed by a short sonication at 50 $^{o}$C using bath ultrasonicator (Branson, Danbury, CT)followed by extrusion through double-stacked polycarbonate membranes with 200 nm pore diameters.Vesicles were diluted to 0.5 mM for analysis. n-Butanol was added to the samples at concentrations from 0.07 M to 0.27 M. The samples were briefly vortexed and stored for 30 min after n-butanol addition before further processing or analysis.

### 3.2. Differential scanning calorimetry (DSC)

Lipid bilayer phase behavior in the DPPC/DPPG vesicles was analyzed by DSC (TA Instruments Nano DSC). Samples were equilibrated at 25 $^{o}$C, and the cell chamber was sealed and pressurized to 3 atm under nitrogen. Samples were analyzed by heating between 25 $^{o}$C and 50 $^{o}$C at a rate of 1 $^{o}$C/min. Pretransition temperature, $T_p$, melting temperature, $T_m$, and melting enthalpy, $\Delta H_m$, were determined using the Universal Analysis software. The melting temperature was taken at maximum peak height.

The membrane/water n-butanol partitioning coefficient, $K_P$, was calculated from DSC results as:

$$\Delta T_m = -\frac{RT_{m,o}^2}{\Delta H_m}\left(\frac{C_b K_P}{C_w + C_l}\right) \qquad (1)$$

where$\Delta T_m$ is the measured change in melting temperature ($T_m - T_{m,0}$), $R$ is the gas constant, $T_{m,0}$ is the melting temperature of DPPC without n-butanol, and $\Delta H_m$ is the lipid melting enthalpy. $C_b$,$C_w$, and $C_l$ are the n-butanol, water, and lipid molar concentrations, respectively.

### 3.3. High performance liquid chromatography (HPLC)

Sample preparation began by taking liposomes without n-butanol and liposomes with n-butanol, and centrifuging the suspensions at 10,000 rpm for 30 min at 4 $^{o}$C (Megafuge 16 R, Germany). The aqueous supernatant was separated from the liposomes and analyzed by HPLC for n-butanol concentration. HPLC was conducted with a resin-based column (Aminex HPX-87H, Bio-Rad, CA) and a refractive index detector (Varian, CA) using with 0.5 mM $H_2SO_4$ as the mobile phase. Standard calibration curves were prepared with aqueous n-butanol solutions containing 0.07 M to 0.27 M n-butanol ($R^2$ = 0.994).

The partition coefficient, $K_P$, was calculated as

$$K_P = \frac{a_b^m}{a_b^w} = \frac{\gamma_b^m x_b^m}{\gamma_b^w x_b^w} \qquad (2)$$

where$a_b$, $\gamma_b$, and $x_b$ are the activity, activity coefficient, and mole fraction of n-butanol, respectively, and the superscript *m* denotes the membrane phase and *w* the water phase. n-Butanol mole fractions were determined directly based on a mole balance.

### 3.4. Dynamic Light Scattering (DLS)

Average size and zeta potential of vesicles at different DPPC:DPPG ratios and n-butanol concentration were measured by Dynamic Light Scattering (DLS) with a Zetasizer Nano ZS instrument (Malvern Instruments Ltd.). This instrument is equipped with 5mW He-Ne laser operating at 633nm. A quartz cuvette was used to

determine the vesicle hydrodynamic diameter a folded capillary cell was used to measure the vesicle zeta potential. The cells were sealed with a cap and secured in the sample chamber of the instrument. DLS was conducted in backscattering mode at an angle of 173$^{o}$ and zeta potential was measured based on laser Doppler electrophoresis.

## 4. Results

### 4.1. DSC studies of membrane phase behavior

DSC was used to investigate the phase behavior of DPPC and DPPC/DPPG vesicles (Figure 4.2). Results for $T_m$ in DI water and 1x PBS were consistent with previous results depicting lipid interdigitation where $T_m$ decreases for the $P_{\beta'} \rightarrow L_\alpha$ transition until a critical n-butanol concentration is reached (0.13 M; Figure 4.2A, B). Above this critical concentration $T_m$ does not change with increasing n-butanol concentration (plateaus), reflecting lipid interdigitation ($L_{\beta I} \rightarrow L_\alpha$). At these conditions the entirety of the bilayers, DPPC and DPPG, were interdigitated ($L_{\beta I}$) confirming that low monovalent salt concentrations (near 0.1 M) have little effect on lipid phase behavior[16]and that DPPG repulsion between inner and outer leaflets was not strong enough to prevent interdigitation.

The trends in $T_m$ are less clear for 10x PBS. In the absence of n-butanol DPPC was not affected by this high salt condition, but $T_m$ increased with DPPG concentration up to 43 $^{o}$C at 1:3 DPPC:DPPG (Figure 4.2C). This increase reflects lipid dehydration and headgroup charge bridging to due to cation binding, which increases tail-tail van der Waals attraction. In the presence of n-butanol there was a near linear decrease in $T_m$ with increasing n-butanol concentration. Results for DPPC

show a modest biphasic effect above 0.13 M indicative of interdigitation, but this feature is less clear with DPPG present.

Results for the $T_p$ of DPPC at all salt concentrations were also consistent with interdigitation where the $L_{\beta'} \rightarrow P_{\beta'}$ transition is replaced by the $L_{\beta'} \rightarrow L_{\beta I}$ transition at 0.13 M n-butanol. Increasing DPPG concentration reduced $T_p$ in DI water and 1x PBS, and eliminated it at 10x PBS. More significantly, the presence of DPPG completely prevented the $L_{\beta'} \rightarrow P_{\beta'}$ transition in the presence of n-butanol.

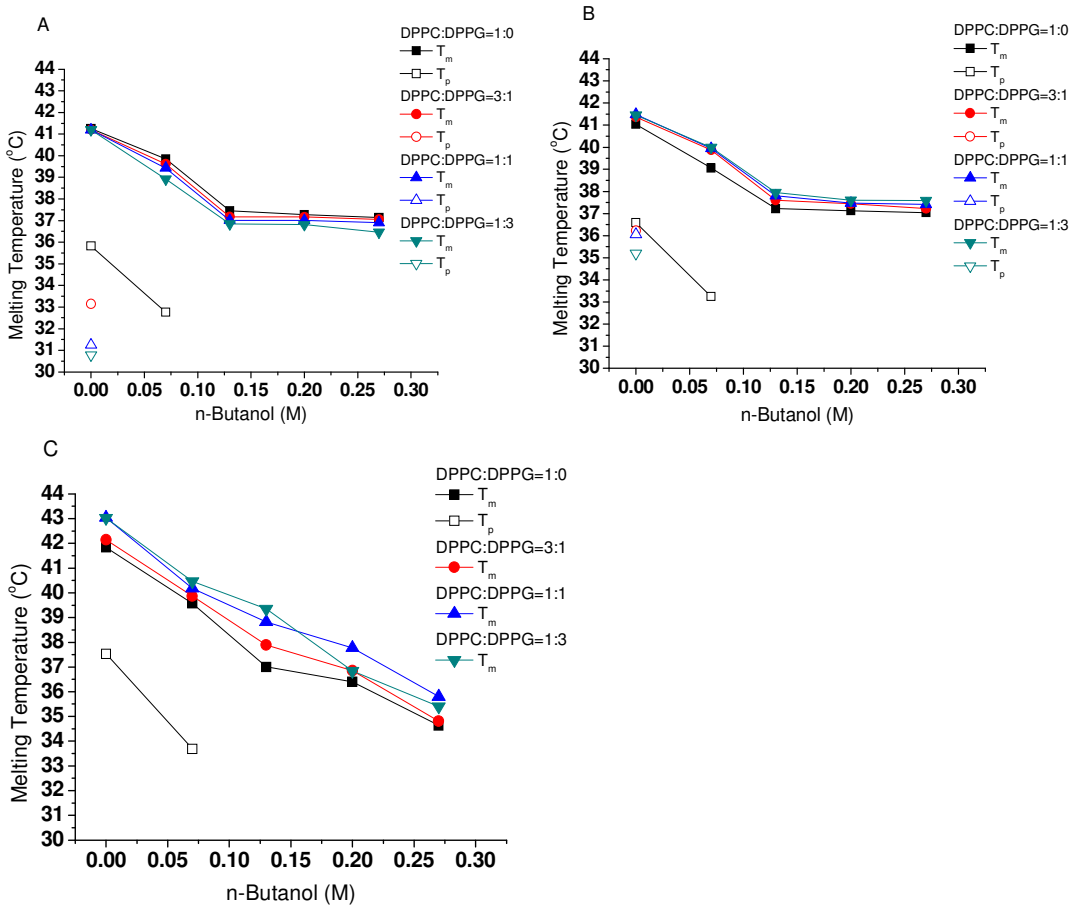


Figure 4.2. DSC membrane phase behavior of vesicles in(A) DI water, (B) 1x PBS, (C) 10x PBS at DPPC:DPPG ratios of (■) 1:0, (●) 3:1, (▲) 1:1, and (▼) 1:3 as a function of n-butanol concentration. Melting temperatures ($T_m$) are shown as filled symbols and pretransition temperatures ($T_P$) are shown as unfilled symbols.

Melting enthalpy, $\Delta H_m$, provides additional evidence of interdigitation and has been shown to increase above the n-butanol interdigitation concentration for the $L_{\beta I} \rightarrow L_\alpha$ transition. Results for $\Delta H_m$ clearly show DPPC interdigitation in DI water and PBS; and the trends observed for DPPC/DPPG also suggest interdigitation in DI water and 1x PBS (Figure 4.3). At 10x PBS it is more difficult to discern interdigitation when DPPG is present. At 1:3 DPPC:DPPG there is a reduction in $\Delta H_m$above 0.13 M n-butanol consistent with the presence of small unilamellar vesicles (SUVs) which exhibit a lower melting enthalpy (~20%) relative LUVs.[22]

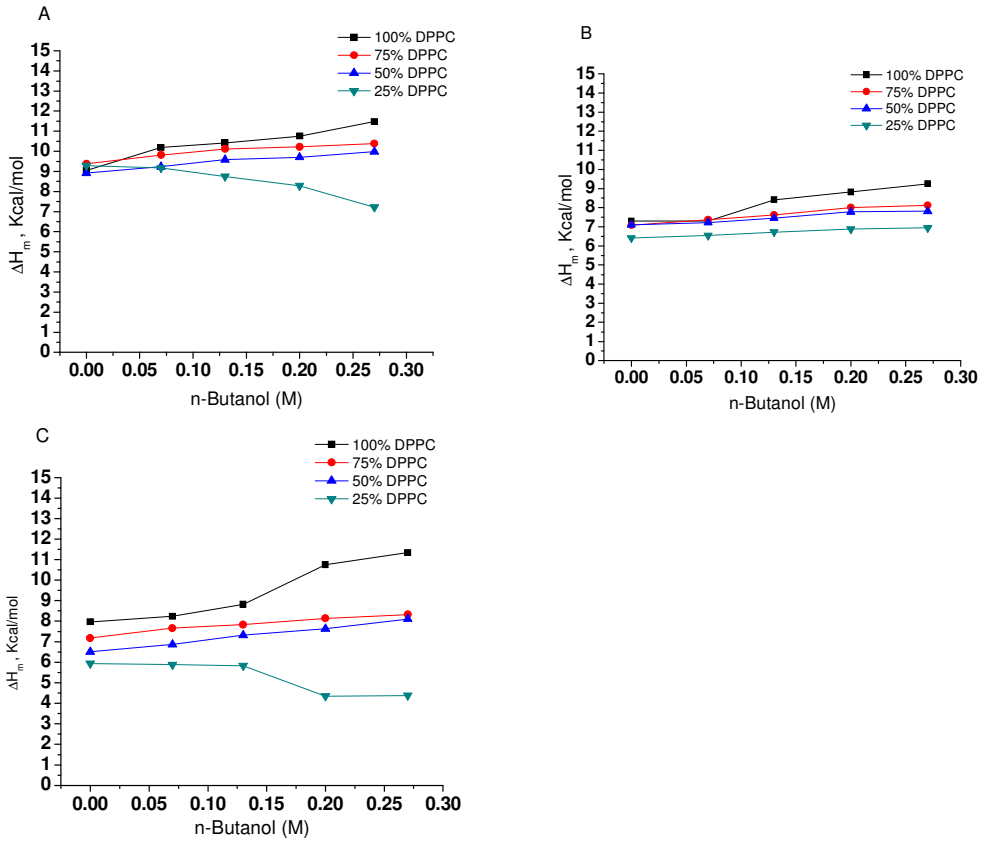


Figure 4.3. Melting enthalpy as a function of n-butanol concentration in (A) DI water, (B) 1x PBSand (C) 10x PBSat DPPC:DPPG ratios of (■) 1:0, (●) 3:1, (▲) 1:1, and (▼) 1:3.

### 4.2. Partitioning of n-butanol into membranes ($K_p$)

n-Butanol partitioning coefficients,$K_p$, were determined from DSC (equation 1) and by HPLC (Figure 4.4). It should be noted that $K_p$ from DSC were calculated based on the linear portion of the $T_m$ graphs before interdigitation while $K_p$ by HPLC was determined below and above the n-butanol interdigitation concentration (0.13 M). Calculated and measured values of $K_p$ for gel phase ($L_{\beta'}$) DPPC in DI water (71 and 141, respectively) were in general agreement with reported values.[23] Collectively, trends for $K_p$ from DSC and HPLC were consistent and showed that (i) $K_p$ increased for DPPC with increasing salt concentration (ca. 2-fold from DI water to 10x PBS), (ii) $K_p$ increased with DPPG concentration in DI water, and (iii) $K_p$ decreased within increasing DPPG concentration in PBS (ca. 2 to 3-fold from 1:0 to 1:3 DPPC:DPPG at 10x PBS). These are the first reported results for n-butanol partitioning into anionic lipid membranes and show that increasing anionic lipid content reduces $K_p$ in the presence of electrolyte.

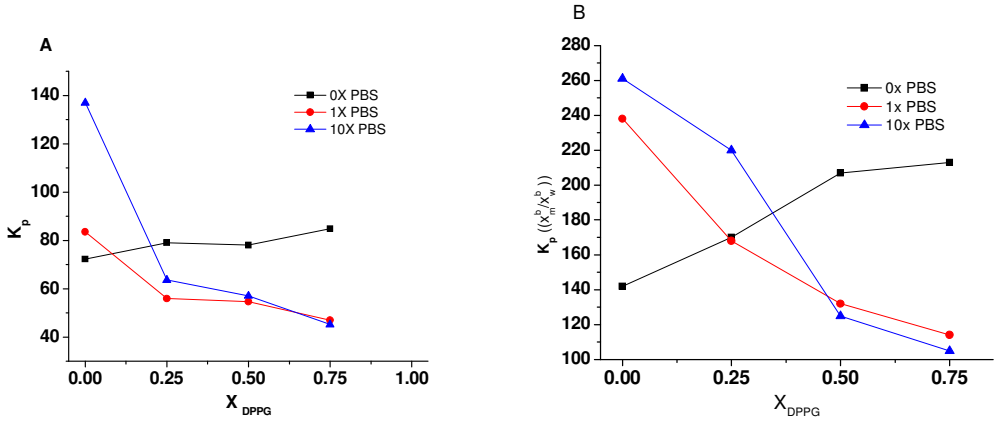


Figure 4.4. (A) n-Butanol partition coefficient, $K_p$, (A) calculated from DSC results and (B) measured by HPLC as a function of DPPG mole fraction and PBS concentration at 0.27 M n-butanol.

Increases in $K_p$ with PBS concentration (i) can be partially explained by the 'salting out' effect of cations on n-butanol water solubility.[24] ASPEN simulation was conducted to determine the effect of $Na^+$ and $K^+$ on the activity coefficient of n-butanol in water (Figure F.1). $Na^+$ reduced the activity coefficient by as much as 37% at NaCl concentrations representing 10x PBS. The effect of $K^+$ was less pronounced. Considering equation 2 for $K_p$, this reduction may explain in part why butanol partitioning increased with PBS concentration assuming that the activity coefficient of n-butanol in the membrane was unchanged. However, trends observed with DPPG concentration are still unclear and will be discussed in more detail below.

**4.3. Vesicle hydrodynamic size**

The effect of DPPG and electrolyte concentration on vesicle size are shown in Figure 4.5 at 1:0 and 1:3 DPPC:DPPG. The average $r_h$ of DPPC vesicles increased with n-butanol interdigitation. For complete interdigitation $r_h$ increases by a factor of $\sqrt{2}$ as the membrane expands laterally. This condition was observed for DPPC in DI water and PBS at 0.27 M n-butanol (the measured increase in $r_h$ from 0 M to 0.27 M n-butanol was $\sim\sqrt{3}$). In contrast, there was a 3-fold increase in $r_h$ in 10x PBS. Increases in $r_h$ for DPPC correlate well with increases in the partitioning coefficients when PBS was used.

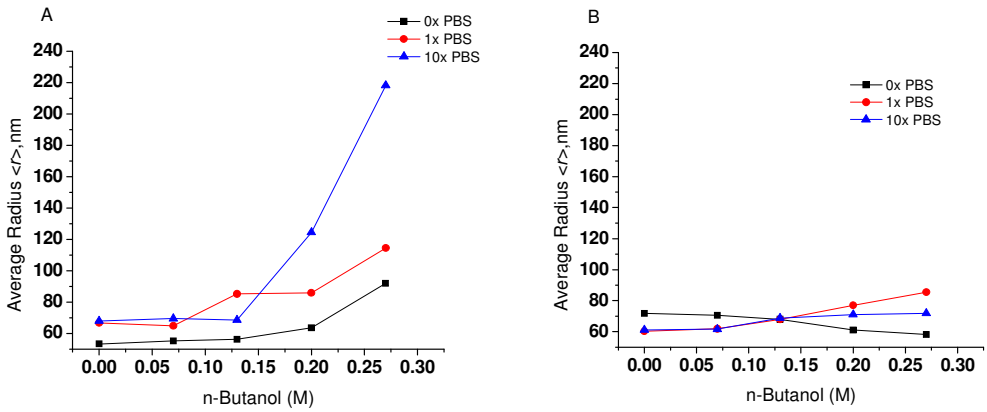


Figure 4.5. Average size of DPPC/DPPG vesicles at DPPC:DPPG ratios of (A) 1:0 and(B) 1:3 as a function of n-butanol and PBSconcentration.

The large increase in DPPC $r_h$ with n-butanol concentration in 10x PBS can be attributed to vesicle aggregation and fusion[18] aided by cation adsorption. n-Butanol partitioning displaced headgroup-bound water molecules that normally yield an repulsive inter-vesicle force that prevents aggregation. $Na^+$ and $K^+$ did not perturb the hydration of the bound water layer, as previously reported,[25] but rather reduced the activity coefficient of n-butanol in water and increased the concentration of n-butanol in the membranes (as discussed for $K_p$). It is unlikely that cation adsorption played a role DPPC vesicle aggregation or fusion.[26]

Not surprisingly, cation adsorption did influence vesicle size in DPPC/DPPG vesicles as $Na^+$ and $K^+$ bound to anionic DPPG. This is clearly depicted by zeta potential measurements at 1:3 DPPC:DPPG in DI water and 10x PBS (Figure F.2). Cation adsorption reduced the increase in $r_h$ with increasing n-butanol concentration in proportion to the concentration of DPPG present within the vesicles (DLS results for 3:1 and 1:1 DPPC:DPPGare shown in Figure F.3). At 1:3 DPPC:DPPG small interdigitated vesicles were observed and with no evidence of aggregation or fusion despite inter-vesicle charge screening at high PBS concentration. Closer examination

of the intensity distribution as a function of $r_h$ (Figure F.4) reveals a shoulder at $r_h$ ~10 nm consistent with DSC results depicting the presence of SUVs at the highest n-butanol concentration (0.27 M).

**5. Discussion**

Interdigitated structures have been studied intensively for PC/short alcohol systems.[2,3,16] However, the effects of electrolyte and charged lipids on alcohol partitioning and interdigitation have not been reported. Results from this work are summarized in Figure 4.6. DPPC/DPPG membranes were interdigitated in DI water and 1x PBS (low salt) below the lipid melting temperature at all DPPC:DPPG ratios despite the fact that increasing DPPG concentration reduced n-butanol partitioning coefficient in PBS. This result differs from previous reports where n-butanol partitioning increased when DPPC membranes transitioned from gel ($L_{\beta'}$) to interdigitated gel ($L_{\beta I}$) phases.[11,23] The membranes were also interdigitated in 10x PBS (high salt), but in this case interdigitated DPPC vesicles exhibited aggregation and fusion, and 1:3 DPPC:DPPG exhibited a mixture of interdigitated SUVs and LUVs. At 3:1 and 1:1 DPPC:DPPG vesicle size increased modestly with n-butanol concentration despite being interdigitated.

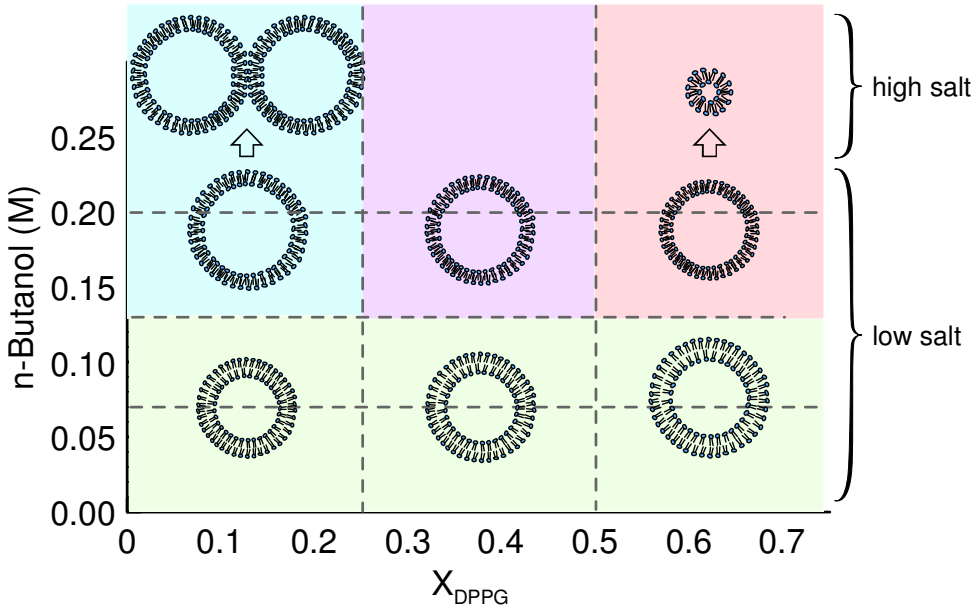


Figure 4.6. Phase diagram at 25 °C for DPPC/DPPG vesicles as a function of n-butanol concentration and DPPG mole fraction ($X_{DPPG}$). Structural transformations associated with increasing salt concentration (low salt to high salt) are shown.

Based on these results, DPPG played a complicated role in influencing n-butanol partitioning and vesicle structure. It did not, however, prevent interdigitation based on the conditions used in this study. DPPG electrostatically stabilized interdigitated vesicles and prevented aggregation and fusion. Interestingly, this stabilization appeared to persist in 10x PBS where the total electrolyte concentration was 1.37 M (predominately NaCl). One would expect that increasing salt concentration would promote greater DPPG packing, and hence more rigid bilayer structures, by screening electrostatic repulsion between PG headgroups. The emergence of SUVs at 1:3 DPPC:DPPG and high n-butanol concentration suggest that n-butanol drove this LUV-SUV shift. Increasing DPPG concentration coupled with n-butanol at the membrane/water interface may have led to higher spontaneous curvature

that the formation of DPPG-rich interdigitated vesicles or micelles as previously observed for bile salts.[27] It is unclear why this did not occur at low salt conditions.

Regarding n-butanol partitioning, DPPG appears to influence $K_p$ through collective hydration and electrostatic interactions. PG headgroups mimic water and exhibit increased solvation and hydrogen bonding capacity compared to PC.[28] Considering that n-butanol displaces interfacial water and itself hydrogen bonds to lipid headgroups, it is expected that $K_p$ would decrease with DPPG concentration. This was observed in PBS and total salt concentration was not a significant factor at or above $X_{DPPG} = 0.5$. At $X_{DPPG} = 0.25$, which is representative of PG content in bacterial membranes, there is discrepancy between $K_p$ values determined by DSC and HPLC, particularly at high salt conditions. At low salt conditions, which mimic physiological $Na^+$ concentrations, $K_p$ did decrease with increasing DPPG concentration ($X_{DPPG}$ from 0 to 0.25).Reductions in electrostatic repulsion between DPPG molecules via salt screening would have increased lipid packing (i.e. reduced area per lipid), which may also have contributed to the decrease in $K_p$.

The mechanism involved in increasing $K_p$ in DI water with increasing DPPG concentration is more elusive. 'Salting out' is a possible factor that may have been driven by the $Na^+$ counter ion of DPPG, but this cannot be the primary cause. It is possible that the increase in $K_p$ arose from difference in lipid packing. In pure bilayers PG posses a larger area per molecule (48.7 $Å^2$) than PC (47.2 $Å^2$) due in part to electrostatic repulsion between PG headgroups.[29] Without charge screening additional area would be available for n-butanol partitioning with increasing DPPG concentration (1.5 $Å^2$ per DPPG). Geometrically, twelve DPPG molecules would be needed to create

the additional space needed to accommodate one n-butanol molecule. This simple analysis neglects membrane expansion due to n-butanol partitioning, which would reduce electrostatic repulsion between DPPG.

## 6. Conclusions

This study illustrates the role of ionic strength on n-butanol partitioning in neutral and anionic membranes, which is important to understanding how heterogeneous model bacterial membranes restructure in response to n-butanol. This work has shows that DPPG concentration and ionic strength have a significant effect on DPPC/DPPG membrane phase behavior, size and n-butanol partitioning. Cation adsorption on DPPC membranes and high n-butanol partitioning (> 0.13M n-butanol) led to interdigitation and a fusion. However, increasing DPPG content in DPPC/DPPG membrane and salts with high n-butanol partitioning did not prevent interdigitation but it did prevented aggregation/fusion and caused a LUV-to-SUV transformation. n-Butanol partitioning was reduced likely due to charge screening via cation adsorption, which packed and rigidified the membrane. To our knowledge this is the first study depicting the effects of ionic strength and n-butanol partitioning intoa mixture of negatively charged and neutral lipids.

## 7. References


(1) Kurniawan, Y.; Venkataramanan, K. P.; Scholz, C.; Bothun, G. D. *J Phys Chem B*, *116*, 5919.

(2) Lobbecke, L.; Cevc, G. *Biochim Biophys Acta***1995**, *1237*, 59.

(3) Zhang, F.; Rowe, E. S. *Biochemistry***1992**, *31*, 2005.

(4) Ly, H. V.; Longo, M. L. *Biophys J***2004**, *87*, 1013.

(5) Rodriguez, J. R.; Garcia, A. E. *Interdiscip Sci*, *3*, 272.

(6) Sapia, P.; Coppola, L.; Ranieri, G.; Sportelli, L. *Colloid. Polym. Sci.* **1994**, *272*, 1289.

(7) Carole, T. M.; Pellegrino, J.; Paster, M. D. *Appl Biochem Biotechnol***2004**, *113-116*, 871.

(8) Harvey, B. G.; Meylemans, H. A. *J Chem Technol Biot***2011**, *86*, 2.

(9) Sikkema, J.; de Bont, J. A.; Poolman, B. *Microbiol Rev***1995**, *59*, 201.

(10) Denich, T. J.; Beaudette, L. A.; Lee, H.; Trevors, J. T. *J Microbiol Methods***2003**, *52*, 149.

(11) Kurniawan, Y.; Venkataramanan, K. P.; Scholz, C.; Bothun, G. D. *J. Phys. Chem. B***2012**, *116*, 5919.

(12) Vanegas, J. M.; Contreras, M. F.; Faller, R.; Longo, M. L. *Biophysical Journal***2012**, *102*, 507.

(13) Carrion, F. J.; Delamaza, A.; Parra, J. L. *Journal of Colloid and Interface Science***1994**, *164*, 78.

(14) Findlay, E. J.; Barton, P. G. *Biochemistry***1978**, *17*, 2400.

(15) Jacobson, K.; Papahadjopoulos, D. *Biochemistry***1975**, *14*, 152.

(16) Koynova, R.; Caffrey, M. *Biochim Biophys Acta***1998**, *1376*, 91.

(17) Ohki, S.; Duzgunes, N.; Leonards, K. *Biochemistry***1982**, *21*, 2127.

(18) Komatsu, H.; Okada, S. *Biochim Biophys Acta***1995**, *1235*, 270.

(19) Garcia-Manyes, S.; Redondo-Morata, L.; Oncins, G.; Sanz, F. *J Am Chem Soc*, *132*, 12874.

(20) *Handbook of clostridia*, 1 ed.; CRC Press: New York, NY, 2004.

(21) Bangham, A. D.; Standish, M. M.; Weissmann, G. *J Mol Biol***1965**, *13*, 253.

(22) Koynova, R.; Caffrey, M. *Biochim. Biophys. Acta***1998**, *1376*, 91.

(23) Zhang, F.; Rowe, E. S. *Biochemistry***1992**, *31*, 2005.

(24) Krisch, M. J.; D'Auria, R.; Brown, M. A.; Tobias, D. J.; Hemminger, J. C.; Ammann, M.; Starr, D. E.; Bluhm, H. *Journal of Physical Chemistry C***2007**, *111*, 13497.

(25) Binder, H.; Zschornig, O. *Chemistry and Physics of Lipids***2002**, *115*, 39.

(26) Mondal Roy, S.; Sarkar, M. *Journal of lipids***2011**, *2011*, 528784.

(27) Hildebrand, A.; Beyer, K.; Neubert, R.; Garidel, P.; Blume, A. *J Colloid Interface Sci***2004**, *279*, 559.

(28) Zhang, Y. P.; Lewis, R. N.; McElhaney, R. N. *Biophysical Journal***1997**, *72*, 779.

(29) Pabst, G.; Danner, S.; Karmakar, S.; Deutsch, G.; Raghunathan, V. A. *Biophysical Journal***2007**, *93*, 513.

# CHAPTER 5

## Differential Homeoviscous Response of *Clostridium Pasteurianum* by Membrane Composition and Structural Adaptations to Butanol Toxicity

Keerthi P. Venkataramanan[a,#], Yogi Kurniawan[b,#], Judy J. Boatman[c], Casandra H. Haynes[c], Katherine A. Taconi[c], Lenore Martin[d], Geoffrey D. Bothun[b,*] and Carmen Scholz[e,*]

[a]Biotechnology Science and Engineering Program, University of Alabama in Huntsville, 301 Sparkman Dr NW, MSB 333, Huntsville, AL 35899. USA.

[b]Department of Chemical Engineering, University of Rhode Island, 16 Greenhouse Rd, 205 Crawford Hall, Kingston, RI 02881.

[c]Department of Chemical and Materials Engineering, University of Alabama in Huntsville, 301 Sparkman Dr NW, EB 130, Huntsville, AL 35899. USA.

[d]Department of Cell and Molecular Biology, University of Rhode Island, 120 Flagg Rd, 393 CBLS, Kingston, RI 02881. martin@uri.edu.

[e]Department of Chemistry, University of Alabama in Huntsville, 301 Sparkman Dr NW, MSB 333, Huntsville, AL 35899. USA. scholzc@uah.edu. Tel: (+1) 256 824 6188; Fax: (+1) 256 824 6349

#-authors KPV and YK contributed equally and are co-first authors.

*authors GB and CS are co-corresponding authors

Prepared for submission to ACS Chemical Biology

## 1. Abstract

*Clostridium pasteurianum* has been shown to ferment glycerol into butanol at higher yields than when sugars are used as the carbon source. *C. pasteurianum'*s potential to use biodiesel-derived crude glycerol as the carbon source has been gaining importance in the recent past. This study investigated the homeoviscous response of *C. pasteurianum* during butanol stress. *C. pasteurianum*'s lipid composition of the plasma membrane during butanol challenge was analyzed. *C. pasteurianum* was found to exert two different homeoviscous responses by altering the composition of the lipid membranes in an attempt to counteract the butanol toxicity. Addition of exogenous butanol to glycerol fermentation when *C. pasteurianum* produced endogenous butanol led to an increase in the ratio of saturated to unsaturated lipids. On the contrary, addition of exogenous butanol to fermentation when *C. pasteurianum* did not produce any endogenous butanol led to a decrease in the ratio of saturated to unsaturated lipids. This counterintuitive finding of an alternate response to butanol toxicity, which is similar to a response observed in gram negative microbes, was verified for the presence of hydrophobic membrane proteins and the ability of the cells to retain butanol productivity. The differential responses for exogenous butanol during the presence and absence of an active butanol biosynthesis indicates that *C. pasteurianum* is a versatile micro-organism that has the potential to be engineered as an industrial butanol producer using crude glycerol, a promising low cost feedstock for butanol production.

## 2. Introduction

*Clostridium pasteurianum,* an anaerobic spore-forming firmicute, ferments glycerol as the sole substrate, resulting in a mixture of butanol, ethanol, and 1,3-propanediol (PDO) along with acetate and butyrate. [1-4]*C. pasteurianum* is of particular interest for butanol production, as it has also been shown to ferment biodiesel-derived crude glycerol as the sole substrate. [3,4]

Butanol is toxic to cells, as it partitions into the cell membrane and affects both the structural and functional integrity of the cell. The extent of solvent toxicity correlates to the log P value, the partition coefficient. Solvents with a log P value less than 4 partition into the lipid membrane bilayer and are considered extremely toxic. Butanol has a log P value of 0.8 and is considered to be one of the most toxic solvents.[5] When *Clostridia* are exposed to solvents, the solvents exhibit a fluidizing effect on the phospholipid bilayer, which causes the organism to alter the lipid composition of the bilayer. This response of bacteria to tolerate toxic solvents by altering the composition of the lipid bilayer is known as homeoviscous response (membrane viscosity is proportional fluidity). To compensate for the fluidizing effects of butanol, *Clostridia* increase the ratio of saturated to unsaturated lipids (S/U) in the lipid membrane, thereby reducing the fluidity of the membrane and increasing butanol tolerance. [6-16]The fluidity of the lipid membrane is inversely related to the amount of saturated fatty acids in the tail of the lipid bilayer. Hence, the bacteria that tolerate more butanol have a much higher S/U ratio in the lipid bilayer. [11] This has been observed to be an essential biophysical process of tolerating butanol in various butanol producing organisms from the genus *Clostridium.* [6-8,10,12,13] It has been established

that composition and distribution of lipids in cell membrane play an essential role not only in maintaining membrane stability, curvature and membrane fluidity but also in modulating protein function and insertion of membrane proteins into the membranes.[17-19] Membrane fluidity is essential for maintaining the proper distribution and diffusion of embedded proteins in membrane. [20]

Membrane lipid composition changes in response to alcohol toxicity with an increase in S/U has been observed in Clostridia, particularly, *C. acetobutylicum*[10] and *C. thermocellum.* [21] Among wild-type and ethanol-adapted (EA) *C. thermocellum,* where the EA cells preserved the optimum level of fluidity in response to ethanol toxicity by increasing the fatty acids chain length of the lipid tails and S/U in the cell membrane; resulting in higher membrane rigidity. Contrastingly, an opposite effect (decreasing S/U) in response to alcohol toxicity has been observed in several other microorganisms including gram positives such as *Lactobacillus heterohiochii, Lactobacillus homohiochii,* gram negatives such as *Escherichia coli*, and yeast,*Saccharomyces cereviisiae.*[22-24]These responses those have a decrease in S/U ratio, but were observed to have longer fatty acid chain lengths. The presence of contrasting responses to counteract the effect of toxic solvents raises the question of why does two distinct responses are required to tolerate the effects of solvents.

Butanol has been shown to affect the membrane by increasing fluidity and hence reducing lipid ordering.[10,25-27] Also, butanol's toxic effects lead to the formation of interdigitated phases and phase separation. [25,28] Overall, butanol can compromise cellular function of the membrane by altering cell fission, fusion, budding, vesicle formation and cell signaling.[28,29] The passive and active transport of substrates and

products is also affected, along with the structure and function of integral membrane proteins. This can hinder the ability of the cell to maintain an internal pH and inhibits membrane-bound ATPases and the uptake of the carbon source (if present), which subsequently inhibits energy generation.[9] Membrane bound ATPases are one such examples, which maintain a transmembrane pH for ATP generation. Butanol inhibits the ATPases and reduces the transmembrane pH resulting in lower ATP formation.[30]

To our knowledge, *C. pasteurianum* membrane lipid composition with or without homeoviscous adaptation has not been examined. Furthermore, the effect of lipid composition on the membrane structure of butanol-tolerant solvent producing bacteria have are unknown. In this study, membrane extracts of *C.pasteurianum* exposed to exogenous addition of different butanol concentrations were analyzed and reconstituted as dispersed bilayer vesicles or monolayers to investigate membrane composition, membrane fluidity, and membrane compressibility.

## 3. Materials and Methods

### 3.1. Materials

All chemicals were purchased from Fisher Scientific and Sigma-Aldrich. Deuterated chloroform ($CDCl_3$) was obtained from Cambridge Isotope Laboratory. Synthetic lipids, 1,2-Dipalmitoyl-*sn*-glycero-3-phosphocholine (DPPC, >99% purity) and 1,2-dioleoyl-*sn*-glycero-3-phosphocholine (DOPC, >99% purity) were obtained from Avanti Polar Lipids, Inc.

### 3.2. Bacterial Strain

The bacterial strain *C. pasteurianum* ATCC 6013 was purchased from American Type Culture Collection and the glycerol stock was maintained as described earlier.[8]

### 3.3. Effect of n-Butanol

The effect of n-butanol (n-butanol was used throughout all experiments) on bacterial growth and the stability and changes in membrane composition were studied by adding butanol to the media containing either glucose or glycerol as the sole carbon source. For investigating the effect of butanol, exogenous butanol was added to the media varied from 0 to 1% (w/v) (0 $gL^{-1}$ to 10 $gL^{-1}$) containing either glycerol (25 $gL^{-1}$) or glucose (50 $gL^{-1}$) in Biebl media.[6] *C. pasteurianum* does not produce butanol when grown on glucose. The cells were allowed to grow in the presence of butanol for 24 hours after which the membrane was extracted. All experiments were conducted with 10% (v/v) inoculum, pre-grown in reinforced clostridial media (RCM).

### 3.4. Extraction of the Cell Membrane

Cell membranes were extracted using the modified protocol of Bligh and Dyer using dichloromethane/methanol mixtures.[28] The cells were harvested (0.5 mL cell suspension) by centrifugation at 13000 rpm for 15 minutes and the pellets were resuspended in 0.5 mL of sterile 1.0% (w/v) NaCl in a 10 mL glass sample tube with PTFE lined caps. To the resuspended pellets, 2 mL of dichloromethane/methanol mixture (1:2 v/v) was added and shaken vigorously for 15 minutes. It was followed by a 2 hour incubation at RT, followed by centrifugation at 2500 rpm and the

supernatant (S1) was collected in a fresh tube. The pellet was again resuspended in 0.5 mL 1.0% NaCl and 2 mL of a dichloromethane/methanol mixture (2:1 v/v) was added to the resuspended pellet and shaken vigorously for 15 minutes. Following a 2 hour incubation, the samples were centrifuged at 2500 rpm and the supernatant (S2) was collected. Supernatants S1 and S2 were combined and 1 mL of dichloromethane and 1 mL of sterile 1.0% NaCl were added. The top phase (aqueous) was removed and the bottom (organic) phase was retained. The solvent was evaporated under a gentle nitrogen stream. Once a dry film was obtained, the headspace was flushed with nitrogen, capped tightly, and stored for further analysis.

### 3.5. NMR Analysis

The dry film of the membrane was dissolved in $CDCl_3$ for $^1$H-NMR analysis. Synthetic lipids, DPPC and DOPC were used as standards for NMR analysis. Various ratios of DPPC and DOPC (1:0, 3:1, 1:1, 1:3 and 0:1) in a total lipid concentration of 10 mM were used for calibration (Figure G.1). The synthetic lipids were dried and dissolved in $CDCl_3$. All $^1$H-NMR spectra were recorded on a Varian™ Unity Inova 500 (500 MHz) spectrometer equipped with a 5 mm triple resonance inverse detectable probe. The percentage of unsaturation in the membrane lipid samples was calculated from the integration ratios of the olefinic hydrogen signals (at 5.31 ppm), using Equation 1.[30]

$$\%unsaturation = \frac{Intensity_{olefenic}}{Intensity_{total}} \times 100 \quad \text{(Eq 1)}$$

### 3.6. Liposome Preparation and Fluorescence Anisotropy

The dry film of the reconstituted cell membrane and 0.1 mM 1,6-diphenyl 1,3,5-hexatriene (DPH) dissolved in chloroformwere mixed and co-evaporated under a

gentle stream of nitrogen until a dry reconstituted cell membrane/DPH film remained. Vacuum was used (~ 60 min) to remove residual solvent from the film. The film was then hydrated with distilled water and maintained at 50°C in a water bath for 1 hour before shaking. The reconstituted membrane/DPH film was suspended as multilamellar liposomes by vigorously shaking for approximately 1 hour. The liposomes were sonicated for 60 min at 50°C, which has been previously shown to yield unilamellar liposomes. A 10 mM DPPC liposomal solution was used as control. Fluorescence anisotropy(Perkin Elmer LS 55) and melting temperature were measured using the L-format configuration with DPH as the hydrophobic bilayer probe from 25 to 50°C at a rate of 1°C/min under continuous mixing as described previously [25].

### 3.7. GC/MS Analysis

The lipid samples were methylated for GC/MS analysis. The dried lipid samples were saponified using 1 mL of 3N sodium hydroxide at 90ºC for an hour and then cooled to RT. The excess sodium hydroxide was neutralized with 1.8 mL of 3.6 N hydrochloric acid at 90ºC for 10 minutes and cooled to RT. The free fatty acids were extracted using 1 mL of hexane and diethyl ether (1:1 v/v). The organic phase was then separated into a dry round bottom flask. The fatty acid hydrolyzates were dried using a rotoevaporator and stored under Argon in desiccators.

The dried fatty acid hydrolyzates were derivatized using a 5 mL borontrifluoride-methanol complex at 60ºC for 5 minutes and then cooled to RT. To the cooled solution, 1 mL water and 1 mL hexane were added and the container shaken multiple times to ensure the transfer of esters into the non-polar solvent. The upper organic layer was removed and transferred into an Erlenmeyer flask containing

5 g of anhydrous sodium sulfate. The flask was incubated at RT to dry overnight. The sodium sulfate was filtered and the hexane solution was transferred into a round bottom flask and dried in a rotoevaporator and the samples were stored under Argon. For GC-MS analysis, samples were dissolved in 250 µL of dichloromethane.

Fatty acid methyl esters (FAME) derivatives were analyzed by a Shimadzu GC-MS QP 2010 system using aSHR5xLB silica capillary column (30m× 0.25mm ID, composed of 100% dimethyl polysiloxane).Manufacturer's instructuion were followed for FAME analysis.The compoundswere identified by comparison with the data in theNIST libraries.The FAME distribution was determined using equation 2:

% FAME = $\frac{Area_{FAME}}{\sum FAME_{area}} \boldsymbol{x100}$(Eq 2)

### 3.8. Surface pressure-area (Π-A) isotherms

*Π-A* isotherms were recorded using a Langmuir trough (model 102M, Nima technology Ltd, UK) with a deposition area of 70 $cm^2$ at 25$^oC$, 37$^oC$ and at 50$^oC$. A Wilhelmy plate connected to an electronic micro-balance was used to measure surface pressure with an accuracy of ± 1µN/m. Isotherms were monitored by NIMA TR 7.4 .vi software. The external water bath system was used to control the subphase temperature. Monolayers were obtained by spreading diluted solutions of lipid samples in chloroform at the air/water interface using a 5 µL microsyringe. The chloroform was allowed to evaporate and the lipid films spread at air/water within 15 min. The system was the equilibrated for 15 min before being compressed at a speed of 10 $cm^2$/min.

### 3.9. Elastic modulus / area compressibility modulus

Mechanical properties of the monolayer films were determined by the compressibility modulus. The elastic modulus ($C_s^{-1}$) / area compressibility modulus is the reciprocal of the compressibility ($C_s$).[31] The elastic modulus corresponds to the elasticity of the Langmuir films under the compression force. $C_s^{-1}$values were defined as: $C_s^{-1} = -A\left(\frac{\partial \pi}{\partial A}\right)_T$ (Eq 3)

where, $A$ is the area per molecule at the particular surface pressure and $\Pi$ is the corresponding surface pressure. A maximum in the elastic modulus ($C_{sMax}^{-1}$)denotes the maximum molecular packing condition of monolayer.

## 4. Results and Discussion

Clostridial species produce various metabolites in the form of acids and solvents, and have to modify the composition of their lipid membranes to tolerate the toxic effects of the produced metabolites. This study is focused on investigating the effect of butanol in*C. pasteurianum* leading to the tolerance response, which involves changes in the lipid membrane composition. These changes in the physical and structural compositions of the membranes were analyzed to examine the relationship between the composition and function of the lipids as it provides *C. pasteurianum* cells an ability to use two different homeoviscous responses to tolerate the toxic effects of butanol.

### 4.1. Effect of Exogenous Butanol

The homeoviscous response of *C. pasteurianum* to the addition of exogenous butanol was studied at two conditions, first by adding exogenous butanol during the endogenous production of butanol by *C. pasteurianum,* i.e., glycerol fermentation

(EB1), and second by adding exogenous butanol while no butanol was produced, i.e. during the fermentation of glucose (EB2). *C. pasteurianum* cultures do not undergo solventogenesis during the fermentation of glucose, as the fermentation is predominantly only in the acidogenic phase, resulting in butyric acid as the major fermentation product with no butanol formation.

Butanol was added at concentrations of 0 g/L (control), 2.5 g/L (0.0335 M), 5 g/L (0.067 M), 7.5 g/L (0.105 M) and 10 g/L (0.134 M), respectively, once the cells reached mid exponential phase. The membranes were extracted after 24 hours of butanol exposure and analyzed using GC-MS, $^{1}$H-NMR, and fluorescent anisotropy. The data from GC-MS on the fatty acid composition (Figure 5.1) showa clear shift from short to long carbon chain saturated fatty acids with increasing butanol concentration. Thelongchain saturated fatty acids ($C_{19}$ to $C_{22}$) are almost completely absent in the control samples with no exogenous butanol present. Similarly, a reduction in the shorter chain fatty acids was observed with an increase in the butanol stress (Figure 5.1). $C_{10}$ fatty acids were completely absent in the cells exposed to higher butanol concentrations, while other shorter fatty acids from $C_{11}$ to $C_{16}$ were found to decrease proportionately with an increase in butanol concentration.

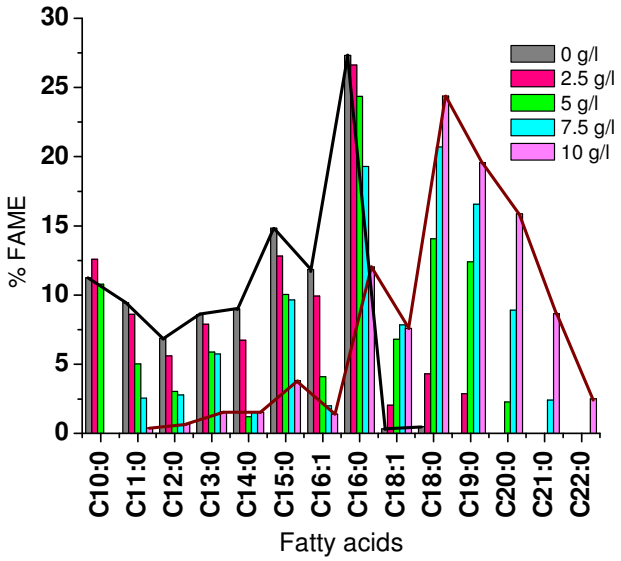


Figure 5.1.Membrane fatty acid distribution during effect of exogenous butanol on glycerol fermentation (EB1) of *C. pasteurianum* analyzed by GC-MS.

In addition to increasing lipid tail length, exogenous butanol addition during glycerol fermentationled to a decrease in the degree of unsaturation (increase in S/U) as determined by $^{1}$H-NMR (Figure 5.2). Comparatively, the fluorescence anisotropy data at 37°C show a decrease in anisotropy with increasing butanol concentration. The anisotropy, <r>, of the unexposed control was found to be 0.12 and was found to reduce as the butanol concentration increased. However, at butanol concentrations of 7.5 and 10.0 g/L the anisotropy remained rather constant or increased marginally. The fluorescence anisotropy of DPH in the membranes is inversely related to the fluidity of the reconstituted lipid membranes. The decrease in the anisotropy indicates the fluidizing effect of butanol on the membrane lipids, which was the impetus for homeoviscous response. The stabilization of the anisotropy at higher butanol concentrations can be explained as the response of the bacteria to tolerate the fluidizing effects of butanol.

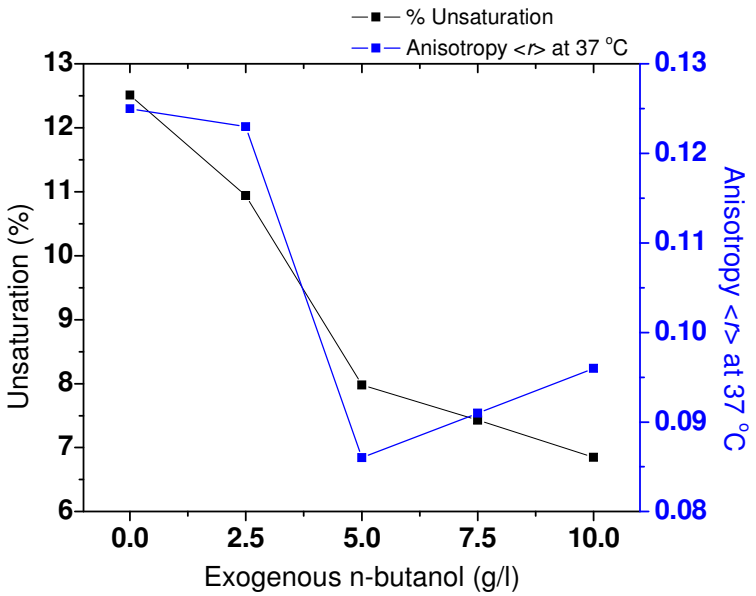

Figure 5.2.Effect of exogenous n-butanol during glycerol fermentation (EB1).

As a control, the change in the degree of unsaturation and anisotropy of the lipid membrane during the production of endogenous butanol was studied and compared (Supplementary material and Figure G.2 and G.3). In this case the degree of unsaturated lipids decreased and the fluorescence anisotropy increased in the absence of exogenous butanol. The difference observed in the anisotropy data is consistent with the previously reported fluidizing effect of butanol observed through fluorescence anisotropy of synthetic lipids and reconstituted membrane lipids.[8,25] Deviations observed in the anisotropy data without and with exogenous butanol depict the additional fluidizing effects of the exogenous butanol on the membrane. The fact that *C. pasteurianum* could not counteract fluidization at high exogenous butanol concentrations despite the clear shift in lipid composition suggests that a homeoviscous 'threshold' exists for combined endogenous + exogenous butanolconcentrations.

The compositional analysis through GC-MS not only supports the results from NMR and fluorescence anisotropy, but also substantiates that *C. pasteurianum* exerts a homeoviscous response to butanol under EB1 condition by two major changes in the fatty acid composition to counteract the fluidity of the toxic butanol. First, *C. pasteurianum* increases the percentage of longer chain fatty acids at the expense of shorter chain fatty acids, and second *C. pasteurianum* increases the ratio of saturated to unsaturated lipids.

The effect of butanol on the lipid composition and the fluidity of the lipid membrane has also been reported for *C. acetobutylicum.*[6,7,10,12]*C. acetobutylicum* produces butanol by fermenting glucose and the effect of butanol challenge was studied during the growth of *C. acetobutylicum* in glucose (butanol producing media).[6,7,10,12]*C. acetobutylicum* tolerates butanol through a homeoviscous response that predominantly involves an increase of saturated fatty acids at the expense of unsaturated fatty acids in the lipid membrane.[6,7,10,12]Lepage *et al.* reported the composition of the *C. acetobutylicum*'s fatty acid composition in the lipid membrane, which consisted of fatty acids from $C_{12}$ to $C_{19.}$ [10] The ratio of the unsaturated to saturated fatty acids was found to be close to 1 in the absence of butanol exposure but the ratio reduced to 0.87 and 0.77 respectively with an exposure to 4 g/L and 8 g/L butanol respectively. This reduction in unsaturation and the concurrent increase in saturated fatty acids in the membrane lipid constitutes the organism's homeoviscous response.

### 4.2. The Differential Response to Butanol Toxicity

The effect of butanol under EB1 conditions showed a conventional homeoviscous response by increasing the fatty acid chain length and the ratio of saturated to unsaturated lipids. To further investigate the sole effect of butanol toxicity,cells were grown in glucose and exposed to exogenous butanol (EB2 conditions). Initially, the EB2 experiment was conducted to match the butanol stress concentration of 0 g/L to 10 g/L, but experiments at higher butanol concentrations of up to 20 g/L were also performed.

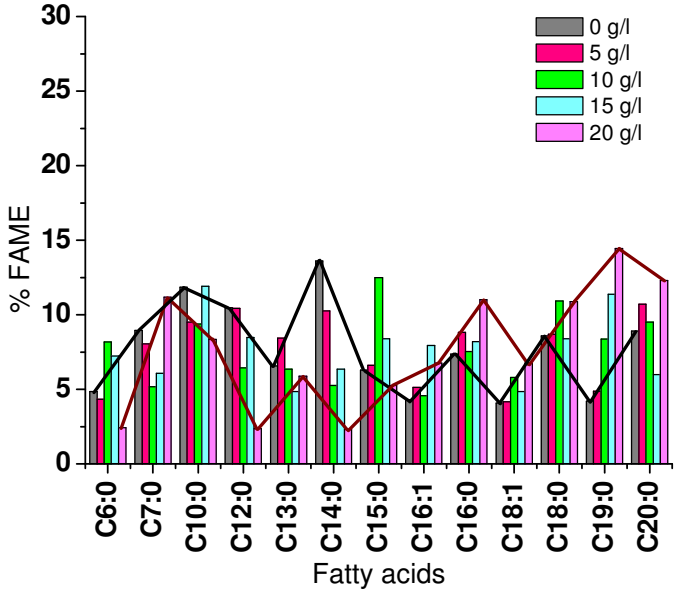


Figure 5.3.Membrane fatty acid distribution during effect of exogenous butanol on glucose fermentation (EB2) of *C. pasteurianum* analyzed by GC-MS.

GC-MS analysis of EB2 membrane extracts identified 13 different fatty acids were identified of which 11 were saturated (Figure 5.3). The data on the composition of the fatty acids shows not only an increase in the degree of unsaturation in the lipids, but also an increase in the percentage of longer chained lipids ($\geq C_{16}$) with an increase in the concentration of exogenous butanol. However the shift towards longer chain

lipids was not nearly as pronounced when *C. pasteurianum* was grown on glycerol and produced butanol (EB1).

The $^{1}$H-NMR results further confirm an increase in the percentage of unsaturation in the fatty acid tails of the lipid membranes,from 2% to 13%. This result is completely contrasting to the results obtained earlier during butanol stress in glycerol fermentation (EB1 conditions, see Figure 5.2). The degree of unsaturation in the lipid membranes increased proportionately with increasing concentration of butanol in the media. For an exogenous butanol concentration of 5 g/L, a small drop in the percentage of unsaturation in the fatty acid tail was observed when compared to the control with no external butanol. The data obtained from fluorescent anisotropy of the reconstituted membrane supported the data obtained from $^{1}$H-NMR (Figure 5.4). The anisotropy, <r>, measured at 37°C decreased with an increase in the butanol concentration in the media and in conjunction with the increase in degree of unsaturation.

Unsaturated lipids are known to reduce membrane fluidity. It has been shown that an increase in the percentage of unsaturated lipids in model liposomes (model membranes from DPPC and DOPC) results in a decrease in fluorescence anisotropy.[25] Furthermore, the addition of butanol to model membranes comprised of DPPC, DOPC, or mixturesof the two have shown a decrease in anisotropy due to the fluidizing effects of butanol on the lipid membrane.[25,29] Butanol fluidizes membranesby reducing inter lipid interactions and the surface tension within the membrane. An increase in the degree of unsaturation in lipid membranes has been shown to augment the fluidizing effects of butanol.[25] Hence, the results obtained from

the addition of exogenous butanol to the cells of *C. pasteurianum*in EB2contradictthe results obtained during EB1. This led to the question of whether other non-lipid entities could be involved in the homeoviscous adaptation of the membrane in EB2.

The lipid composition of the cells also varied considerably when the cells are grown on glycerol and glucose in the absence of exogenous butanol. Lipid chain lengths as low as $C_6$ were observed during glucose fermentation, while the shortest lipid chain length in glycerol fermentation was $C_{10}$. A similar distinction is also observed in the maximum chain length for the two carbon sources.

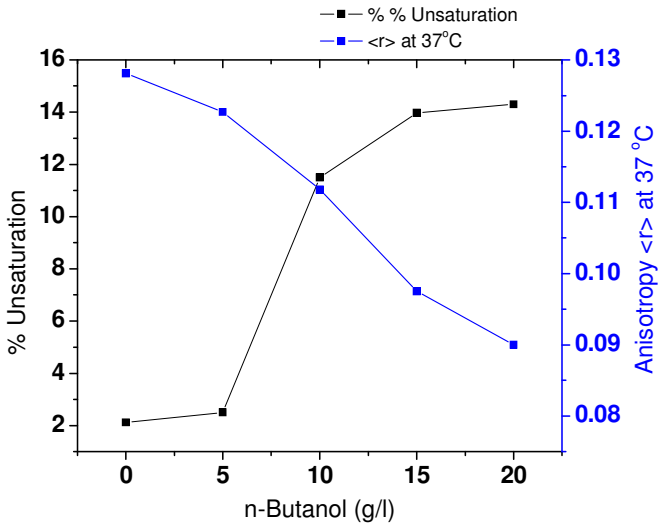

Figure 5.4.Exogenous effect of butanol during glucose fermentation (EB2).

The increase in unsaturation (exogenous butanol with glucose, EB2) cannot be explained by a homeoviscous adaptation, as it led to an increase in the fluidity of the membrane consistent with the toxic effect of butanol (Figure 5.3 and 5.4). However, an increase in unsaturation in the lipid membrane of cells exposed to solvent stress has been reported for *E. coli* during ethanol stress and for *C. butyricum* during 1,3-PDO stress. [14,32] Dombek and Ingram reported that the plasma membrane became more rigid during ethanol challenge experiments, but the extracted lipid membrane

exhibited higher fluidity in comparison to the control cells that were unexposed to ethanol[32]. This shows that the rigidity of the membrane is not only dependent on the ratio of saturated to unsaturated fatty acids, or the presence of shorter or longer fatty acids, but is also dependent on the lipid to protein ratio in the membrane.[33]Membrane proteins can rigidify the membrane regardless of lipid composition and, based on the method used to obtain membrane extracts, they were likely present in the reconstituted vesicles.[34,35] Hence, an increase in protein:lipid ratiomay account for the net increase in the rigidity of the membrane and compensates for the increase in fluidity as a result of the increased unsaturation of the lipid tails (Figure 5.3). These changes in rigidity could not be detected through fluorescence anisotropy experiments.

During the formation of butanol (EB1), the bacteria must be synthesizing butanol efflux pumps in the membrane that serve as butanol transporters to the extracellular environment. [36] Dunlop *et al.* have shown that cloning and expressing of efflux pumps from different microorganisms for various solvents resulted in an increase of solvent tolerance. [36] However, overexpression of butanol and iso-butanol efflux pumps did not improve butanol tolerance,leading to the conclusion that the toleration of butanol is a complex phenomenon.[36]

**4.3. *Π–A*isotherms ofreconstituted cell membrane (RM) monolayers**

The surface pressure and elasticity modulus of RM monolayers were examined to gain more understanding of lipid-lipid and (possible) lipid-protein interactions. *Π–A*isotherms of RM monolayers spread at air/water interfaces are shown in Figure 5.5 for the first compression cycle where *A* ($cm^2/\mu g$) was based on the mass of the membrane extract. Fluorescence anisotropy data indicated that the membranes (EB1)

were in a fluid state, which, in a two-dimensional lipid monolayer, is analogous to a liquid expanded (*LE*) or disordered state. *Π* of RM monolayers was lower than *Π* of monolayers of saturated/unsaturated phospholipid[33,37] and E.coli lipid membrane extract.[17] In addition to 37°C, temperatures at 25°C and 50°C were employed to determine if two-dimensional lipid phase changes could be elicited.

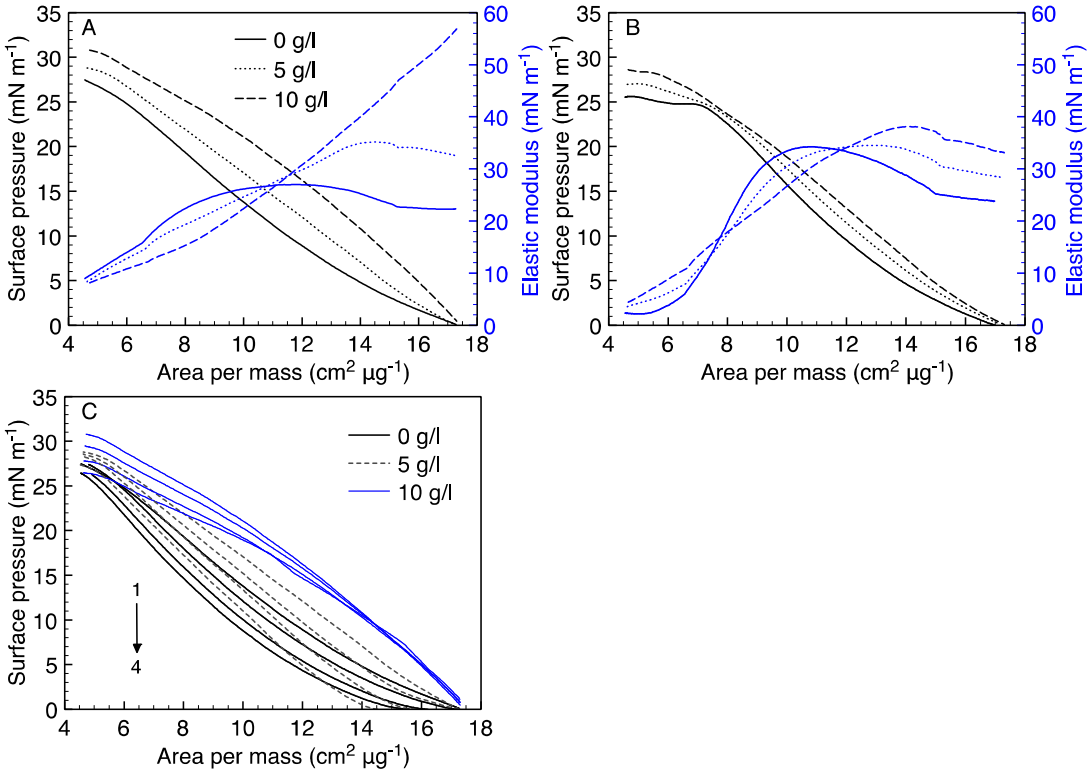


Figure 5.5.*Π–A* isotherms of reconstituted membrane monolayers at air/water interfaces at (A) 37°C, (B) 25°C, and (C) 50°C at 0, 5, and 10 g/l butanol (solid lines). The elastic modulus is shown (dashed lines) based on equation X (solid lines). The legend shown in (A) applies to (B) and (C). (D) *Π–A* isotherms at 37°C during monolayer compression over four sequential compression/expansion cycles.

At 37°C there was a continuous increase in *Π*with decreasing *A* suggesting that the RM monolayers existed in a *LE*state (Figure 5.5A). RM monolayers exhibited high surface pressures with increasing n-butanol added during EB1 conditions. This result is consistent with the observed homeoviscous response where lipid chain length increased with increasing exogenous n-butanol concentration. As lipid chain length

increases the average interfacial area occupied by each lipid molecules increased, which led to a rise in $\Pi$at higher $A$. This behavior persisted at 25°C, where this lower temperature was used to artificially rigidify the RM monolayers to detect possibly changes in monolayer phase behavior and monolayer collapse (Figure 5.5B). While no phase changes were observed, the collapse pressure ($\Pi_{collapse}$, Table 1*),* denoted by a plateauing of the $\Pi$–$A$ isotherm as $A$ approaches zero, increased from 25 mN/m at 0 g/l n-butanol to 28.5 mN/m. This increase reflects stronger van der Waals attraction between longer lipids chains.

Table 5.1. Parameters related to the maximum elastic moduli and collapse ($A \rightarrow 0$) of RM monolayers (EB1 conditions).

| n-Butanol (g/l)[a] | T (°C) | C-1max (mN/m) | $\Pi_{max}$ (mN/m) | $A_{max}$ ($cm^2/\mu g$) | $\Pi_{collapse}$ (mN/m) | $A_{collapse}$ ($cm^2/\mu g$) |
|---|---|---|---|---|---|---|
| 0 | 37 | 27.0 | 9.5 | 11.7 | n.d. | n.d. |
| | *25* | *34.2* | *13.0* | *10.8* | *24.6* | *7.4* |
| 5 | 37 | 35.1 | 3.7 | 14.5 | n.d. | n.d. |
| | *25* | *34.6* | *8.6* | *13.0* | *25.0* | *7.5* |
| 10 | 37 | 57 | 0.4 | 17.3 | n.d. | n.d. |
| | *25* | *38.3* | *7.0* | *14.1* | *28.0* | *6.1* |

Although there is no direct evidence of membrane proteins present within the RM monolayers, there is qualitative evidence at 37°C based on the shape of the $\Pi$–$A$ isotherms, the elastic moduli, and $\Pi$–$A$ isotherm hysteresis over multiple compression/expansion cycles. Concerning isotherm shape, RM monolayers from 0 g/l exhibited a common 'concave up' lipid isotherm where surface pressure rises steeply as lipid molecules pack together (decreasing $A$). The maximum compressibility occurs where the slope is greatest, typically at the midpoint where the isotherm is the steepest. In contrast the isotherm shape of RM monolayers from 10 g/l exhibit a 'concave down' isotherm, which indicates that intermolecular repulsion is greatest at

the lowest surface pressures or highest areas. This is reflected in the elastic moduli where it increases continuously with increasing $A$ – i.e. the monolayer becomes less rigid or more compressible within increasing surface pressure or decreasing $A$. Results at 5 g/l where intermediate. This behavior has not been reported for lipids, but it has for proteins. At low $\Pi$or high A, proteins are extended or denatured at the air/water interface. With compression, proteins are compacted and can undergo an extended to globular transition and/or even be expelled or 'squeezed out' from the interface into the bulk phase. Consecutive compression/expansion cycles support this concept. At 0 and 5 g/l decreases in the 'lift-off' area where $\Pi$ begins to rise suggest that material is being expelled from the RM monolayer into the bulk phase or that strong intermolecular attraction exists that yields irreversible clustering once compressed. In contrast, the lift-off area at 10 g/l does not change consistent with reversible protein conformational changes.

Based on our interpretation data, the effect of protein can be interpreted as shown in Figure 5.5. Temperature affected the structure of membrane proteins and lipid. At low temperature (T< 37°C), proteins remained in native state and lipid tails were ordered. At low compression ($\Pi<\Pi_{Collapse}^{protein}$ ) and low temperature, folded-hydrophobic protein at 0 g/l butanol displaced within lipid membrane monolayers and water molecules remained between the hydrophilic lipid head groups. As a result, repulsive contribution at polar headgroup was high, and attractive van der Waals interactions between lipid tails were low promoting a weak molecular packing. At high surface pressure, $\Pi>\Pi_{Collapse}^{protein}$ external pressure compressed the folded protein network until it failed and displaced from the interface, forming collapsed protein

multilayers in the aqueous bulk phase near to the interface; thus, the collapse phase appeared (Figure 5.5B).

Protein content in RM increased with increasing EB2. As a result, the increased amount of the hydrophobic proteins at 10 g/l adsorbed at air/water interface increasing$\Pi$. At high temperature (T> 37°C) lipid tails were disordered and proteins were unfolded increasing the protein relaxation, the displacement and the elasticity. Even though monolayer was under high surface pressure, the membrane elasticity at 10 g/l butanol was higher than the membrane elasticity at 0 g/l butanol. This indicates that the protein at air/water interface did not occur due to the orogenic displacement of unfolded protein (Figure 5.6).

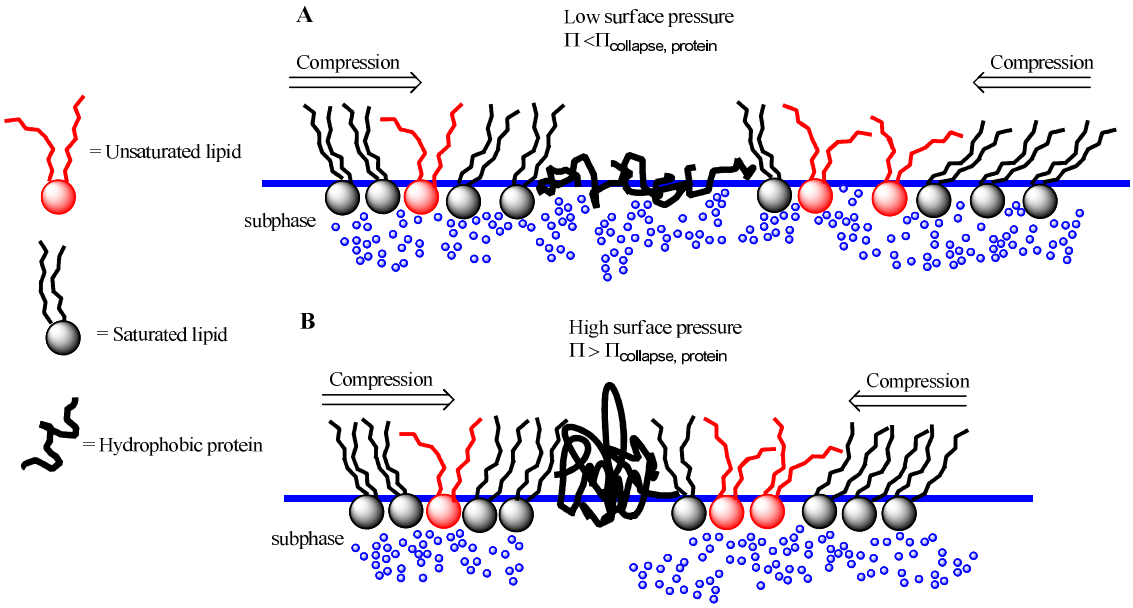


Figure 5.6.Schematic illustration depicting an isothermal-structural response of (A) relaxation phenomena in protein at low surface pressure, (B) "orogenic'' hydrophobic proteins at high surface pressure T= 25°C.

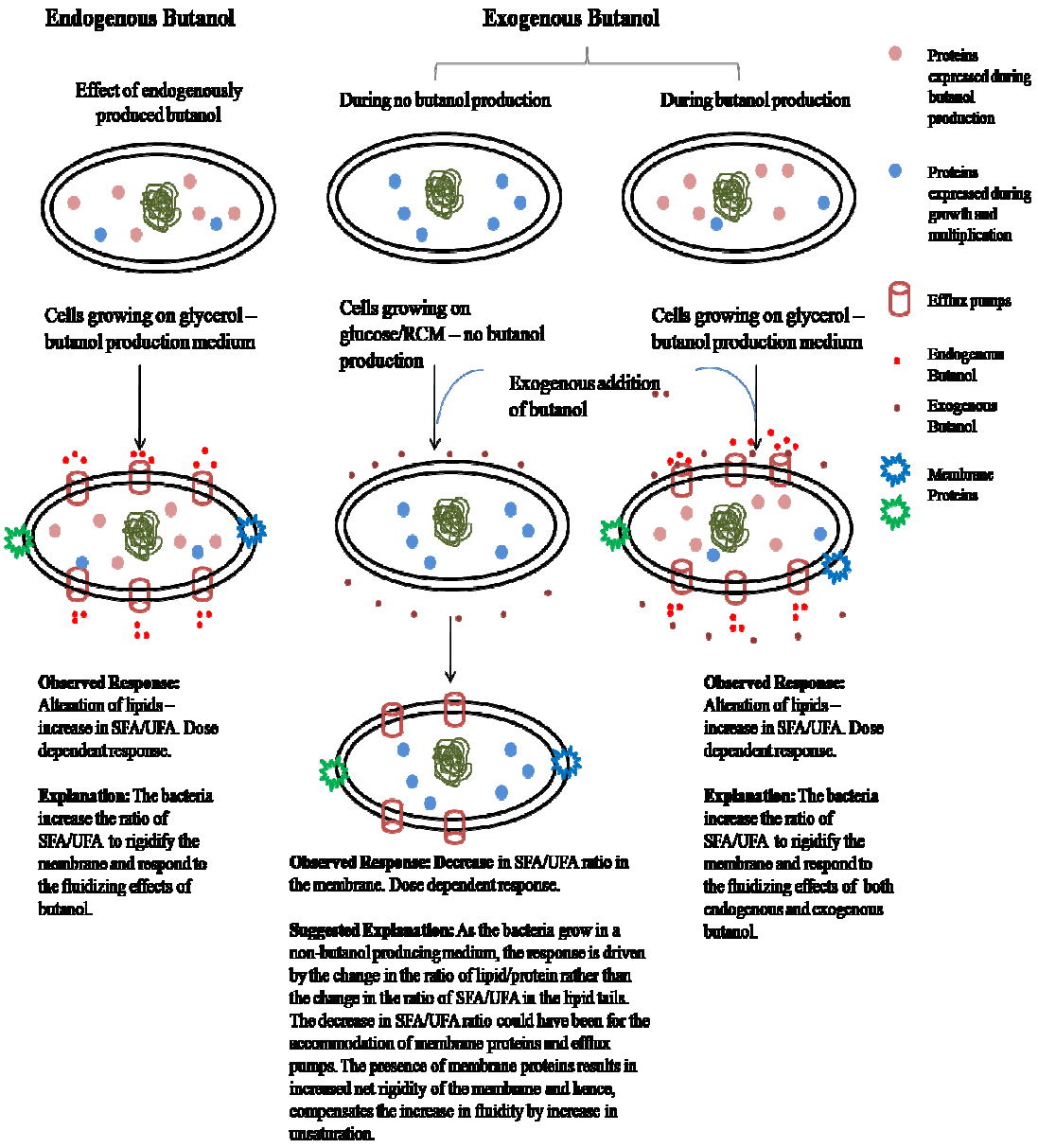


Figure 5.7.Homeoviscous response of *C. pasteurianum* to endogenous, exogenous and endogenous (EB1) & exogenous butanol (EB2).

## 5. Conclusions

This study is the first report of the analysis of the homeoviscous adaptation to butanol by *C. pasteurianum*and this study is also the first study that quantifies lipid composition in *C. pasteurianum*. The analysis of the extracted membranes from cells exposed to various concentration of butanol under two different conditions (i) butanol production by glycerol fermentation (EB1) and (ii) no butanol production by glucose fermentation (EB2), resulted in two completely different responses with respect to the changes in the composition of the lipids. During butanol production, when stressed with exogenous butanol, *C. pasteurianum* responds by increasing the ratio of the saturated to unsaturated fatty acids in the membrane. This is also the response found in other butanol producing species of C*lostridia*, along with the response exhibited by other microbes towards tolerating toxic organic compounds.[14-16,38]*C. pasteurianum* exhibits a different response when grown on glucose (no butanol produced), and challenged with exogenous butanol, which can be explained on the hypothesis of altering the ratio of the protein to lipids in the membrane (Figure 5.6 and 5.7). This hypothesis was further confirmed using by *Π-A*isotherms and the presence of hydrophobic membrane proteins in the lipid membrane of *C. pasteurianum* during EB2.

A comprehensive view of butanol-tolerant *C. pasteurianum* ATCC 6013 in membrane fluidity and Langmuir monolayer isotherm at the air-water interface was presented. The results reveal*the changes on structure and integrity of the cell membranes counteracting butanol toxicity in media was dependent on* the level of lipid-lipid interactions and the lipid-protein interactions. Homeoviscous cell

membrane altered S/US ratios and protein content in respond to exogeneous butanol. Unsaturated fatty acid of lipid and membrane proteins played a major role to influence the membrane elasticity and the phase behavior. When unsaturated lipid ratio decreased with high n-butanol concentration, reconstituted cell monolayer experienced in high surface pressure due to a greater attractive attraction within saturated tails of lipids, an increased folded protein molecules and a rigid packing as indicated by an increase of elasticity modulus and molecular areas.

At 25°C *Π-A* isotherms membrane monolayer showed in the *LE* phase and the collapse phase. The collapse phase on membrane monolayers was able to observe because of a greater attractive interaction of saturated lipids and a displacement of lipid monolayers on collapse protein network at the interface. At 50°C *Π-A* isotherms membrane monolayer exhibited a *G-LE* phase transition and *LE* phase. The *G-LE* phase transition appeared due to a low interaction of lipid-lipid and lipid-protein associating with disordering protein and lipid structure (Figure 5.6). This study implies the effect of unsaturated lipids and proteins on membrane monolayers and helps our understanding of the mechanism of butanol tolerant membrane by *C. pasteurianum* could be utilized to develop cultures in higher concentrations of butanol leading to more cost-effective and more efficient on butanol production.

Apart from the changes in the composition of lipids in the membrane, the response to toxic solvent also involves various changes in the intracellular components such as expression of heat shock proteins and their role in protein turnover, changes to the composition of cell wall with a possible activation of sporulation and maintenance

of cell's energy requirements under stress conditions through the carbohydrate or glycolytic pathway. [39]

The result from this study substantiates the assumption that a correlation exists between the modes of homeoviscous response, which are in turn, dependent on the activation of butanol production pathway. Furthermore, the existence of two different homeoviscous adaptations to butanol challenge in *C. pasteurianum*, demonstrates the potential of this organism to be studied further in terms of proteomics, functional genomics and metabolic engineering for the development of an industrial strain. The unavailability of the genome sequence and the proteome data must be addressed to explore butanol production and tolerance in *C. pasteurianum*. In the meantime, methods to use genomic and metabolic information from closely related species can be explored to establish a platform that can be used to perform transcriptional analysis of *C. pasteurianum* during butanol stress.

## 6. References


(1) Biebl, H. *J Ind Microbiol Biotechnol* 2001, *27*, 18.

(2) Dabrock, B.; Bahl, H.; Gottschalk, G. *Appl Environ Microbiol* 1992, *58*, 1233.

(3) Taconi, K. A.; Venkataramanan, K. P.; Johnson, D. T. *Environmental Progress & Sustainable Energy* 2009, *28*, 100.

(4) Venkataramanan, K. P.; Boatman, J. J.; Kurniawan, Y.; Taconi, K. A.; Bothun, G. D.; Scholz, C. *Appl Microbiol Biotechnol* 2012, *93*, 1325.

(5) Sardessai, Y.; Bhosle, S. *Res Microbiol* 2002, *153*, 263.

(6) Baer, S. H.; Blaschek, H. P.; Smith, T. L. *Appl Environ Microbiol* 1987, *53*, 2854.

(7) Baer, S. H.; Bryant, D. L.; Blaschek, H. P. *Appl Environ Microbiol* 1989, *55*, 2729.

(8) Baut, F.; Fick, M.; Viriot, M. L.; Andre, J. C.; Engasser, J. M. *Appl Microbiol Biotechnol* 1994, *41*, 551.

(9) Bowles, L. K.; Ellefson, W. L. *Appl Environ Microbiol* 1985, *50*, 1165.

(10) Lepage, C.; Fayolle, F.; Hermann, M.; Vandecasteele, J. P. *J Gen Microbiol* 1987, *133*, 103.

(11)Liu, S. Q.; Qureshi, N. *N Biotechnol* 2009, *26*, 117.

(12)Vollherbst-Schneck, K.; Sands, J. A.; Montenecourt, B. S. *Appl Environ Microbiol* 1984, *47*, 193.

(13)Isar, J.; Rangaswamy, V. *Biomass & Bioenergy* 2012, *37*, 9.

(14)Heipieper, H. J.; Weber, F. J.; Sikkema, J.; Keweloh, H.; Debont, J. A. M. *Trends Biotechnol* 1994, *12*, 409.

(15)Lăzăroaie, M.Mechanisms Involved In Organic Solvent Resistance in Gram-Negative Bacteria

(16)Ramos, J. L.; Duque, E.; Gallegos, M.-T.; Godoy, P.; Ramos-González, M. I.; Rojas, A.; Terán, W.; Segura, A. *Annual Review of Microbiology* 2002, *56*, 743.

(17)Lopez-Montero, I.; Arriaga, L. R.; Monroy, F.; Rivas, G.; Tarazona, P.; Velez, M. *Langmuir* 2008, *24*, 4065.

(18)Lingwood, D.; Kaiser, H. J.; Levental, I.; Simons, K. *Biochem Soc Trans* 2009, *37*, 955.

(19)Simons, K.; Ikonen, E. *Nature* 1997, *387*, 569.

(20)Lenaz, G. *Biosci Rep* 1987, *7*, 823.

(21)Timmons, M. D.; Knutson, B. L.; Nokes, S. E.; Strobel, H. J.; Lynn, B. C. *Applied Microbiology and Biotechnology* 2009, *82*, 929.

(22) Beaven, M. J.; Charpentier, C.; Rose, A. H. *Journal of General Microbiology* 1982, *128*, 1447.

(23)Ingram, L. O. *Journal of Bacteriology* 1982, *149*, 166.

(24)Uchida, K. *Biochimica Et Biophysica Acta* 1974, *348*, 86.

(25)Kurniawan, Y.; Venkataramanan, K. P.; Scholz, C.; Bothun, G. D. *J Phys Chem B* 2012, *116*, 5919.

(26)Aguilar, L. F.; Sotomayor, C. P.; Lissi, E. A. *Colloids and Surfaces a-Physicochemical and Engineering Aspects* 1996, *108*, 287.

(27)Iiyama, S.; Toko, K.; Murata, T.; Ichinose, H.; Suezaki, Y.; Kamaya, H.; Ueda, I.; Yamafuji, K. *Biophys Chem* 1992, *45*, 91.

(28)Cevc, G. *Studia Biophysica* 1982, *91*, 45.

(29)Lobbecke, L.; Ceve, G. *Biochimica Et Biophysica Acta-Biomembranes* 1995, *1237*, 59.

(30)Papoutsakis, E. T. *Curr Opin Biotechnol* 2008, *19*, 420.

(31)Duncan, S. L.; Larson, R. G. *Biophys J* 2008, *94*, 2965.

(32)Dombek, K. M.; Ingram, L. *J Bacteriol* 1984, *157*, 233.

(33)Yan, W. F.; Piknova, B.; Hall, S. B. *Biophysical Journal* 2005, *89*, 306.

(34)Gwynne, J. T.; Mahaffee, D.; Brewer, H. B.; Ney, R. L. *Proceedings of the National Academy of Sciences of the United States of America* 1976, *73*, 4329.

(35)Sparrow, C. P.; Parthasarathy, S.; Steinberg, D. *Journal of Lipid Research* 1988, *29*, 745.

(36)Dunlop, M. J.; Dossani, Z. Y.; Szmidt, H. L.; Chu, H. C.; Lee, T. S.; Keasling, J. D.; Hadi, M. Z.; Mukhopadhyay, A. *Mol Syst Biol* 2011, *7*.

(37)Lucero, A.; Nino, M. R. R.; Gunning, A. P.; Morris, V. J.; Wilde, P. J.; Patino, J. M. R. *Journal of Physical Chemistry B* 2008, *112*, 7651.

(38)Segura, A.; Duque, E.; Mosqueda, G.; Ramos, J. L.; Junker, F. *Environmental microbiology* 2002, *1*, 191.

(39)Huffer, S.; Clark, M. E.; Ning, J. C.; Blanch, H. W.; Clark, D. S. *Appl Environ Microbiol* 2011, *77*, 6400.

# CHAPTER 6

# CONCLUSIONS AND FUTURE WORK

## 6.1. Conclusions

While many studies have examined the effects of n-butanol on lipid membrane, an understanding of how microorganisms that exhibit homeoviscous adaptation to counteract n-butanol toxicity is lacking. For example, some cells increase and some decrease the SFA/UFA lipid ratio and the biophysical basis for this is unclear. The influence of unsaturated lipids and anionic lipids on n-butanol partitioning into cell membranes was examined using unilamellar liposomes, monolayers, and reconstituted membranes of *Clostridium pasteurianum* as model cell membranes. We hypothesized that increasing unsaturated lipid and decreasing anionic lipids ratio in electrolyte solution increase butanol partitioning into membrane. Experimental techniques were developed and implemented to quantify butanol partitioning and mechanical structure.

Thin film hydration technique was used to form mixed liposomes from zwitterionic saturated lipid (DPPC) and unsaturated lipid (DOPC) at different ratios. n-Butanol was added to the liposomal solution up to 0.27 M and the interactions were studied using differential scanning calorimetry (DSC), high pressure liquid chromatography (HPLC), and fluorescence spectrometry to characterize the thermodynamic and structural cell membrane. Phase behavior of DPPC/DOPC bilayer membrane was dependent on n-butanol concentration and continuous phase (DPPC in gel phase or DOPC in fluid phase). The presence of DOPC in DPPC/DOPC membrane

did not prevent interdigitation and DOPC with n-butanol partition promoted a $L_\beta$-like DPPC phase. Below the interdigitation concentration (<0.13 M n-butanol), the numbers of n-butanol partitions into membrane correlated with the molecular fraction of DOPC in fluid phase. Above the interdigitation concentration the numbers of n-butanol partitions into membrane was dependent upon which phase was continuous.

To gain insight further of the interaction between coexisting phases in DPPC/DOPC membrane and n-butanol, heterogeneous monolayer membrane of DPPC/DOPC with n-butanol was examined using Langmuir balance trough and fluorescence microscope. Lipid phase behavior, lipid packing, and monolayer elasticity were evaluated by surface pressure-area (*Π-A*) analysis. n-Butanol partitioning into DPPC monolayers led to lipid expansion and decreased elasticity. With increasing DOPC content, lipid expansion became greater. At equimolar DPPC/DOPC, n-butanol accumulation was amplified at the interface between coexisting liquid expanded (*LE*, DOPC-rich) phases and liquid condensed (*LC*, DPPC-rich)domains. Consequently, *LE-LC* line tension was reduced, and the domain size and morphology of *LC* domains were changed.

Due to the negatively charged cell membrane and the effects of ionic strength, the interaction between mixed liposomes from zwitterionic and anionic lipids (DPPC/DPPG) and n-butanol were also examined extensively. Thin film hydration technique and extrusion were used to form uniformly mixed large unilamellar vesicles (LUVs). This work has experimentally proved that DPPG concentration and ionic strength have a great effect on DPPC/DPPG membrane phase behavior, size and n-butanol partitioning. Above interdigitation concentration (>0.13 M n-butanol), n-

butanol partitioning into membrane transformed the $L_{\beta'}$ phase to the$L_{\beta l}$ phase without considering DPPG content and salt concentration. Increasing DPPG content in the DPPC/DPPG membrane and salts above 0.13 M n-butanol concentration, aggregation/ fusion could be prevented and the emergence of SUVs could be apparent. This indicates that DPPG and salt promoted more rigid bilayer structures and reduced butanol partition, by screening electrostatic repulsion between PG headgroups.

This dissertation also examined membrane composition, membrane phase behavior, and membrane fluidization of butanol adapted *C. pasteurianum*. The work revealed that the changes on structure and integrity of the cell membranes counteracting butanol toxicity in media were dependent on the level of lipid-lipid interactions and the lipid-protein interactions. The presence of extracted-hydrophobic protein in reconstituted membrane using Bligh and Dyer method was able to observe by evaluating membrane phase behavior, packing and elasticity through detailed analysis of surface pressure-area isotherms at different temperatures. Unsaturated fatty acid of lipid and membrane proteins played a major role to influence the membrane elasticity and the phase behavior. Using Langmuir balance method, lipid-protein and lipid-lipid interaction were able to identify. When unsaturated lipid ratio decreased with high n-butanol concentration, reconstituted cell monolayer experienced in high surface pressure due to a greater attractive attraction within saturated tails of lipids and an increased of protein contents in cell membrane adsorbed at air/water interface. A rigid molecular packing was indicated by an increase of elasticity modulus and anisotropy.

Collectively, this work shows a truly novel aspect inclusive of the importance of gel-fluid or LE-LC interfaces on partitioning; membranes containing DOPC or DPPG are still interdigitated; salt can enhance interdigitation and/or change liposome structure; *C. pasteurianum* responds by increasing lipid tail length and protein content; and *C. pasteurianum* monolayers can be used to probe homeoviscous response. To our knowledge, these works are the first study that has ever been done.

**6.2. Future work**

As introduced in chapter 1, the major lipid components of bacterial cell membranes consist of phosphoethanolamine (PE), phosphoglycerol (PG), and diphosphatidylglycerol (DPG).Thus, unilamellar vesicles and monolayer membranes composed of PE or DPG will be well-suited to improve our understanding of bilayer perturbations in a more realistic system.

In chapter 2, the interactions between DPPC/DOPC liposome and n-butanol have been examined. With considering the insertion of ergosterol in the DPPE/DOPE liposome, it may reinforce the membrane to tolerate high n-butanol concentration.[42]This may give more informative that ergosterol as an additive insertion may be applicable to reduce the membrane fluidity and hinder n-butanol to partition in the membrane.

In chapter 3, elasticity modulus, Gibbs free energy of mixing, and membrane phase of DPPC/DOPC monolayer have been examined. However, considered the insertion of ergosterol in the DPPE/DOPE monolayer with n-butanol adsorption will be favorable to understand how ergosterol interacts with lipid to reduce n-butanol partition. The effect of ergosterol and n-butanol on surface pressure and elasticity will

give an insight of Gibbs free energy of mixing, line tension and size distributions of domains.

Chapter 4 has demonstrated the role of ionic strength on butanol partitioning into DPPC/DPPG. To gain more insight, comparing self-assemblies of ergosterol/DPPG/DPPE liposomes in water and PBS will be favorable to obtain a better understanding of the role of the additive insertion and salts in modulating n-butanol partition. The effects of salts and ergosterol may change the morphologies and phase behavior of the charged lipid membrane.

Chapter 5 has studied the effect of exogenous n-butanol concentration on the lipid composition, phase behavior and elasticity of the homeoviscous *C. pasteurianum.* However, the expression of protein in the homeoviscous *C. Pasteurianum* has not been evaluated. Thus, comprehensive analysis on the membrane proteome of *C. pasteurianum* wild type strain and its butanol-tolerant mutant will be very useful to reveal the protein expression related to n-butanol tolerance. This comparative membrane proteomics study, together with lipid membrane study will bring a systemic understanding of the n-butanol effects on cellular physiology of C.*pasteurianum*.

The main focus of this dissertation was to evaluate the interaction of n-butanol with liposomes, monolayers, reconstituted membranes, and use that fundamental knowledge to understand the n-butanol partitioning into membrane associated with membrane fluidity and lipid composition. The future work may focus on design of more realistic and stable the bacterial membrane and develop a systemic

understanding of interactions between lipid and protein membrane in butanol-adapted cell membrane.

## 6.3. References

(1) Vanegas, J. M.; Contreras, M. F.; Faller, R.; Longo, M. L. *Biophysical Journal***2012**, *102*, 507.

# APPENDIX A

## Differential scanning calorimetry (DSC)

DSC measures the temperatures and heat flows correlated to phase transitions in materials as a function of time and temperature.[98] These measurements provide quantitative and qualitative information about physical and chemical changes that involve endothermic or exothermic processes, or changes in heat capacity. There are two cells; sample cell and reference cell. The heat flows to the sample cell and a reference cell at the same temperature and the difference of heat is recorded as a constant pressure and a function of temperature that increased at a constant rate. The heat flow is equivalent to enthalpy changes ($\Delta H$).

Heat flow = $\left(\frac{\Delta q}{\Delta t}\right) = \left(\frac{\Delta H}{\Delta t}\right)$ = enthalpy changes = $\left(\frac{\Delta H}{\Delta t}\right)_{sample} - \left(\frac{\Delta H}{\Delta t}\right)_{reference}$

where $\left(\frac{\Delta q}{\Delta t}\right)$ is the heat flow measured in mcal/sec.$\Delta H$ can be determined by correcting suitable baseline which affects the transition and measuring the total integrated zone below the thermogram peak representing the total heat energy uptake by the sample.

The heat flow difference can be either positive (endothermic process) or negative (exothermic process). For example, the dipalmitoylphosphatidylcholine (DPPC) phase transition between gel phase to fluid crystalline phase is an endothermic process where the reference cell needs more heat to increase in temperature to the same extent with sample cell.[99] DSC can also determine the melting temperature of phase transition. Figure A.1 demonstrates melting behavior of DPPC lipids; pretransition ($T_p$, gel phase to ripple phase) and main transition ($T_m$, ripple phase to liquid phase).

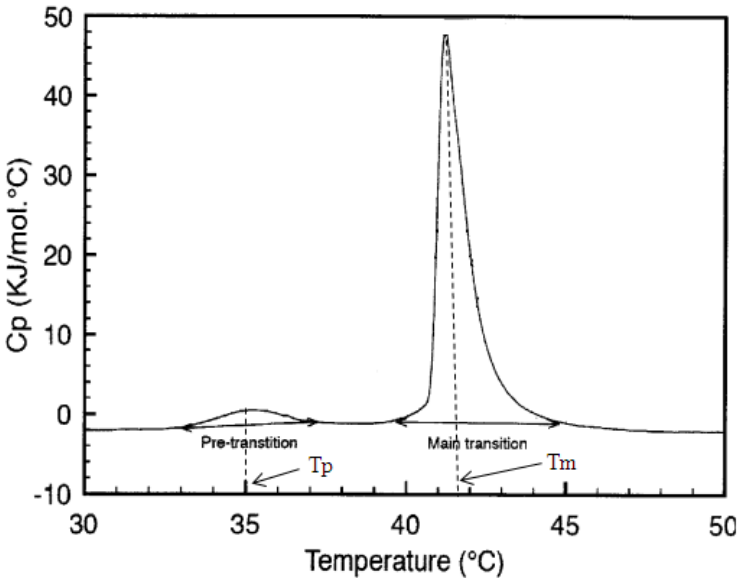


Figure A.1.DSC thermogram of DPPC lipid exhibiting pre-transition and main transition curves and temperatures.

## References

(1) Gill, P.; Moghadam, T. T.; Ranjbar, B. *J Biomol Tech*, **2010**, *21*, 167.

(2) Killian, J. A. *Biochimica Et Biophysica Acta-Reviews on Biomembranes***1998**, *1376*, 401.

## APPENDIX B

### Dynamic light scattering (DLS)

*Size measurement*

DLS measures Brownian motion (random movement of particles) which is related to the size of the particles.[100] Sample is suspended within a liquid. The larger the particle, the slower the Brownian motion will be. Smaller particles move faster due to bombardment by the solvent or water. The velocity of the Brownian motion is related to diffusion coefficient, *D*, of particles which is to determine the hydrodynamic diameter of the particles, *d,* via the Stokes-Einstein equation (assuming spherical particle). The hydrodynamic diameter is defined as

$$d(H) = \frac{kT}{3\pi\eta D}$$

Where *d(H)* is hydrodynamic diameter, *D* is difussion coefficient, *k* is Boltzmann's constant, *T* represents temperature, and $\eta$ represents viscosity.[101]

*Zeta potential measurement*

DLS can measure zeta potential of colloidal solution to predict and control dispersion stability by determining the electrophoretic mobility which is expressed as

$$U_p = \frac{\Delta v \lambda_o}{2\, nE \sin\left(\frac{\theta}{2}\right)}$$

Where $U_p$ is the electrophoretic mobility, $\Delta v$ is the Doppler frequency shift, $\lambda o$ is the wavelength of the laser in vacuum, *n* is the index of refraction of the medium, *E* is the electric field applied and $\theta$ is the scattering angle.

The electrophoretic mobility is obtained by conducting an electrophoresis experiment on the sample and measuring the velocity of the particles using Laser Doppler Velocimetry (LDV). LDV measures the movement of charged particles in an

electric field which utilizes the Doppler Effect. When a voltage is applied to a pair of electrodes of the cell holding sample, charged particles are attracted to the oppositely charged electrode and then their velocity is measured and expressed in unit field strength as their mobility. Viscous forces acting on the particles tend to oppose this movement. When equilibrium is reached between these opposing forces, the particles move with constant velocity which is a function of the strength of electric field, the dielectric constant, viscosity of the medium, and zeta potential. Thus, zeta potential can be determined from the electrophoretic velocity of the particles using Helmholtz-Smoluchowski equation

$$\zeta = \frac{U_P}{\varepsilon\eta} = \frac{V_p E}{\epsilon\eta}$$

where $\zeta$ is the zeta potential, $V_p$ is the electrophoretic velocity, $\varepsilon$ is the permittivity, and $\eta$ is the viscosity of the medium.[101]

## References

(1) Alexander, M.; Dalgleish, D. G. *Food Biophysics***2006**, *1*, 2.

(2) Chu, B.; Lin, F. L. *Journal of Chemical Physics***1974**, *61*, 5132.

## APPENDIX C

### Fluorescence anisotropy (FA)

The changes of membrane fluidity are determined quantitatively through steady-state fluorescence spectroscopy by using a probe molecule to penetrate into hydrophobic part of the lipid membrane.[102] 1,6-diphenyl-1,3,5-hexatriene (DPH) is common fluorescent probe molecule for measuring membrane fluidity in biological membranes.[103]

When DPH is embedded within the hydrophobic tails of lipid bilayer, rotational motion of DPH is inhibited by the hydrophobic tails of the lipids (Figure C.1) resulting in fluorescence emission.[103] The degree of the rotational motion of DPH is associated with the fluorescence intensity of DPH which is a function of the membrane fluidity.

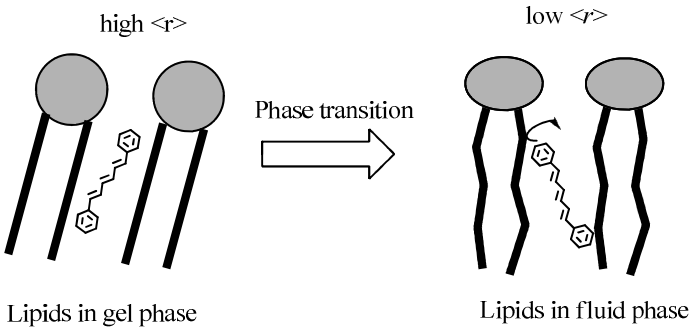


Figure C.1. DPH located within hydrophobic lipid tails of monolayer membrane from a gel phase to a liquid phase.

When <*r*> increases, the fluidity of the membrane is low whereas when <*r*> decreases, the fluidity of the membrane is high. Figure C-2 represents a fluorescence anisotropy result exhibiting the anisotropy of DPPC/DOPC liposomes as a function of temperature and DPPC/DOPC molar ratios.

Fluorescence anisotropy (<r>) is defined as:

$$< r >= \frac{I_{VV} - I_{VH}}{I_{VV} + GI_{VH}}$$

where $I$ represents the fluorescence intensity, the subscripts $V$ and $H$ represent the vertical and horizontal orientation of the excitation and emission polarizers, respectively, and $G$ is the grating factor ($G = I_{HV}/I_{VH}$), which accounts for the correction factor of the sensitivity of the instrument towards vertically and horizontally polarized light.

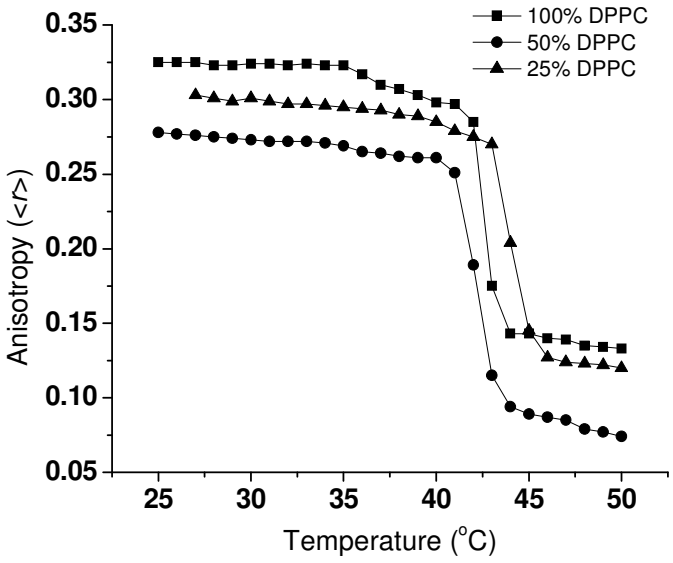


Figure C.2. Steady-state fluorescence anisotropy is expressed as a function of temperature (°C) and DPPC/DOPC ratios (0.1 mM Lipid in DI water with DPH:lipid molar ratio of 1:400) under atmospheric pressure.

## References

(1) Lentz, B. R.; Barenholz, Y.; Thompson, T. E. *Biochemistry***1976**, *15*, 4529.

(2) Parasassi, T.; Conti, F.; Glaser, M.; Gratton, E. *Journal of Biological Chemistry***1984**, *259*, 4011.

## APPENDIX D

### Langmuir Blodgett (LB)

A Langmuir Blodgett monolayer technique is used to measure the surface pressure of amphiphilic molecules in monolayer at air/water interface.[104] The molecular density at the air/water interface with constant temperature is altered with moveable barriers in a Langmuir-Blodgett (LB) film balance. By moving barriers the film density decreases (compression) or increases (expansion), which changes the surface tension, $\gamma$, of the air-water interface which is measured by Wilhelmy plate (Figure D-1).

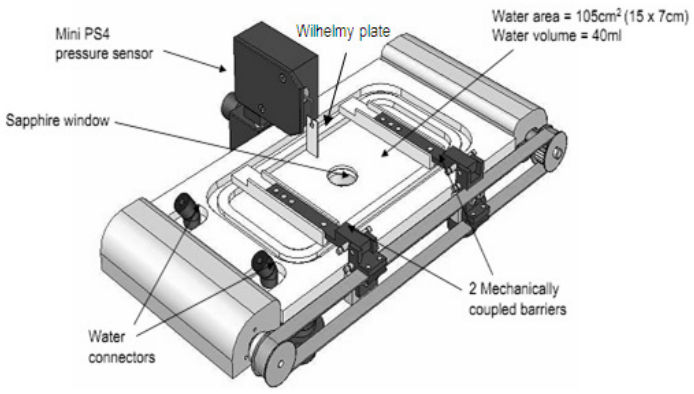


Figure D.1. A schematic of the Langmuir-Blodgetttrough.

Surface pressure, $\Pi$, of monolayer at water surface can be calculated as $\Pi = \gamma_o - \gamma$, where, $\gamma_o$ is surface tension of water without amphiphilic molecules present and $\gamma$ issurface tension of water with amphiphilic molecules present.

Plots of the surface pressure $\Pi$ versus the molecular area, $A$, of the amphiphiles at constant temperature $T$ (isotherms) shows the $\Pi$- $A$ isotherms which provide information on the monolayer state or phase transitions and the compression modulus ( Figure D.2).

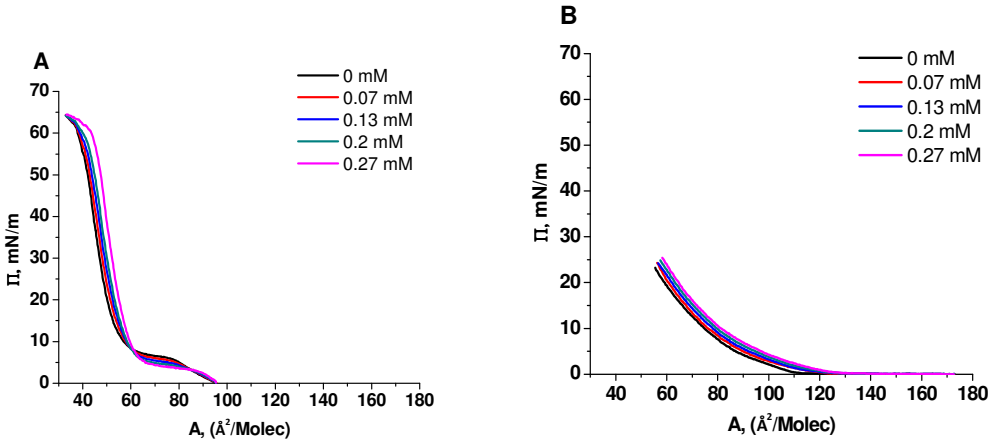


Figure D.2. *Π–A* isotherms ofDPPC/DOPC monolayerson butanol-water/air interface at different ratios of (A) 1:0, (B) 0:1 at 25°C as a function of n-butanol concentrations.

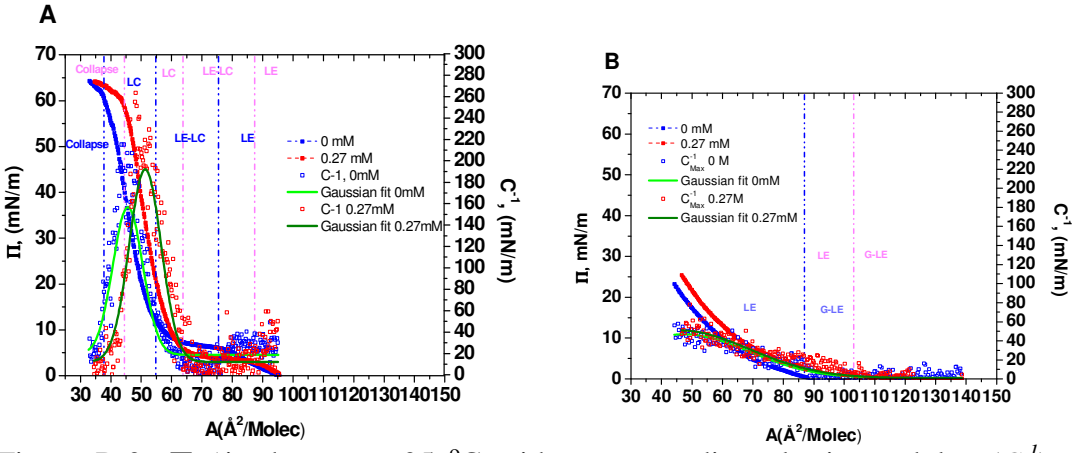


Figure D.3. *Π–A*isotherms at 25 °C with corresponding elastic modulus ($C^{-1}$) and phase diagrams of DPPC/DOPC monolayers at (A) 1:0 and (B) 0:1 DPPC:DOPC ratios for 0 mM and 0.27 mM n-butanol in the subphase.

## References

(1) Roberts, G. G. *Advances in Physics***1985**, *34*, 475.

(2) Guzman, E.; Liggieri, L.; Santini, E.; Ferrari, M.; Ravera, F. *Colloids and Surfaces a-Physicochemical and Engineering Aspects***2012**, *413*, 174.

## APPENDIX E

### Miscibility and thermodynamic stability of the mixed monolayers

To explore the nature of DPPC/DOPC interactions influenced by n-butanol, the thermodynamic stability of the mixed monolayers was examined based on the excess free energy of mixing, $\Delta G_{Mix}^{E}$.

$$\Delta G_{Mix}^{E} = N_A \int_0^{\pi} (A_{12} - X_1 A_1 - X_2 A_2) d\pi$$

where$A_1$ and $A_2$ are the molecular areas of pure DPPC and pure DOPC, respectively,$A_{12}$is the molecular area of mixed DPPC/DOPC without n-butanol present, $\Pi$is surface pressure and $N_A$is Avogadro's constant.[105-107]If the components form an ideal mixture, $\Delta G_{Mix}^{E}$ equals zero. Negative values of $\Delta G_{Mix}^{E}$ indicate that the DPPC/DOPC film is more thermodynamically stable (attractive interlipid forces) than the pure monolayers; whereas positive values of $\Delta G_{Mix}^{E}$represents instability (repulsive interlipid forces) and phase separation.[106,107]

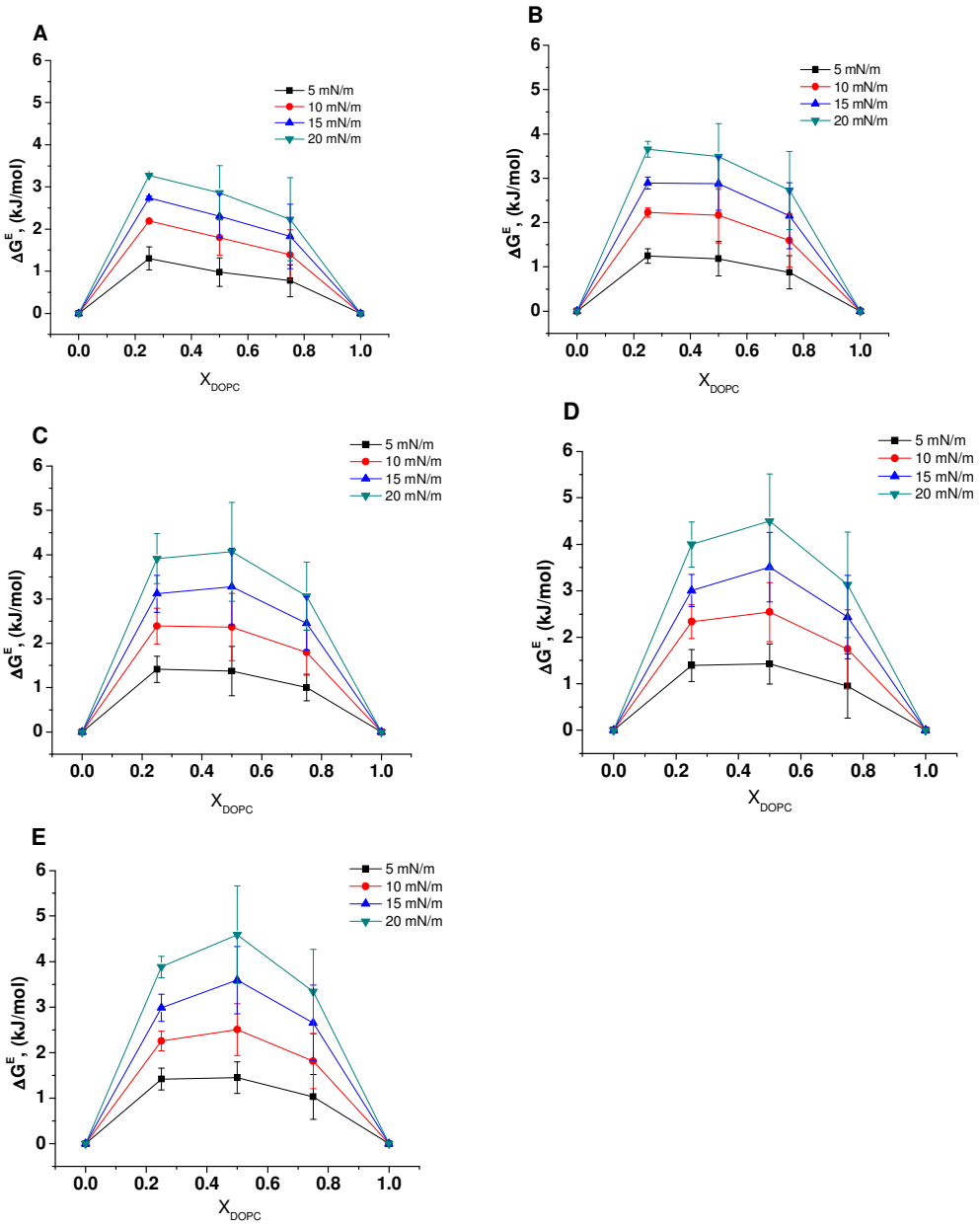


Figure E.1.The excess Gibbs energy of mixed DPPC/DOPC monolayers as a function of DPPC mole fractions at different surface pressures and at different butanol concentrations of (A) 0 mM, (B) 0.07 mM, (C) 0.13 mM, (D) 0.2 mM, (E) 0.27 mM at 25°C.

## References


(1) Bordi, F.; Cametti, C.; Venanzio, C. D.; Sennato, S.; Zuzzi, S. *Colloids and Surfaces B: Biointerfaces***2008**, *61*, 304.

(2) Chen, K. B.; Chang, C. H.; Yang, Y. M.; Maa, J. R. *Colloids and Surfaces a-Physicochemical and Engineering Aspects***2000**, *170*, 199.

(3) Panda, A. K.; Vasilev, K.; Orgeig, S.; Prestidge, C. A. *Materials Science & Engineering C-Materials for Biological Applications***2010**, *30*, 542.

# APPENDIX F

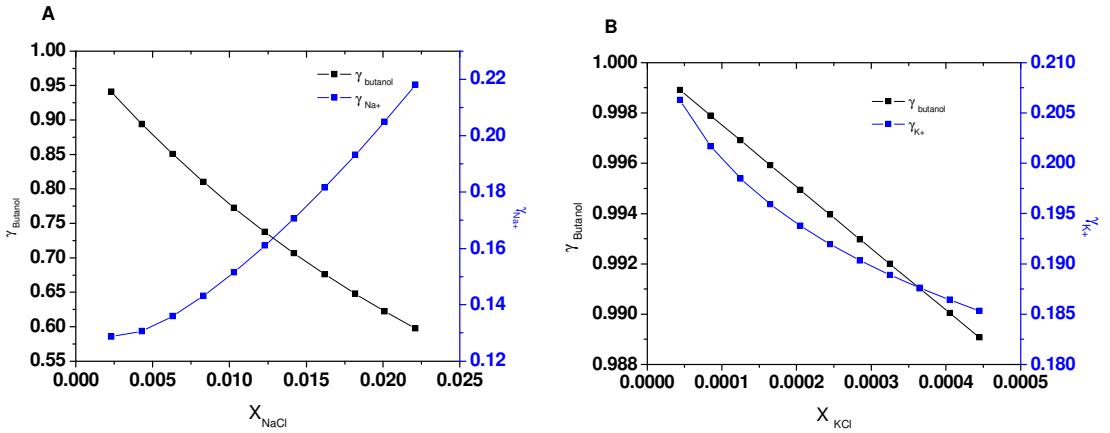


Figure F.1.Activity coefficient of n-butanol as a function of (A) NaCl and (B) KCl mole fraction computed by ASPEN based on the NRTL-RK model.

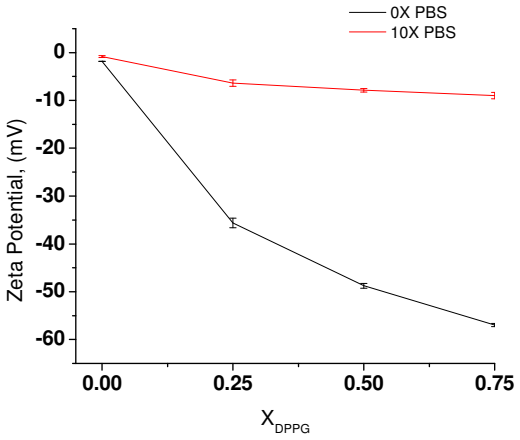


Figure F.2.Zeta potential of DPPC/DPPG liposome as a function of DPPG mole fractions and PBS solution concentrations.

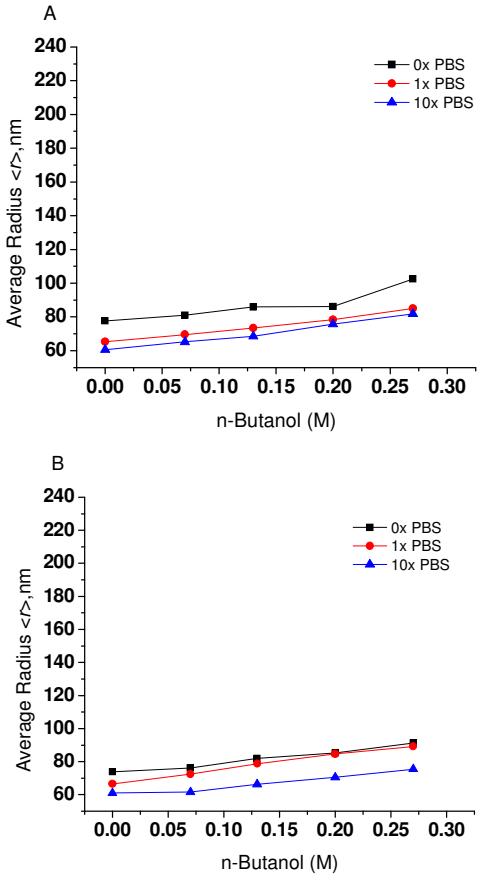


Figure F.3.Average size of DPPC/DPPG liposome at different ratios (A) 25% DPPG, (B) 50% DPPG as a function of different butanol concentrations and PBS.

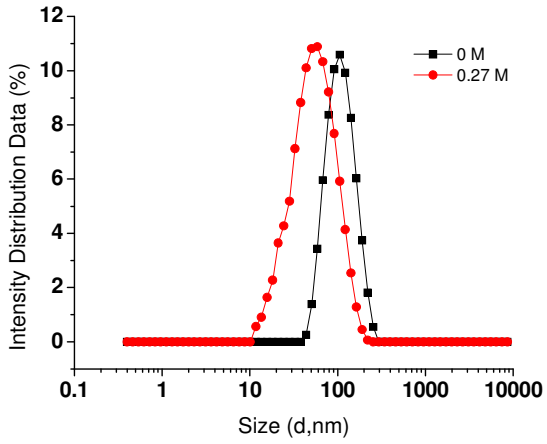


Figure F.4. Intensity distribution data of 75% DPPG liposome as function of liposome hydrodynamic diameter at different butanol concentration in 0x PBS.

# APPENDIX G

**Determination of percentage unsaturation using NMR**

The unsaturation in the fatty acid tails of the lipids was analyzed using $^{1}$H-NMR using synthetic lipids for calibration. Specifically, DPPC and DOPC (10 μM, total) were mixed to obtain lipid mixtures in the ratio of 1:0, 3:1, 1:1, 1:3 and 0:1, thereby generating samples of varied degrees of unsaturation. The $^{1}$H-NMR of the samples is shown in Figure G.1.

The peak for the unsaturation (-C*H*=C*H*-) is observed at 5.35 ppm (Figure G.1B)[1,2]. The $^{1}$H-NMR of 100 % DPPC, does not show a peak, as DPPC is a saturated lipid (Figure G.1B). The area of the peak progressively increased with an increase in the ratio of DOPC in the samples with respect to DPPC (Figure G.1B). The area of the peak was calculated by normalizing the area of the terminal methyl group (-C$H_3$) observed at 0.88 ppm to 6 ppm (due to the presence of two fatty acid tails per lipid molecule and hence, two methyl groups with 6 protons). All other peaks between 1.0 ppm and 4.5 ppm correspond to the rest of the protons on the lipid moiety[1,2]. The peak at 5.20 ppm corresponds to the single proton on the center carbon of the glycerol molecule and integrates to 1 (Figure G.1C).

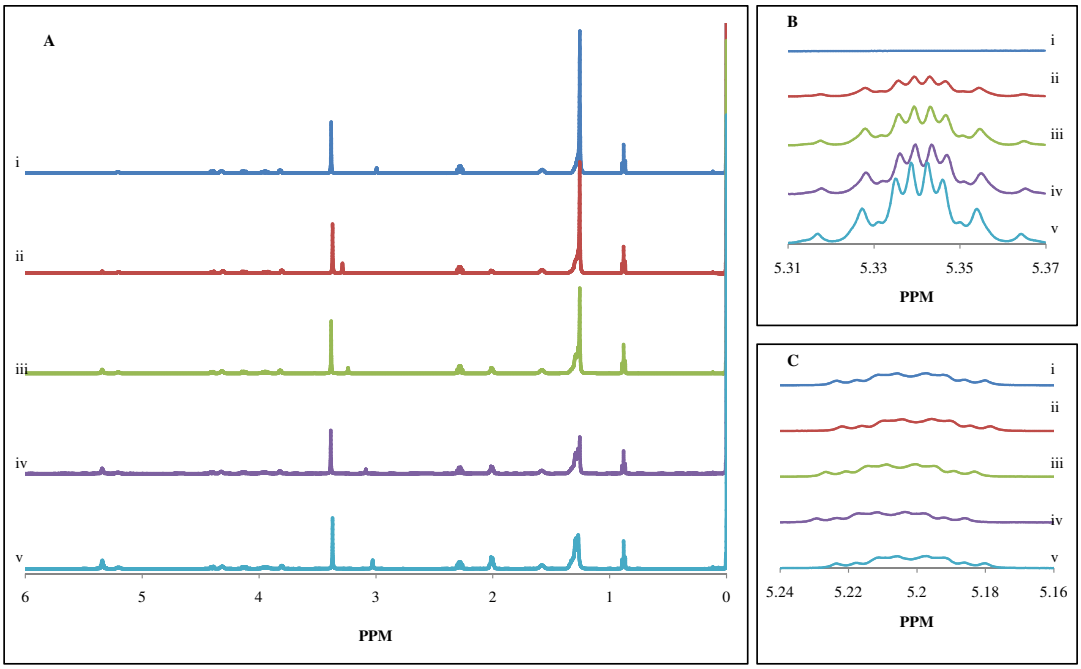


5.34 ppm; (C) Comparison of of the proton on glycerol at 5.20 ppm.

**Effect of Endogenous Butanol**

The effect of endogenously produced butanol on the bacterial lipid membrane was studied by growing the bacteria in conditions that resulted in the formation of butanol at different concentrations from 0 g/L to 10 g/L (0.134 M). Growing the bacteria in a dual carbon source of glycerol (butanol producer) and glucose (not a butanol producer) resulted in the formation of higher butanol titers. Hence, for the studies on the homeoviscous response during endogenous butanol formation, cells were grown in glucose (10 g/L) and glycerol (10 g/L to 50 g/L), resulting in butanol formation between 0 g/L and 10 g/L. The membranes were extracted from the stationary phase cultures and the extracted membranes were analyzed using $^{1}$H-NMR

and DPH fluorescent anisotropy. Figure G.2 summarizes the results from $^{1}$H-NMR and fluorescent anisotropy.

The anisotropy of the lipid membranes of *C. pasteurianum* increased with increasing amounts of butanol being synthesized by the cells (Figure G.3). Furthermore, the degree of unsaturation in the fatty acid tails decreased with the corresponding increase in the titers of butanol produced endogenously. An increase in the anisotropy indicated a decrease in fluidity and hence, an increase in the rigidity of the membrane. The data on the degree of unsaturation obtained from $^{1}$H-NMR, supports the trend observed in the data from the fluorescent anisotropy (Figure G.2 and G.3). In summary, an increase in the amount of butanol produced by the cells led to a more rigid membrane.

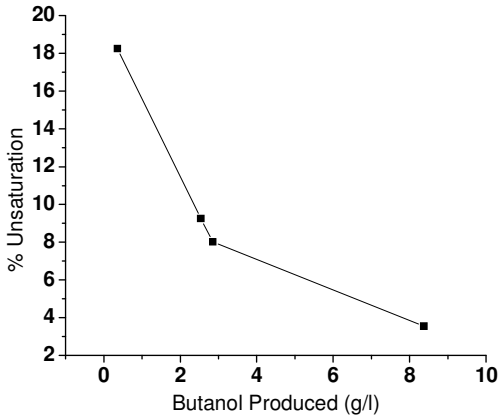


Figure G.2. Degree of unsaturation in the reconstituted of *C. pasteurianum* producing differentamounts of butanol during glycerol fermentation measured by $^{1}$H-NMR.

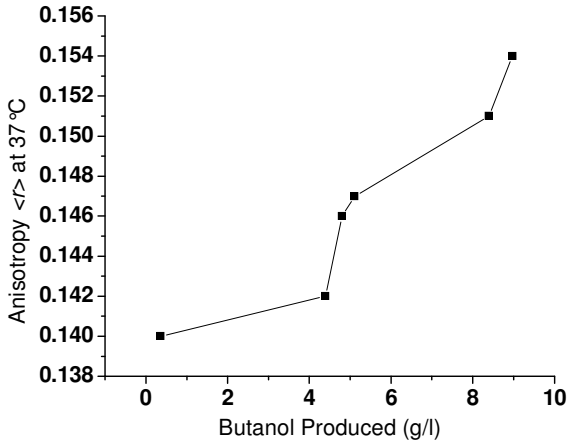


Figure G.3. DPH fluorescence anisotropy of membrane lipids of *C. pasteurianum* during endogenous butanol production during glycerol fermentation.

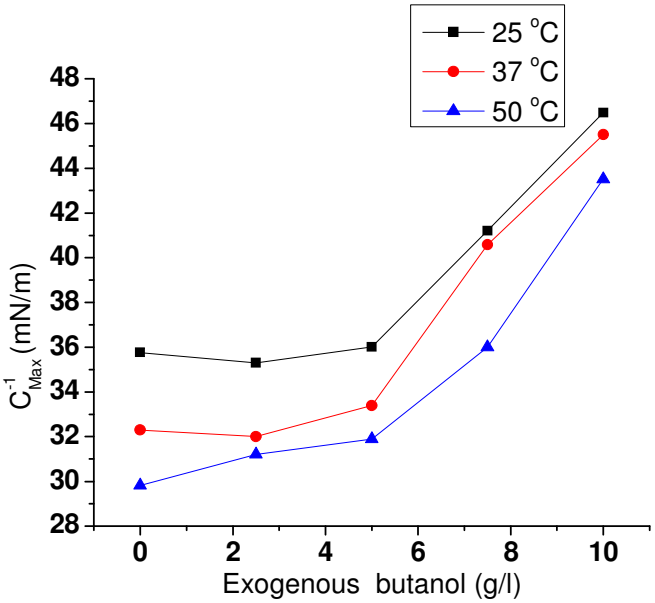


Figure G.4. Maximum elastic modulus of reconstituted membrane monolayer at 25°C (black), 37°C (red), and 50°C (blue) as a function of exogenous butanol.